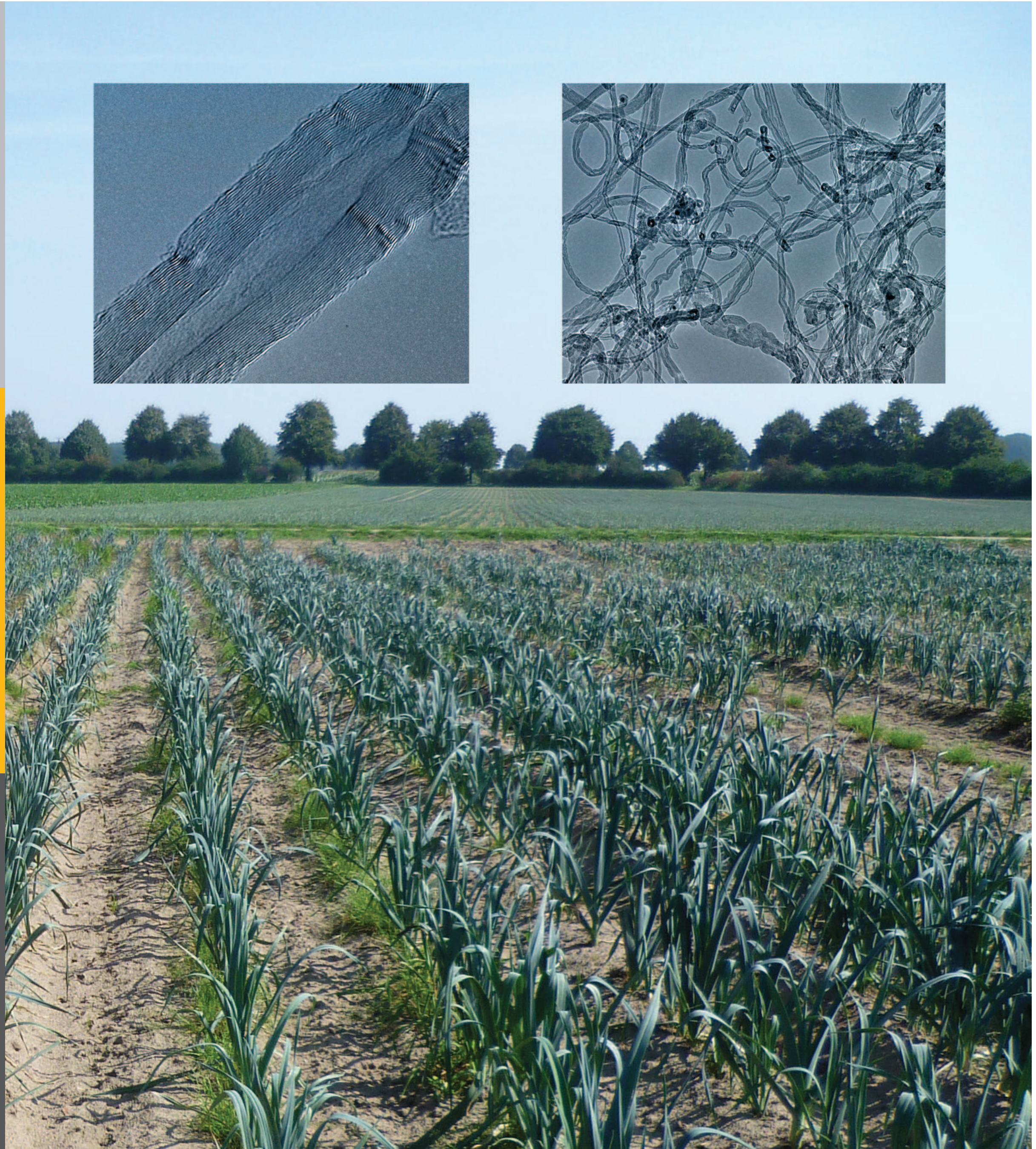

Transport and deposition of functionalized multi-walled carbon nanotubes in porous media

Daniela Kasel

JÜLICH
FORSCHUNGSZENTRUM

Schriften des Forschungszentrums Jülich
Reihe Energie & Umwelt / Energy & Environment Band / Volume 201

Forschungszentrum Jülich GmbH
Institute of Bio- and Geosciences (IBG)
Agrosphere (IBG-3)

Transport and deposition of functionalized multi-walled carbon nanotubes in porous media

Daniela Kasel

Schriften des Forschungszentrums Jülich
Reihe Energie & Umwelt / Energy & Environment Band / Volume 201

ISSN 1866-1793 ISBN 978-3-89336-929-4

Bibliographic information published by the Deutsche Nationalbibliothek.
The Deutsche Nationalbibliothek lists this publication in the Deutsche Nationalbibliografie; detailed bibliographic data are available in the Internet at http://dnb.d-nb.de.

Publisher and Distributor:	Forschungszentrum Jülich GmbH Zentralbibliothek 52425 Jülich	
	Tel:	+49 2461 61-5368
	Fax:	+49 2461 61-6103
	Email:	zb-publikation@fz-juelich.de www.fz-juelich.de/zb
Cover Design:	Grafische Medien, Forschungszentrum Jülich GmbH	
Printer:	Grafische Medien, Forschungszentrum Jülich GmbH	
Copyright:	Forschungszentrum Jülich 2013	

Schriften des Forschungszentrums Jülich
Reihe Energie & Umwelt / Energy & Environment, Band / Volume 201

D 82 (Diss.,RWTH Aachen University, 2013)

ISSN 1866-1793
ISBN 978-3-89336-929-4

The complete volume is freely available on the Internet on the Jülicher Open Access Server (JUWEL) at www.fz-juelich.de/zb/juwel

Abstract

The aim of this study was to gain more profound knowledge on the transport and deposition of functionalized multi-walled carbon nanotubes (MWCNTs) in porous media. The use of ^{14}C-labeled MWCNTs allowed investigations into very low concentrations and the determination of retention profiles. Transmission electron micrographs revealed that the MWCNTs exhibited average outer diameters of 10–50 nm and average lengths of up to several µm. The functionalization of the MWCNTs with nitric acid induced oxygen containing functional groups and reduced the amount of metal catalysts on the nanotubes. Since nanoparticles do not behave like solutes but rather like colloids, the applicability of the available experimental setups and procedures was evaluated for carbon nanotubes. The nanoparticles could not be injected using a sample loop or an irrigation head. Therefore, the MWCNTs were applied to the columns directly by a pump or a pipette, respectively.

The effect of the input concentration (C_o) and sand grain size on the transport and retention of MWCNTs was investigated in water-saturated sand columns at conditions unfavorable for attachment (repulsive electrostatic forces). These experiments were performed at very low C_o (0.005–1 mg L^{-1}), low ionic strength (1 mM KCl), and high flow rate (0.64 cm min^{-1}). The breakthrough curves (BTCs) for MWCNTs typically did not reach a plateau, but exhibited an asymmetric shape that slowly increased during breakthrough. The retention profiles (RPs) exhibited a hyper-exponential shape with greater retention near the column inlet. The collected BTCs and RPs were simulated using a numerical model within the HYDRUS-1D code that accounted for both time- and depth-dependent blocking functions on the retention coefficient. For a given C_o, the depth-dependent retention coefficient and the maximum solid phase concentration of MWCNTs were both found to increase with decreasing grain size. These trends reflect greater MWCNTs retention rates and a greater number of retention locations in the finer textured sand. The normalized concentration of MWCNTs in the effluent increased and the RPs became less hyper-exponential with higher C_o due to enhanced blocking/filling of retention locations. This concentration dependency of MWCNT transport increased with smaller grain size because of the effect of pore structure and the shape of MWCNTs on their retention. In particular, MWCNTs have a high aspect ratio, and it was hypothesized that MWCNTs may create a porous network with an enhanced ability to retain further MWCNTs, especially in smaller grain-sized sand and at higher C_o. Results demonstrate that model simulations should accurately account for observed behavior of both BTCs and RPs to make reliable predictions on MWCNT transport.

Investigations with more environmentally relevant conditions were conducted in water-unsaturated soil columns with undisturbed and repacked samples from two natural soils (loamy sand and silty loam) using low flow rates (0.008 cm min^{-1}). Additionally, a field lysimeter experiment was performed to provide long-term information on a larger scale. In all experiments, no breakthrough of MWCNTs was detectable and more than 85% of the applied radioactivity was recovered in the soil profiles. No significant differences were found between the determined particle concentrations and the shape of the RPs of a repacked and an undisturbed column and two different soil types. The retention profiles exhibited a hyper-exponential shape with greater retention near the column or lysimeter inlet. They were successfully simulated using a numerical model that accounted for depth-dependent retention. The high retention of MWCNTs in the soils was likely caused by the physical and chemical heterogeneity of the soils including a non-uniform pore size distribution, the low flow rate, and the water saturation degree.

In conclusion, the results of the experiments under environmentally relevant conditions (unsaturated flow, low C_o, undisturbed soil) indicated that soils may act as a strong sink for MWCNTs. Therefore, little transport of MWCNTs is likely to occur in the vadose zone, which implies a limited potential for groundwater contamination in the investigated soils. The effect of MWCNTs on the transport of environmental pollutants is an interesting topic for further research. Preliminary adsorption experiments with the organic pollutant chlordecone (CLD) on the loamy sand soil and the MWCNTs showed that CLD strongly adsorbed to both soil and MWCNTs. Thus, transport experiments should be performed to clarify the influence of MWCNTs on CLD transport.

Zusammenfassung

Das Ziel dieser Arbeit war es, fundierte Kenntnisse über den Transport und die Deposition funktionalisierter mehrwandiger Kohlenstoffnanoröhren (MWCNTs) in porösen Medien zu gewinnen. Die Verwendung radioaktiv-markierter (^{14}C) MWCNTs ermöglichte die Untersuchung sehr niedriger Konzentrationen und die Erfassung von Tiefenprofilen. Transmissionselektronenmikroskopische Aufnahmen zeigten, dass die MWCNTs äußere Durchmesser von durchschnittlich 10–50 nm und Längen von bis zu mehreren µm aufweisen. Die Funktionalisierung der MWCNTs mit konzentrierter Salpetersäure erzeugte sauerstoffhaltige funktionelle Gruppen und reduzierte den Gehalt an Metallkatalysatoren an den Nanoröhren. Da Nanopartikel sich nicht wie gelöste Stoffe sondern wie Kolloide verhalten, war es notwendig die Anwendbarkeit der vorhandenen Versuchsaufbauten für den MWCNT-Transport zu überprüfen. Der Eintrag der Partikel in die Säule mittels Probenschleife oder Beregnungskopf stellte sich als ungeeignet heraus. Aus diesem Grund wurden die MWCNTs mittels Pumpe bzw. Pipette direkt auf die Säule gegeben.

Der Einfluss der Ausgangskonzentration (C_o) und der Sand-Korngröße auf den Transport und die Deposition der MWCNTs wurde in wassergesättigten Sandsäulen untersucht. Dabei herrschten, aufgrund elektrostatischer Abstoßung, ungünstige Bedingungen für die Anlagerung der MWCNTs an die Sandoberfläche (attachment). Die Versuche wurden bei sehr niedrigen Ausgangskonzentrationen (0,005–1 mg L^{-1}), niedrigen Ionenstärken (1 mM KCl) und hohen Fließraten (0.64 cm min^{-1}) durchgeführt. Die Durchbruchskurven (BTCs) für die MWCNTs erreichten dabei kein Plateau sondern hatten eine asymmetrische Form mit einem langsamen Anstieg über die Zeit. Die Tiefenprofile (RPs) hatten eine hyper-exponentielle Form mit höherer Retention nahe dem Säuleneinlass. Die ermittelten BTCs und RPs wurden mit einem numerischen Modell innerhalb des HYDRUS-1D Codes simuliert. Dieses Modell berücksichtigte sowohl zeit- als auch tiefenabhängige „Blocking"-Funktionen des Retentionskoeffizienten. Bei gleichbleibender C_o nahmen der tiefenabhängige Retentionskoeffizient und die maximale MWCNT-Konzentration in der festen Phase mit abnehmender Korngröße zu. Dies ist die Folge von höheren Retentionsraten und einer größeren Anzahl an Retentionsplätzen in feinerem Sand. Zunehmende C_o führten zu einem Anstieg der MWCNT-Konzentration im Eluat und weniger hyper-exponentiellen Tiefenprofilen. Dieser Effekt ist auf erhöhtes „Blocking"/Auffüllen von Retentionsplätzen bei höheren Partikelkonzentrationen zurück zu führen. Diese Konzentrationsabhängigkeit des MWCNT-Transports nimmt aufgrund

des Einflusses der Porenstruktur und der Form der MWCNTs mit abnehmender Korngröße des Sandes zu. Insbesondere sind die MWCNTs in Längsrichtung deutlich größer als im Durchmesser, weshalb die Hypothese aufgestellt wurde, dass die MWCNTs ein zusätzliches poröses Netzwerk im Sand kreieren in dem weitere MWCNTs zurück gehalten werden können. Dabei wird erwartet, dass dieser Effekt in feinkörnigem Sand und bei hoher C_o besonders ausgeprägt ist. Die Ergebnisse zeigen, dass Modellsimulationen sowohl das beobachtete Verhalten der Durchbruchskurven als auch der Tiefenprofile berücksichtigen müssen, um den MWCNT-Transport verlässlich vorherzusagen.

Untersuchungen unter umweltrelevanteren Bedingungen wurden unter wasser-ungesättigten Bedingungen in ungestörten und gepackten Proben zweier natürlicher Böden (lehmiger Sand und schluffiger Lehm) bei niedrigen Fließraten (0,008 cm min^{-1}) durchgeführt. Zusätzlich sollte ein Feldlysimeterversuch Informationen über das Langzeitverhalten der MWCNTs auf einer größeren Skala liefern. In keinem der Versuche waren MWCNTs im Eluat messbar und mehr als 85% der Radioaktivität wurden im Tiefenprofil nachgewiesen. Dabei wurden keine signifikanten Unterschiede in den gemessenen Partikelkonzentrationen und den Tiefenprofilen zwischen gestörtem und ungestörtem Boden sowie den beiden Bodentypen gefunden. Die Tiefenprofile waren hyper-exponentiell mit höherer Retention nahe des Säulen- bzw. Lysimetereinlasses und wurden erfolgreich mit einem numerischen Model simuliert das tiefenabhängige Retention annimmt. Die hohe Retention der MWCNTs in den Böden war vermutlich bedingt durch die physikalische und chemische Heterogenität der Böden (z.B. ungleichmäßige Porengrößenverteilung), die niedrige Fließrate und den Wassersättigungsgrad.

Insgesamt lassen die Resultate der umweltrelevanten Versuche (ungesättigter Fluss, niedrige C_o, ungestörter Boden) vermuten, dass Böden als starke Senke für MWCNTs fungieren. Daher wird nur ein geringer Transport der MWCNTs in der vadosen Zone und damit eine geringe Gefahr der Grundwasserkontamination in den untersuchten Böden erwartet. Überdies ist der Einfluss der MWCNTs auf den Transport von Umweltschadstoffen ein interessantes Thema für weitere Untersuchungen. Erste Adsorptionsversuche mit dem organischen Schadstoff Chlordecon (CLD) an lehmigen Sandboden und MWCNTs zeigten eine starke Adsorption von CLD an beide Adsorbenzien. Basierend darauf sind Transportversuche notwendig um den Einfluss der MWCNTs auf den CLD-Transport zu klären.

Table of contents

1. Introduction

Nanotechnology is a relatively new and rapidly developing area of industrial production and scientific research (Farré et al., 2009). Within this field of interest, nanoparticles (NPs) have gained more and more attention because of the increasing ability to synthesize, modify, and use these materials (Nowack and Bucheli, 2007). In addition, concerns about their potential health effects have risen. Nanoparticles exhibit special physico-chemical properties caused by their small size and the fact that 40–50% of the atoms reside on the NP's surface (Farré et al., 2009; Nel et al., 2006). The term nanoparticle is not strictly defined, but among researchers there is a consensus that particles with at least one dimension smaller than 100 nm are called nanoparticles regardless of their chemical composition (Klaine et al., 2008; Nowack and Bucheli, 2007; Wiesner et al., 2006). In general, there are various types of nanoparticles with differences in their chemical compositions and structures, e.g., silver NPs, titanium dioxide NPs, nano zerovalent iron, fullerenes, and carbon nanotubes. Considering the increasing use of synthetic NPs in industrial and household applications, there is no doubt that they can be released into the environment (Boxall, 2007; Lecoanet et al., 2004). Thus, besides studies on ecotoxicity, profound information on the environmental fate of engineered NPs is needed. This thesis is focusing on the transport and deposition of carbon nanotubes because they are one of the most commonly used engineered nanoparticles (Tian et al., 2012) and their production and commercial use are rising continuously (Zhang et al., 2011).

1.1 Carbon nanotubes

Carbon nanotubes (CNTs) are a relatively new class of nanoparticles. The first public description of their synthesis was in 1991 (Iijima, 1991). Later, CNTs were found in the melt water of a 10,000 year old Greenland ice core indicating that they are airborne materials of natural origin and also present in the contemporary air (Murr et al., 2004). Nevertheless, especially engineered CNTs are of interest because their annual global production is above several thousand tons (De Volder et al., 2013).

Properties

Two types of CNTs (Figure 1) are most commonly distinguished and produced: single-walled carbon nanotubes (SWCNTs, Figure 1a) are individual graphene tubes and multi-walled carbon nanotubes (MWCNTs, Figure 1b) are tubes within tubes consisting of more than two carbon walls (Sinnott, 2002). In the following, the abbreviation CNTs includes both SWCNTs and MWCNTs.

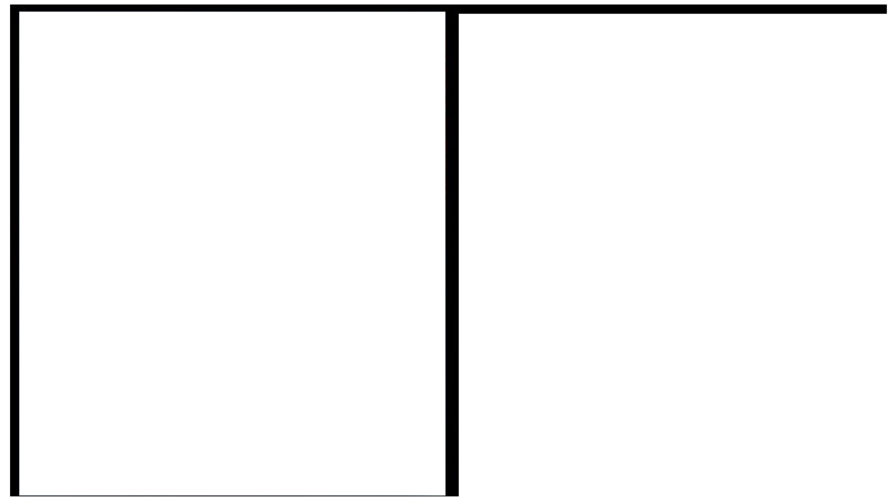

Figure 1. Schematic illustrations of a single-walled carbon nanotube (a) and a multi-walled carbon nanotube (b). Reprinted from Pillay (2012).

In contrast to the majority of known nanoparticles, CNTs are not spherical, but needle-shaped particles (Iijima, 1991; Mauter and Elimelech, 2008). With diameters between 10 and 50 nm and lengths of up to several µm, CNTs exhibit a high aspect ratio (Jaisi et al., 2008; Petersen et al., 2011) and a high strength-to-weight ratio (Maynard, 2007). In principle, CNTs are rolled up graphene sheets composed of sp^2 carbon atoms arranged in fused benzene rings (Mauter and Elimelech, 2008; Petersen et al., 2011). Carbon nanotubes exhibit characteristic electronic, chemical, and physical properties (Liu et al., 2009; Mattison et al., 2011), e.g., excellent thermal and electrical conductivities (Maynard, 2007). They also significantly increase modulus and strength of plastics (Baughman et al., 2002). Furthermore, CNTs act as strong adsorbents for organic pollutants (Chen et al., 2007; Li et al., 2012a; Lu et al., 2005; Peng et al., 2003).

Synthesis

To date, there are several methods for CNTs synthesis available (e.g., arc-discharge evaporation, catalytic chemical vapor deposition, pulsed laser vaporization of graphite, and high-pressure CO decomposition). The most common procedure is the catalytic chemical vapor deposition (De Volder et al., 2013; Jorio et al., 2008) although all of these methods involve high temperatures and often result in substantial metal impurities (Baughman et al., 2002). These residual metal catalyst particles (e.g., Co, Fe, Ni) may influence the properties of CNTs like sorption of organic chemicals, electrical conductivity, and toxic potential (Hull et al., 2009; Li et al., 2012a; Pumera, 2007).

Modification

In general, carbon nanotubes are very hydrophobic and aqueous suspensions can only be stabilized by adding dispersing agents (e.g., surfactants or polymers) or by modification/functionalization of CNTs (Batley et al., 2012; Jiang et al., 2003; Tian et al., 2010). Polymer-functionalization for example enables the embedding of CNTs into nanocomposites (Sun et al., 2002) and oxidation with strong acids (e.g., nitric acid) enhances the stability of CNTs in aqueous suspensions due to the introduction of functional groups (Smith et al., 2009; Sun et al., 2002). These acid treatments also remove metal impurities but can cause other impurities and shortening of CNTs (Baughman et al., 2002). In addition, the application of a strong physical force, e.g., sonication, is needed to separate CNT agglomerates and to produce homogeneous dispersions (Mauter and Elimelech, 2008).

Applications

To date, CNTs are used in numerous commercial applications: as filler material in various nanocomposites, e.g., for sport products, antistatic coatings or aerospace and automotive applications (De Volder et al., 2013; Hussain et al., 2006; Sangermano et al., 2008; Schlagenhauf et al., 2012; Sun et al., 2002), in solar cells, field emitter displays, and as catalysts converting endothermic reactions to exothermic which reduces the temperature and improves the selectivity of the reaction (Mauter and Elimelech, 2008). Additionally, numerous potential applications for CNTs including conductive and high-strength composites, energy storage and energy conversion devices, sensors, radiation sources, hydrogen storage media, semiconductor devices, probes, and interconnects have been proposed (Hussain et al., 2006). Furthermore, CNTs were considered for a variety of bio-applications (Sun et al., 2002). Jorio et al. (2008) number the total market share of carbon-fiber composites to nearly one billion US dollars subdivided into 70% aerospace, 18% sporting goods, 7% industrial equipment, 2% marine, and 3% miscellaneous.

Carbon nanotubes are also prospects as adsorbents in water filtration membranes (e.g., desalination membranes) (Mauter and Elimelech, 2008). Considering their high sorption capacity for metal ions, radionuclides, and organic compounds, CNTs could also be used for soil and groundwater remediation (Pan and Xing, 2012). Due to their high aspect ratio, large accessible surface area, and well developed mesopores, CNTs possess the potential to adsorb bacterial pathogens, natural organic matter, and cyanobacterial toxins from water, making CNTs interesting for drinking water purification (Upadhyayula et al., 2009). But this use has not yet been considered for large scale applications because of its high costs and the risk of CNT release into the environment (Upadhyayula et al., 2009). Up to now, disposal and reuse procedures for CNTs are not available but required (De Volder et al., 2013).

Risks

This widespread use and a lack of regulations for CNT disposal can undoubtedly result in their release into the environment, especially into soils and waters (Jaisi and Elimelech, 2009; Klaine et al., 2008; Köhler et al., 2008; Nowack and Bucheli, 2007). Therefore, it is essential to investigate the ecotoxicity and environmental fate of CNTs.

Several studies provide information on the environmental risks of CNTs, but there is still a lack of knowledge especially concerning their ecotoxicity (Eckelman et al., 2012). The ecotoxicity of CNTs may depend on their concentration, size, shape, functionalization, the amount and location of metal impurities, and the exposure medium (e.g., soil, sediment, or water). Kang et al. (2008) demonstrated that SWCNTs exhibited significantly greater toxic effects towards bacteria than MWCNTs. Furthermore, modification of CNTs may also result in more reactive and thus more toxic particles (Simon-Deckers et al., 2009). Simon-Deckers et al. (2009) also state that the toxicity of MWCNTs towards bacteria was independent of their purity. They found a bactericidal effect of both purified and iron containing MWCNTs on a specific strain of *Escherichia coli* due to damage of the cell membrane and hypothesize that the location of metal impurities (e.g., inside the tubes) affects their ecotoxicity (Simon-Deckers et al., 2009). Another study showed that metal impurities released from carbon nanomaterials exhibited toxic effects towards different aquatic organisms (Hull et al., 2009).

Some studies revealed that there was no acute toxicity and negligible absorption of SWCNTs and MWCNTs spiked to soil or sediments into the cellular tissues of oligochaetes (Petersen et al., 2008b), two estuarine invertebrates (Ferguson et al., 2008;

Petersen et al., 2010), an earth worm (Petersen et al., 2008a), and a lugworm (Galloway et al., 2010). For MWCNTs dispersed in water only, Petersen et al. (2009a) found accumulation in the gut of a water flea but no absorption into cellular tissues. Direct exposure of CNTs via intratracheal instillation or subcutaneous implantation caused toxic effects to rats, mice, and guinea pigs (Grubek-Jaworska et al., 2006; Koyama et al., 2006; Lam et al., 2004; Warheit et al., 2004). Another study reported toxic effects of SWCNTs dispersed in water to rainbow trout (Smith et al., 2007) and an estuarine copepod (Templeton et al., 2006). Schäffer et al. (2011) found an incorporation of MWCNTs by algae, daphnia, fish, and benthic worms after exposure to contaminated medium. The MWCNTs were also found in the cells of the organisms and were mostly, but not completely, removed when the organisms were transferred to MWCNTs free medium (Schäffer et al., 2011).

At high concentrations, CNTs were found to cause growth inhibition of green algae due to shading and agglomeration of cells with CNTs (Schwab et al., 2011). In addition, MWCNTs can absorb to the root surfaces of rice plants and may thus constrain uptake of water and nutrients (Lin et al., 2009). In contrast, another study revealed that MWCNTs promoted germination of tomato seeds and referred this to penetration of MWCNTs into the seeds leading to enhanced water uptake (Khodakovskaya et al., 2009). In conclusion, these studies are somehow contradictory and further information on the ecotoxicological effects of CNTs, especially at realistic exposure scenarios, is needed.

Carbon nanotubes and the environment

There is no doubt that MWCNTs, and engineered NPs in general, can finally be released to the environment through point sources (e.g., production facilities, landfills, or wastewater treatment plants), nonpoint sources (abrasion of materials containing MWCNTs), accidental release (e.g., during transport), or intentional release (e.g., for groundwater remediation) (Jaisi and Elimelech, 2009; Köhler et al., 2008; Nowack and Bucheli, 2007; Pan and Xing, 2012).

In general, the environmental behavior of nanoparticles is highly controlled by their colloidal stability. Aggregation leads to larger particles that are trapped in pore spaces or settled through sedimentation (Nowack and Bucheli, 2007). Thus, it is more likely that single particles and small aggregates enter the groundwater compared to large aggregates. Therefore, stabilization of nanoparticles is a key factor controlling their environmental fate. Functionalized CNTs are of special interest because the modification does not only increase their stability in aqueous suspensions but also increase their mobility in the environment (Mattison et al., 2011). Finally, CNTs can be released as agglomerates or as individual particles. Recently, the release of free-standing individual CNTs from CNT-embedded nanocomposites was demonstrated (Schlagenhauf et al., 2012).

Interaction with organic pollutants

Since organic pollutants tend to adsorb onto CNTs (Chen et al., 2007; Li et al., 2012a; Lu et al., 2005; Peng et al., 2003), CNTs may affect the fate and mobility of these chemicals in natural environments. Adsorption of organic pollutants onto CNTs may decrease their bioavailability (Petersen et al., 2009b) and decrease toxic effects to organisms. Nevertheless, a CNT-facilitated transport (co-transport) of organic pollutants could lead to enhanced migration of contaminants (Cheng et al., 2005) and increase the risk of groundwater contamination. After long periods of agricultural use, pollutants adsorbed to soils may be remobilized by CNTs introduced to this soil. Chlordecone (CLD), for example, is an organochlorine pesticide and was frequently applied from 1972 to 1993 in large amounts to banana plantations in the French West Indies resulting in a long-term contamination of soils with this persistent organic pollutant (Levillain et al., 2012). Because of the high sorption capacity of CNTs, it is possible that the CLD might be remobilized or even more immobilized in these soils in the presence of CNTs. Therefore, simultaneous investigations of CNTs and diverse emerging organic pollutants in porous media are necessary in order to evaluate the co-dependencies.

Transformation

So far, CNTs were believed to be one of the most biologically non-degradable man-made materials (Lam et al., 2004). But recently, degradation in the presence of horseradish peroxidase and myeloperoxidase, respectively, was proven (Som et al., 2011). Thus, a transformation of CNTs in the environment might also be possible and may affect their properties, fate, persistency, bioavailability, and ecotoxicity (Som et al., 2011). In fact, the CNTs were significantly shortened during the degradation process (Russier et al., 2011) which may influence their transport behavior. In addition, Liu et al. (2010) found that degradation of CNTs depends on their surface functionalization: carboxyl functionalized CNTs were shortened and transformed into ultrafine carbonaceous debris whereas unmodified, ozone-treated, and aryl-sulfonated CNTs were not degradable.

To assess potential risks to the environment, it is important to gain knowledge on the environmental fate of CNTs. However, the fate and effects of CNTs in the environment are still not well understood (Saleh et al., 2008). The transport of CNTs through porous media is therefore of considerable interest regarding potential risks to organisms and human health (Mattison et al., 2011). Thus, information on transport and deposition of (functionalized) CNTs in porous media, especially undisturbed soils, is needed.

1.2 Transport of carbon nanotubes in porous media

To date, there are numerous studies available reporting on CNT transport in different porous media and its sensitivity to a diversity of experimental conditions including ionic strength (IS), pore water velocity, and collector grain size (Jaisi and Elimelech, 2009; Jaisi et al., 2008; Liu et al., 2009; Mattison et al., 2011; Tian et al., 2010; Tian et al., 2012). Despite this research, transport and retention processes for CNTs are still not completely understood (Mattison et al., 2011). The following chapters summarize the most important research results and knowledge gaps.

1.2.1 Transport at water-saturated conditions

Several of the aforementioned studies were addressed to the transport of SWCNTs and MWCNTs in packed sand columns under water-saturated conditions. In general, the mobility of stabilized particles will be higher compared to non-stabilized ones and the stability strongly depends on the solution chemistry. Jaisi al. (2008) showed that SWCNT deposition due to filtration decreased with decreasing ionic strength, decreasing valence of the ions, and the presence of humic acid. The stabilizing effect of natural organic matter was reported (Hyung et al., 2006) for aqueous CNTs suspensions and Wang et al. (2008) also found enhanced mobility of CNTs in porous media when the particles were coated with humic acid. Furthermore, SWCNTs stabilized with sodium dodecylbenzenesulfonate (SDBS) exhibited high mobility in water-saturated quartz sand when the columns were flushed with SDBS (Tian et al., 2010; Tian et al., 2011).

The effect of the flow rate on MWCNT transport was investigated by Liu et al. (2009). They reported that the transport of MWCNTs decreased significantly with decreasing flow rate and that including a blocking term into the model significantly improved the fit of the normalized effluent concentration which slowly increased with time. The importance of blocking for MWCNT retention was also stated by Mattison et al. (2011) together with a reduction of MWCNT transport with decreasing collector grain size.

The chemical composition of the porous media also affects the transport of MWCNTs. Tian et al. (2012) proposed a high importance of the surface charge on collector grains and CNTs. They state that functionalized CNTs will be strongly retained in natural porous media containing high amounts of positively charged metal oxihydroxides due to the negatively charged carboxylic groups.

The effect of particle shape and size was also investigated for CNTs. One of the first publications compared the transport of needle-shaped SWCNTs and spherical fullerol NPs (Lecoanet et al., 2004). They found a high breakthrough of SWCNTs which occurred faster than for fullerol and referred this to an alignment of the SWCNTs and thus lengthwise transport through the pores (Lecoanet and Wiesner, 2004). In addition, Wang et al. (2012b) demonstrated that retention was higher for MWCNTs with lengths greater than 8 µm compared to shorter MWCNTs. O'Carroll et al. (2013) referred lower mobility of MWCNTs with smaller diameter compared to those with larger diameters to enhanced Brownian motion and thus more collisions.

All of the above mentioned studies determined a certain mobility of CNTs in quartz sand in dependence of the ambient conditions. But none of these studies considered the effect of CNT input concentration on their transport behavior. Furthermore, the CNT input concentrations investigated so far were more than nine orders of magnitude higher than it was estimated for most environmentally relevant scenarios (Gottschalk et al., 2009). This is an important aspect to consider because the input concentration has been demonstrated to significantly influence colloid deposition (Bradford and Bettahar, 2006; Bradford et al., 2009) and this concentration effect was also found to depend on the grain size (Bradford and Bettahar, 2006). In general, transport studies at low CNT concentrations are of interest for fundamental research because initial model estimates predict very low CNT concentrations in soils in the range of several ng kg^{-1} (Gottschalk et al., 2009; Mueller and Nowack, 2008). Although one has to consider that environmental concentrations of CNTs will depend on their source and on hydro-geochemical conditions. However, recent studies only investigated input concentrations significantly higher than 1 mg L^{-1} (Jaisi and Elimelech, 2009; Jaisi et al., 2008; Liu et al., 2009; Mattison et al., 2011; Tian et al., 2010; Tian et al., 2012).

In addition, most of the studies on CNT mobility did not determine retention profiles (RPs), but only breakthrough curves (BTCs). Thus, information on retention profiles for CNTs is still very scarce (Wang et al., 2012b), although retention profiles provide needed information on the mass balance and give useful insight on the controlling mechanisms of retention (Bradford and Bettahar, 2005). Furthermore, breakthrough curves and retention profiles both need to be accurately simulated by numerical models in order to reliably predict environmental fate and risk of colloids (Bradford et al., 2003).

Columns filled with quartz sand serve as simplified model systems for investigations of fate and mobility of colloids or chemicals. Nevertheless, investigations of natural porous media, like undisturbed soil, are necessary. To date, the transport of CNTs in field soils has received very limited attention (Fang et al., 2013; Jaisi and Elimelech, 2009). One of the first studies available on SWCNTs transport in repacked soil under water-saturated conditions only used a part of the sand fraction (420–1000 µm) of this soil (Jaisi and Elimelech, 2009). They observed only little breakthrough of functionalized SWCNTs and concluded that straining was a major reason for the enhanced retention of SWCNTs in soil.

In general, soil is expected to be a more important sink for nanoparticles than sand because its chemical composition and pore size distribution are more heterogeneous (Pan and Xing, 2012). However, preferential flow paths in soils (e.g., root or earthworm channels) (Camobreco et al., 1996) and natural organic matter dissolved in pore water (Jaisi and Elimelech, 2009) may enhance transport through the vadose zone. Undisturbed soil cores and lysimeter are therefore much closer to environmental conditions than packed sand columns. Up to now, there was no study found on the transport and retention of MWCNTs in undisturbed soil cores or lysimeter.

1.2.2 Transport at water-unsaturated conditions

To get closer to environmental conditions, transport processes under unsaturated conditions have to be considered. These are much more complex than processes in saturated porous media because of the presence of the air phase (Gargiulo et al., 2007b; Tian et al., 2011). In unsaturated porous media, higher retention is expected and retention mechanisms can differ to some extent compared to water-saturated conditions. More details on transport mechanisms operating under water-unsaturated conditions can be found in Chapter 2.2. Since unsaturated conditions are present in the vadose zone, it is important to gain knowledge on the mobility of colloids and NPs in unsaturated porous media in order to assess the risk of groundwater contamination. Unfortunately, information on CNT transport in water-unsaturated porous media is very rare (Tian et al., 2011). In line with the literature review for this thesis, there was only one study found on the transport of CNTs in unsaturated quartz sand. Tian et al. (2011) used SDBS-dispersed SWCNTs and reported high mobility in three different sized sands. They also stated that no attachment to the air-water interface took place in the presence of surfactants and that retention only occurred at water contents < 0.1. Since SDBS solution is not expected to be present in natural environments, studies at more realistic scenarios are required.

1.3 Chlordecone

Chlordecone (CLD, Figure 2) is a very stable molecule, with low water solubility and a very low volatility. It is one of the most persistent organochlorine pesticides (Cabidoche and Lesueur-Jannoyer, 2012) and is very hydrophobic. CLD strongly adsorbs onto natural organic matter (high K_{oc}) (Cabidoche and Lesueur-Jannoyer, 2012). Almost 20 years after the prohibition of CLD, soils, fresh and coastal waters, aquatic biota, and crops in the French West Indies are still contaminated due to its long-term application in the 1970s and 80s (Cabidoche and Lesueur-Jannoyer, 2012).

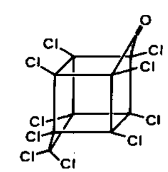

Figure 2. Molecular structure of chlordecone. Reprinted from Hammond et al. (1979).

The insecticide was highly retained in soils of the area of application, though the persistence was found to depend on the soil type. Cabidoche et al. (2009) projected centuries up to a millennium for the remediation of contaminated soils through lixiviation. Cabidoche and Lesueur-Jannoyer (2012) showed that soil contamination resulted in an uptake of CLD by crops, the magnitude depending on the type of soil and crop. They state that accumulation in the plants was too low to consider them for phytoremediation but high enough to affect food production. Due to its high hydrophobicity, CLD tends to bioaccumulate along the food chain (Coat et al., 2006). In the French West Indies, a high CLD contamination of various wild and farmed aqueous species was found indicating that the main route of contamination for humans is food (Coat et al., 2006). As mentioned in Chapter 1.1, CNTs act as strong adsorbents for organic chemicals and because of its structure and properties, CLD is expected to highly adsorb onto CNTs.

1.4 Objectives and outline of the thesis

The aim of this study was to provide new insights into the environmental behavior and fate of functionalized MWCNTs by investigating their transport and retention in saturated and unsaturated porous media. In contrast to the respective literature, this study investigated the transport of MWCNTs at very low, environmentally relevant concentrations.

– **Characterization of carbon nanotubes.** Since the physico-chemical properties of nanoparticles influence their colloid stability and thus their mobility, the characterization of functionalized MWCNTs prior to transport experiments was important (Chapter 4.1) in order to obtain information on these parameters.

– **Transport and retention of multi-walled carbon nanotubes in saturated porous media.** Evaluating the effect of input concentration and grain size on the transport of MWCNTs in water-saturated quartz sand columns was one important objective of this study (Chapter 4.2). In addition, this study intended to provide new essential information on MWCNT deposition by determining retention profiles in addition to the breakthrough curves. The numerical modeling of the retention profiles and the breakthrough curves provides information on MWCNT mass balance and retention mechanisms. Finally, this study highlights the importance of considering input concentration and retention profiles for the reliable prediction of MWCNT transport and fate.

– **Transport of carbon nanotubes in natural soils.** Another goal was to work on scenarios that were more environmentally relevant compared to other studies, e.g., undisturbed soil, unsaturated conditions, and low flow rates. To date, only a few studies have reported on CNT transport under unsaturated conditions and in (undisturbed) soils, respectively. This study aimed to improve our knowledge of the transport and retention of MWCNTs in natural undisturbed soils, particularly under water-unsaturated conditions (Chapter 4.3). This includes a comparison of two soil types (silty loam and loamy sand) in laboratory column experiments and a field lysimeter study.

2. Theoretical background

In order to understand the processes underlying MWCNT transport, some theoretical background knowledge is inevitable. Since nanoparticles behave basically like colloids, understanding of colloidal processes is also important to understand the environmental fate and risk of nanoparticles (Pan and Xing, 2012). The most important theories for the observed behavior of MWCNTs are summarized in this chapter.

2.1 Stability of colloids

The transport of colloids strongly depends on the stability of their suspensions because aggregation results in increased particle sizes and thus enhanced deposition (Grassian, 2008). In general, the aggregation/deposition of NPs is controlled by interactions between particles themselves as well as between particles and collector surfaces (Petosa et al., 2010). Normally, the surfaces of colloids in aqueous suspension are charged and therefore attract the counter ions of the liquid which form an electric double layer around the particle (Grassian, 2008). This electric double layer consists of a layer strongly associated with the surface, the Stern layer and a diffusive layer (Yates et al., 1974). The Derjaguin–Landau–Verwey–Overbeek (DLVO) theory describes the stability of a suspension by calculating the total interaction energy (Van Eerdenbrugh et al., 2008). The total interaction energy is the sum of repulsive (electrostatic double-layer interactions) and attractive forces (van der Waals forces) impacting a nanoparticle when converging another particle or a collector surface (Petosa et al., 2010).

Figure 3 shows the repulsive and attractive forces as well as the resulting total interaction energy as a function of distance between interacting particles or particles and surfaces. If repulsive forces are dominating, the interaction energy shows positive values and the suspension is stable. In case of dominating attractive forces, the DLVO model contains a primary and a secondary minimum separated by an energy barrier. The energy barrier controls particle aggregation by its height (Petosa et al., 2010).

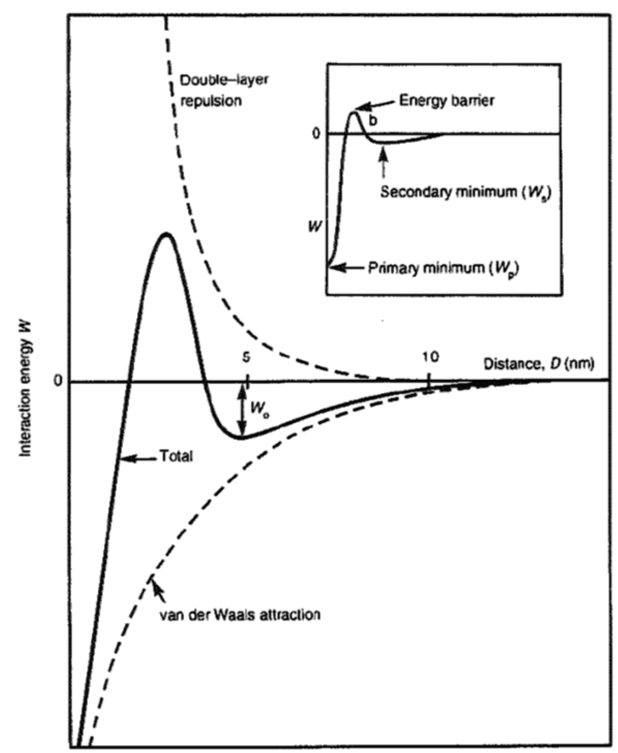

Figure 3. Illustration of the classical DLVO theory with definitions for critical points on the curve, where W_o is the depth of the potential energy minimum. Reprinted from Waychunas (2001).

The electrical potential at the boundary between the Stern and the diffusive layer is the so called Zeta potential. It has a strong influence on the stability and mobility of colloids in suspensions and in porous media, respectively and it depends strongly on the physico-chemical conditions (e.g., ionic strength and pH) of the system (Grassian, 2008). At low ionic strengths, the repulsion between particles and collectors is large because they are surrounded by thick diffusive layers and deposition takes place only in the secondary minimum (Franchi and O'Melia, 2003). Increasing ionic strength will lead to a compression of the electrical double layer of both particles and sand grains, resulting in a higher particle aggregation and deposition because repulsive interactions, the energy barrier, and the zeta potential are reduced (Franchi and O'Melia, 2003; Vecchia et al., 2009). The critical coagulation concentration is an important characteristic of colloid suspensions and is defined as the minimum salt concentration at which the energy barrier will fall into the negative range and the particles start to aggregate (Hsu and Liu, 1998;

Waychunas, 2001). Since the DLVO theory was originally developed for spherical particles, it has its limitations for CNTs (Tian et al., 2011) and there is, to my knowledge, no theory available for tubular-shaped particles.

In summary, a NP suspension is unstable when the total free energy of the system decreases and the particles aggregate (Wiesner and Bottero, 2007). Because of their small size, NPs are expected to be less stable compared to colloids and thus, less mobile (Grassian, 2008). This makes the transport of nanoparticles more complex than for microscale particles (Lin et al., 2010).

2.2 Transport of colloids

Transport of colloids is mainly controlled by the physico-chemical processes of interception, Brownian diffusion, and sedimentation (Lin et al., 2010). The contact between colloids in the fluid streamlines and the collector grains is called interception (Grassian, 2008). Sedimentation occurs when the density of the colloids exceeds the density of the fluid and the colloids move vertically out of the streamlines and towards the collector grains (Grassian, 2008). Brownian motion is the thermal enhanced random motion of (small) particles (Grassian, 2008). In addition, NPs can be physically retained by pore straining which is the deposition of particles or aggregates in pores too small for them to pass (Lin et al., 2010). These processes are illustrated in Figure 4 for spherical particles.

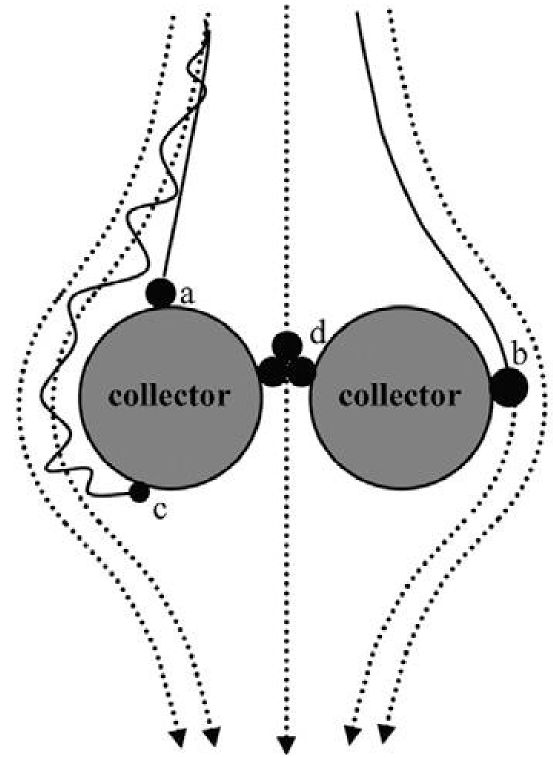

Figure 4. Scheme of filtration mechanisms of colloids (small black spheres) in porous media. The dotted lines represent the fluid streamlines and the black lines the particle paths. Colloids can attach to the collector through gravitational sedimentation (a), interception (b), and Brownian diffusion (c). Large particles or aggregates may be physically retained by small pores (straining, d). Reprinted from Lin et al. (2010).

Because of their small size, the dominant mechanism of NP transport is supposed to be diffusion (Lin et al., 2010). The high diffusivity of NPs increases the number of collisions with the collector grains and enhances aggregation (Lin et al., 2010). The filtration of particles by the porous medium is mainly controlled by physico-chemical colloidal interactions between particles and surfaces which is influenced by the solution chemistry (e.g., pH, ionic strength, organic carbon content), particle size, fluid velocity, collector grain size, and water temperature (Lin et al., 2010). Nevertheless, the shape of nanoparticles and colloids also strongly influences their stability and transport (Pan and Xing, 2012).

2.2.1 Transport processes in saturated porous media

Since saturated porous media consist of a water phase and a solid phase, particles can be present in the water phase and at the solid-water interface and their mobility is influenced by particle-particle and particle-solid interactions (Grassian, 2008). The main mechanisms for colloid removal from the water phase are solid-water interface attachment and pore straining (Grassian, 2008). Attachment is the fixation of colloids after collision with collector grains (Bradford et al., 2004) and is controlled by the physico-chemical processes described in Chaper 2.2 and in Figure 4. In general, particles with a surface charge opposite to the porous media will have low mobility because they will be attracted by the surfaces (Grassian, 2008). At conditions unfavorable for attachment (dominating repulsive forces), pore straining is the major mechanism for colloid retention in porous media and is controlled by the particle size and the pore size distribution (Grassian, 2008).

2.2.2 Transport processes in unsaturated porous media

In unsaturated porous media, the presence of a third phase, the air phase, is expected to limit transport and to make transport processes more complicated compared to saturated conditions because additional retention mechanisms are operating (Gargiulo et al., 2007b). The following mechanisms of colloid retention occur in unsaturated porous media: attachment to the solid-water and the air-water interface, pore straining, and film-straining (Torkzaban et al., 2008). Pore straining can be enhanced compared to saturated conditions because large pores are already drained in unsaturated porous media and thus not accessible. In partially water-saturated porous media, thin water films are formed around the grain surfaces and influence the particle transport. If the water film is thick enough compared to the particle size, the colloids will not attach to the collector grains and be transported to deeper layers. If the colloid size exceeds the water film thickness, particles are retained by the so called film-straining (Wan and Tokunaga, 1997).

2.3 Colloid filtration theory

The classical colloid filtration theory (CFT) is a very common approach to help understanding and predicting the transport of colloids, bacteria, and nanoparticles in porous media (Lin et al., 2010; Nelson and Ginn, 2005). It is based on the attachment of colloids to the solid-water interface of a single spherical grain collector and neglects the influence of pore structure (Bradford et al., 2006). The CFT includes a first-order attachment coefficient to describe a spatially constant deposition and allows the numerical modeling of exponential retention profiles (Bradford et al., 2006).

The CFT is based on the one-dimensional advection-dispersion equation (ADE) with terms for one site kinetic retention and a total mass balance defined as (Harvey and Garabedian, 1991):

$$\theta \frac{\partial C}{\partial t} + \rho \frac{\partial S}{\partial t} = D\theta \frac{\partial^2 C}{\partial x^2} - q\theta \left(\frac{\partial C}{\partial x} + kC \right) \tag{1}$$

where θ [-] is the volumetric water content, ρ [ML^{-3}, where M and L denote units of mass and length, respectively] is the bulk density of the porous media, t [T; T denotes units of time] is the time, x [L] is the spatial coordinate, q [LT^{-1}] is the flow rate, C [N_cL^{-3}, where N_c is the number of particles] is the particle concentration in the aqueous phase, S [N_cM^{-1}] is the solid phase particle concentration, D [L^2T^{-1}] is the hydrodynamic dispersion coefficient, and k [-] is the attachment coefficient.

The attachment coefficient, k is given as (Bradford et al., 2006):

$$k = \frac{3(1-\theta)q}{2d_c} \eta \alpha q \tag{2}$$

where d_c [L] is the mean diameter of the collector grains, η is the experimentally determined single collector efficiency, more precisely the frequency of contact between particles and the solid phase, and α [-] is the sticking efficiency (the quantification of actual attachment of colloids on collector grains) (Nelson and Ginn, 2005). In general, the CFT defines the theoretical single collector efficiency as sum of the contact efficiencies due to interception, sedimentation, and diffusion (Liu et al., 2009).

Unfortunately, the CFT cannot fully explain observed transport behavior of nanoparticles because it is basically valid for favorable attachment conditions and different mechanisms are operative under conditions that are unfavorable for attachment (Bradford et al., 2006). The CFT is specially limited for particles with a high aspect ratio because it assumes collectors and colloids to be spherical (Liu et al., 2009). Since the collision efficiency of colloids increases with increasing aspect ratio (Salerno et al., 2006), not only the processes covered by CFT (e.g., gravitational sedimentation, Brownian diffusion and interception) but additional physical processes are important (Pan and Xing, 2012) to understand the transport of nanoparticles.

2.4 Extension of colloid filtration theory

It is known that the CFT has some limitations (Bradford et al., 2004). For example, it cannot describe a tailing of the breakthrough curve (Mattison et al., 2011) or a hyper-exponential shape of the retention profile (Bradford and Bettahar, 2006). Therefore, it is necessary to extend the CFT by further mechanisms controlling colloid transport in porous media (Bradford et al., 2003). The numerical simulations are more accurate when further processes of colloid/nanoparticle transport and retention are included but the mathematical model will become more complex (Pan and Xing, 2012). Therefore, only the most important model assumptions for the study presented in this thesis are summarized in this chapter.

The solid phase particle mass balance equation corresponding to the above described ADE is given as (Gargiulo et al., 2007a):

$$\rho \frac{\partial S}{\partial t} = \theta k_1 \psi C - k_2 \rho S \qquad (3)$$

where k_1 [T^{-1}] is the first-order retention coefficient, k_2 [T^{-1}] is the first-order detachment coefficient, and ψ [-] is a dimensionless function to account for time and depth- dependent retention. When ψ is equal to 1, the CFT, assuming only attachment and detachment, applies. In general, tailing of the BTC is a hint for detachment (Mattison et al., 2011).

2.4.1 Straining

As mentioned in Chapter 2.2, straining (Figure 4) is the retention of larger particles or aggregates in smaller or dead-end pores (Lin et al., 2010). It is especially important at unfavorable attachment conditions and can explain some of the limitations known for CFT (Bradford et al., 2006). Straining is an important process governing NP retention in quartz sand and soil under water-saturated conditions (Jaisi and Elimelech, 2009; Mattison et al., 2011). Straining of spherical colloids increases with decreasing water content and decreases with increasing flow rate (Torkzaban et al., 2008).

To mathematically describe pore straining, a depth-dependent retention function is included into the model with the parameter ψ of Equation 3 given as (Bradford et al., 2003):

$$\psi_1 = \left(\frac{d_c + x}{d_c}\right)^{-\beta} \tag{4}$$

where d_c [L] is the median diameter of the sand grains and β [-] is an empirical variable that controls the shape of the retention profile. This assumption helps to describe retention profiles of hyper-exponential shape (Bradford and Bettahar, 2006).

2.4.2 Blocking

Another important mechanism influencing NP transport is site-blocking (Figure 5) which assumes a finite number of retention locations of the porous media (Liu et al., 2009; Mattison et al., 2011). The effect of blocking is that the retention of particles decreases with time due to a decreasing number of available attachment sites. Extension of the CFT by a site-blocking term allows a reasonable fit of experimental BTCs where the normalized effluent concentration does not reach a plateau (Liu et al., 2009; Mattison et al., 2011).

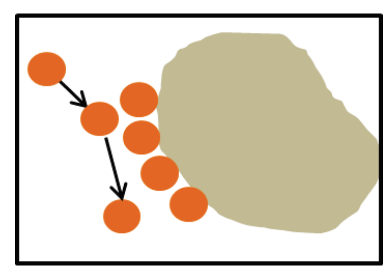

Figure 5. Schematic display of colloid blocking in porous media. The spherical colloids (orange) attach to the collector's surface and block the retention positions for further particles resulting in an increase of particle breakthrough with time.

To include the blocking function into the numerical model, the parameter ψ of Equation 3 is given as (Gargiulo et al., 2007a):

$$\psi_2 = \left(1 - \frac{S}{S_{max}}\right) \tag{5}$$

where S_{max} [N_cM^{-1}] is the maximum solid phase particle concentration as an exponential function of the specific surface area of collectors grains (Mattison et al., 2011). The blocking function is particularly useful in describing a reduction in MWCNT retardation when the normalized effluent concentration of particles (C/C_o) slowly increases with time (Mattison et al., 2011). This means, when S approaches S_{max}, the blocking function will become zero indicating that all retention locations are filled and C/C_o will increase towards 1 (Mattison et al., 2011).

2.5 Adsorption theory

Adsorption describes the association of a dissolved compound (adsorbate) onto a solid phase (adsorbent) (Li, 2011). In general, the adsorption process is characterized by adsorption isotherms showing the ratio between the adsorbed and the dissolved amount of the adsorbate (Allen et al., 2004). In order to reveal the underlying sorption process, these sorption isotherms can be described by different models. The most important models are summarized below.

Linear model

The linear model is the simplest model describing adsorption and is based on Henry's law. It assumes that the amount of adsorbate on the solid phase is proportional to its concentration in the aqueous phase. Furthermore, it implies that the adsorption is independent from the adsorbed concentration of the compound (Grathwohl, 1990).

The linear model is described as:

$$q_e = K_d C_e \tag{6}$$

where q_e [g kg^{-1}] is the solid phase equilibrium concentration, C_e [g L^{-1}] is the liquid phase equilibrium concentration, and K_d [L kg^{-1}] is the adsorption constant (Allen et al., 2004).

Since it was found that hydrophobic organic solutes preferably adsorb to the organic matter, the adsorption constant (K_d) of these solutes in soil is frequently normalized by the organic carbon content (Li, 2011):

$$K_{oc} = \frac{K_d}{f_{oc}} \tag{7}$$

where K_{oc} [L kg^{-1}] is the partition coefficient and f_{oc} [kg kg^{-1}] is the organic carbon content.

Freundlich model

The empirical Freundlich model is frequently used to describe non-linear adsorption isotherms (McGinley et al., 1993). It assumes that adsorption occurs onto heterogeneous sorption sites and is mathematically described by the following equation:

$$q_e = K_F C_e^{1/n} \tag{8}$$

where K_F [µg$^{(1-1/n)}$ L$^{1/n}$ g^{-1}] is the Freundlich coefficient relating to the capacity of the adsorbent and n reflects the surface heterogeneity of the adsorption sites and describes the nonlinearity of the curve (Weber et al., 1992). The isotherm exhibits a convex shape when $1/n < 1$ and a value of $1/n = 1$ represents a linear isotherm where K_F is equal to the adsorption constant K_d (Blume et al., 2010).

Langmuir model

The Langmuir model is also an empirical model for the description of non-linear adsorption isotherms and was originally designed to describe the adsorption of gas molecules (Blume et al., 2010). It assumes equal adsorption sites, no interactions between adsorbed molecules, only one adsorption mechanism operating, and only one layer of adsorbed molecules (monolayer adsorption) (Blume et al., 2010). At equilibrium, saturation is achieved and no further adsorption can occur which is reflected by a plateau of the isotherm (Allen et al., 2004). This model is widely applied and can be described as follows:

$$q_e = \frac{QK_LC_e}{1 + K_LC_e} \quad (9)$$

where Q [µg kg^{-1}] is the limited adsorption capacity of the monolayer and K_L [L µg^{-1}] is the Langmuir coefficient referring to the affinity of the adsorbate to the surface of the adsorbent (Li, 2011).

3. Materials and methods[1]

3.1 Carbon nanotubes

Radioactively (^{14}C) labeled MWCNTs were prepared by catalytic chemical vapor deposition (Bayer Technology Services GmbH, Leverkusen, Germany) using ^{14}C-benzene as feedstock gas. The synthesis procedure was a slightly modified lab-scale setup of the Baytubes® production process (Bierdel et al., 2007). The specific radioactivity of the ^{14}C-labeled MWCNTs was approx. 3.2 MBq mg^{-1}. After synthesis, the MWCNTs were boiled in 70% nitric acid (Sigma-Aldrich Chemie GmbH, Steinheim, Germany) for 4 h under reflux to remove residual metal catalysts and to enhance their stability in the aqueous phase by addition of oxygen-containing functional groups (e.g., carboxylic groups) to their surfaces (Nagasawa et al., 2000; Pumera, 2007; Smith et al., 2009; Xia et al., 2007). Afterwards, the MWCNTs were removed from the acid by filtering through a 0.45 µm polytetrafluoroethylene (PTFE) membrane (Sartorius AG, Göttingen, Germany) and washing with deionized water until a neutral pH-value was achieved in the filtrate (Mattison et al., 2011). Finally, the functionalized MWCNTs were dried in an oven at 45 °C and stored at room temperature until use.

For transport experiments, nanoparticle suspensions of different concentrations were prepared. For water-saturated column experiments, 1 mg of ^{14}C-labeled functionalized MWCNTs were added to 1 L of 1 mM KCl solution and ultrasonicated for approximately 10 minutes at 65 watts using a cup horn sonicator (Branson Sonifier® W-250, Danbury, CT, USA) until no aggregates were visible. To obtain suspensions with lower MWCNTs concentrations (0.01 and 0.005 mg L^{-1}), the stock suspensions (1 mg MWCNTs L^{-1}) were diluted with 1 mM KCl to achieve the desired concentrations. The concentration of the MWCNT suspensions was assessed by measuring the radioactivity of five 2.5 ml aliquots. Each aliquot was added to 5 mL of scintillation cocktail (Insta-Gel Plus, PerkinElmer, Rodgau, Germany), shaken, and the radioactivity was measured by a liquid scintillation counter (LSC, Perkin Elmer, Rodgau, Germany). A low standard deviation of the radioactivity measured in five replicates, indicated that the MWCNT suspensions were homogeneous.

[1] Contains parts from "Water Research 47, Kasel, D., Bradford, S. A., Šimůnek, J., Heggen, M., Vereecken, H., Klumpp, E., Transport and retention of multi-walled carbon nanotubes in saturated porous media: Effects of input concentration and grain size. 933-944, 2013" and "Environmental Pollution 180, Kasel, D., Bradford, S. A., Šimůnek, J., Pütz, T., Vereecken, H., Klumpp, E., Limited transport of functionalized multi-walled carbon nanotubes in two natural soils. 152-158, 2013", with permission from Elsevier.

For water-unsaturated transport experiments, nanoparticle suspensions with concentrations of 10 mg L^{-1} were prepared. Therefore, 1 mg of ^{14}C-labeled functionalized MWCNTs were added to 100 mL of 1 mM KCl solution and ultrasonicated for approximately 10 minutes at 65 watts using the previously described cup horn sonicator until no aggregates were visible. Afterwards, five 0.5 ml aliquots were each added to 5 mL of the scintillation cocktail and 2 mL of water, to obtain the correct ratio between scintillator and aqueous phase. Then all samples were shaken and the radioactivity was measured with the liquid scintillation counter.

3.2 Chlordecone

Radioactively (^{14}C) labeled chlordecone (CLD, also known as Kepone, CAS number 143-50-0) with a specific radioactivity of 2.94 MBq mg^{-1}, dissolved in acetone (1.46 g L^{-1}, Moravec Biochemicals, Inc., Brea, CA, USA) was used for adsorption experiments. To obtain the desired CLD concentration, the ^{14}C-labeled material was mixed with non-labeled chlordecone (Sigma-Aldrich Chemie GmbH, Steinheim, Germany), also dissolved in acetone (160 mg L^{-1}). For sorption experiments, two stock solutions (0.01 and 1 mg L^{-1}) of CLD were prepared by pipetting a specific amount of labeled and unlabeled material into a volumetric flask. After the acetone was evaporated, the flasks were filled to the required volume with 1 mM KCl. For sorption isotherms, these stock solutions were diluted in the correspondent ratio. The radioactivity of 2.5 mL of each solution was measured in 5 mL of scintillation cocktail using the LSC.

3.3 Quartz sands

Three quartz sands with different median grain sizes were applied: two high purity quartz sands (Quarzwerke GmbH, Frechen, Germany) with an average grain size of 350 µm and 240 µm, and a sterile fused silica sand (Teco-Sil®, C-E Minerals, King of Prussia, PA, USA) with an average grain size of 607 µm. The sands were sequentially treated for 2 h with 65% nitric acid to remove metal oxides and then with 10% hydrogen peroxide to eliminate organic material (Mattison et al., 2011). The sands were repeatedly rinsed with deionized water following both acid and peroxide treatments until a neutral pH was achieved in the rinse water. After the washing procedure, the organic carbon content of the sands was below 0.01 wt%, the total iron was below 0.02 wt%, and the total aluminum was below 0.05 wt%.

The electrophoretic mobility of milled sand samples (pH 8.5) was determined in 1 mM KCl solution using a Zetasizer Nano (Malvern Instruments GmbH, Herrenberg, Germany). The electrophoretic mobility values for the sands were -3.90×10^{-8} (240 µm), -4.47×10^{-8} (350 µm), and -3.15×10^{-8} $m^2V^{-1}s^{-1}$ (607 µm).

3.4 Soils

Soil samples from the upper 30 cm of two well characterized agricultural field sites in Germany were used as natural porous media for transport experiments. In particular, a loamy sand soil (Gleyic Cambisol) from the test site in Kaldenkirchen-Hülst (KAL) and a silty loam soil (Orthic Luvisol) from the test site in Merzenhausen (MRZ) were investigated (Unold et al., 2009a). The electrophoretic mobility of the soils (0.1 wt%) in 1 mM KCl solution (pH 8.5) was measured with the previously described Zetasizer Nano. The physico-chemical characteristics of the two soils are summarized in Table 1.

Table 1. Physico-chemical properties of the soils from Kaldenkirchen-Hülst (KAL, loamy sand) and Merzenhausen (MRZ, silty loam).

	unit	KAL	MRZ
Clay (< 2µm)*	% mass	4.9	15.4
Silt (2–63 µm)*	% mass	26.7	78.7
Sand (> 2000 µm)*	% mass	68.5	5.9
pH (0.01 M $CaCl_2$)*		5.9	6.2
Total organic matter*	% mass	1.1	1.3
Cation exchange capacity*	$cmol_c kg^{-1}$	7.8	11.4
Iron[#]	%	0.8	1.5
Electrophoretic mobility	$m^2V^{-1}s^{-1}$	-2.7E-8	-3.2E-8

* data reprinted from Unold et al. (2009a)
[#] data reprinted from Kasteel et al. (2010)

Undisturbed soil samples were collected in columns made of polyvinyl chloride with a length of 10 cm and an inner diameter of 8 cm using a metal adaptor with a sharp front. The adaptor was mounted on the bottom of the column and placed on top of the soil. Afterwards, the column was straightly pushed stepwise into the plough layer of the soil with the help of a water-level. Between the pushing steps, the surrounding soil was removed and at the end, the filled column could be easily removed from the soil. Finally, the soil at the bottom of the column was cut with a knife to obtain an even surface. For repacked soil columns and sorption experiments, disturbed soil samples were taken, sieved to a fraction < 2 mm and air dried.

3.5 Characterization of carbon nanotubes

The MWCNTs were characterized with the help of unlabeled MWCNTs derived from benzene and functionalized in the same way as the radioactively labeled ones. Morphological properties of MWCNTs were identified using a transmission electron microscope (TEM, Philips CM20 FEG, FEI Company, Eindhoven, The Netherlands) at the Ernst Ruska-Centre for Microscopy and Spectroscopy with Electrons, Forschungszentrum Jülich GmbH, Germany. Therefore, a drop of MWCNT suspension was placed onto a carbon-coated copper grid, dried, and inserted into the TEM. For elemental analysis of the samples, the TEM was coupled with an energy-dispersive X-ray spectroscope (EDX).

Metal catalysts in the MWCNT powder were quantified before and after the acid treatment with inductively coupled plasma-mass spectrometry (ICP-MS, Agilent 7500ce, Agilent Technologies, Inc., Böblingen, Germany). Oxygen containing functional groups on the MWCNTs, induced by the functionalization procedure, were identified by X-ray photoelectron spectroscopy (XPS, Phi 5600, Physical Electronics Inc., Chanhassen, MN, USA).

In addition to the characterization of the powder, the stability and electrophoretic mobility of unlabeled MWCNT suspensions were determined. The critical coagulation concentration of 10 mg L^{-1} MWCNTs in KCl (1 to 100 mM) and $CaCl_2$ (0.1 to 10 mM) solutions was determined by visual observations over a 24 h period. The hydrodynamic radius was determined immediately after suspension preparation and after 1 and 24 hours by dynamic light scattering (DLS) using the Zetasizer Nano. The electrophoretic mobility of MWCNT suspensions (1 mg L^{-1}, 1 mM KCl, pH 8.5) was measured with the same machine.

3.6 Water-saturated column setup

Stainless steel columns with an inner diameter of 3 cm and a length of 12 cm were used for water-saturated transport experiments. The column ends were fitted with a stainless steel plate (1 mm openings) and a PTFE mesh (200 µm mesh size) to support the sand/soil and to ensure a uniform flow. The columns were incrementally filled with porous medium by trickling sand/soil and deionized water into the column, and then tapping the column with a rubber mallet. The packed column was connected to a pump (MCP V 5.10, Ismatec SA, Glattbrugg, Switzerland) on the inlet side and a fraction collector (Foxy Jr. ®, Teledyne Isco Inc., Lincoln, NE, USA) on the outlet side. A Darcy velocity of 0.62–0.66 cm min^{-1} (Table **2**) was applied for all water-saturated experiments; equivalent to a pore water velocity of 1.39–1.66 cm min^{-1}. The flow direction was from the column bottom to the top. Preliminary transport studies were conducted using an empty column to determine losses of MWCNTs due to the experimental setup. The initial concentration of MWCNTs (C_o) that was applied to the column was corrected for these losses. A schematic overview of the water-saturated column setup is shown in Figure 6.

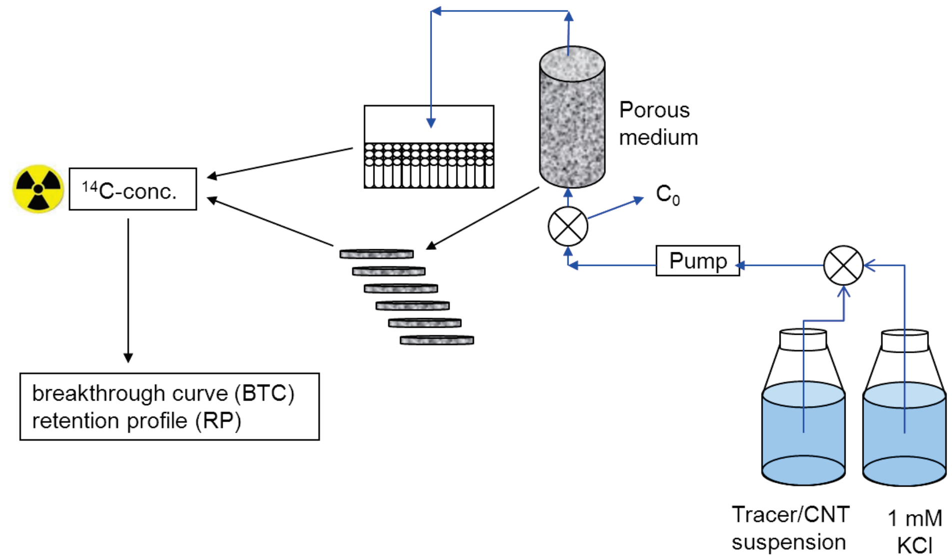

Figure 6. Schematic overview of the water-saturated column setup. The applied MWCNT concentration was determined using a valve just before the column inlet. The flow direction was from bottom to top.

There are different procedures for the injection of colloids in column transport experiments described in the literature. According to Kretzschmar et al. (1997), injecting colloids with a short pulse has advantages compared to the traditionally used long-pulse method because the smaller amount of injected particles reduces the likelihood of blocking or filter ripening and only small amounts of colloids are needed. This might be advantageous especially when their availability is limited. The use of injection loops with different volumes (e.g., 96 µL, 250 µL) is described elsewhere (Grolimund et al., 1998; Jaisi and Elimelech, 2009). Another possibility is described by Lecoanet et al. (2004), where the authors injected different types of nanoparticles as step of at least four pore volumes using a syringe pump and stopped the experiment during the plateau of particle breakthrough.

In general, stable suspensions in water were only attainable when relatively low MWCNT concentrations were applied. In addition, concentration effects in the column might occur when a highly concentrated MWCNT suspension is used. Nevertheless, a sufficient amount of MWCNTs has to be applied to the column to allow their detection in the leachate even if they are highly retained in the porous media. Therefore, it was not reasonable to apply a small pulse of MWCNTs. In consequence, three pore volumes (90 mL) of MWCNT suspension (1 mg L^{-1}) were injected to obtain a distinct BTC. As application tools, a PTFE sample loop, a stainless steel sample loop, and the direct injection without any sample loop (Figure 6) were compared. For the first two methods, the sample loops with a holding capacity of three pore volumes (approx. 90 mL) were consecutively connected to the pump and the column. The loops were filled with the inert tracer and the MWCNTs, respectively, which were then flushed through the column with background solution. For direct injection the reservoirs of inert tracer and MWCNTs were connected to the column using a pump.

The BTCs resulting from runs conducted with these three application methods are shown in Figure 7. Without any sample loop, the resulting BTC was of the typically observed shape (Liu et al., 2009). In contrast, both sample loops caused a delayed MWCNT breakthrough and a strong tailing of the BTC compared to the direct application with the pump. These results indicate that there was no continuous application of MWCNTs to the column.

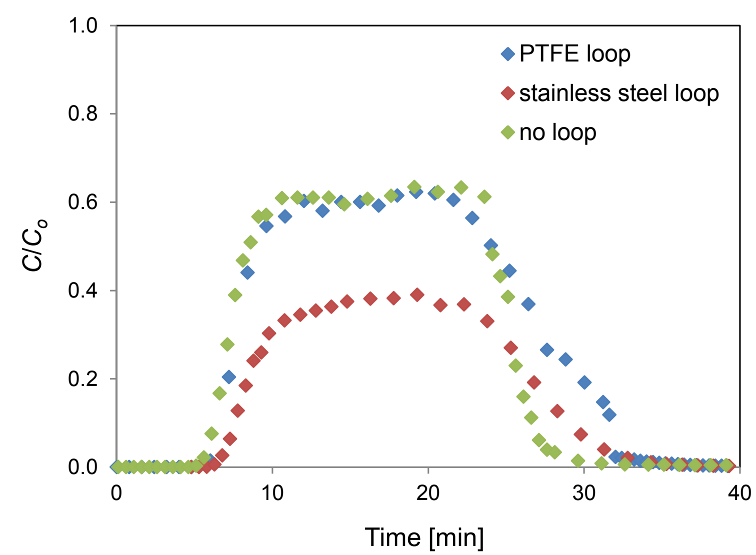

Figure 7. Breakthrough curves of MWCNTs (1 mg L^{-1}, three pore volumes) in 607 µm quartz sand using different methods for particle application: a PTFE sample loop, a stainless steel sample loop, and direct injection without sample loop.

Additionally, a control experiment without column was performed to test if the outflow of the sample loops was constant. Therefore, the stainless steel loop was filled with ^{14}C-labeled MWCNT suspension and flushed with background solution for another 5 pore volumes. The samples were collected every 30 s at the outlet site of the sample loop. Figure 8 shows the normalized MWCNT concentration flushed out of the stainless steel loop over time. For the duration of MWCNT application (18 min) a C/C_o of 1 would be expected, but it was only 0.8 at the beginning and decreased continuously with time. Thus, the sample loop affected the application of MWCNTs to the column. This resulted in an overestimation of the injected MWCNT concentration.

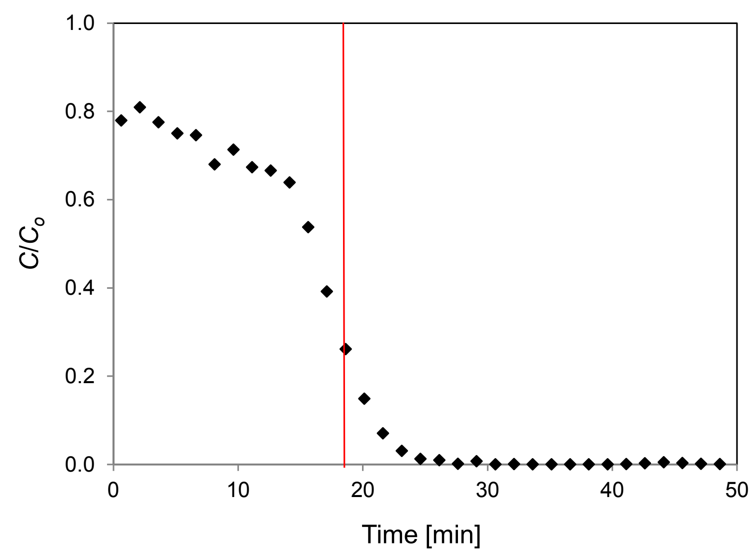

Figure 8. Outflow concentration of MWCNTs flushed through the stainless steel sample loop with 1 mM KCl. The red line indicates the end of the injection pulse (approx. 3 pore volumes).

Because both sample loops negatively affected the application of MWCNTs to the saturated column, the MWCNTs were finally applied without any sample loop. In addition, the actual applied MWCNT concentration was determined directly in front of the column using a valve (Figure 6) and considered as C_o.

For transport experiments, each wet-packed column was rinsed with around 30 pore volumes of 1 mM KCl solution before starting a transport experiment. A pulse of approximately 3 pore volumes of a conservative tracer (1 mM KBr) was applied to determine the column porosity and dispersivity. Afterwards, this tracer was flushed again with 1 mM KCl until background levels were achieved. Effluent solutions were collected by the fraction collector every 30 seconds (e.g., 2.3 mL per vial). The effluent bromide concentrations were determined by a high performance liquid chromatograph (STH 585, Dionex, Sunnyvale, CA, USA) equipped with a UV-detector (UV2075, Jasco, Essex, UK).

The same procedure was repeated for the MWCNT suspensions. The applied MWCNT concentration was determined using a valve just before the column inlet. The effluent concentrations of MWCNTs were measured using the previously discussed liquid scintillation counter method. Retention profiles for MWCNTs were also determined after recovery of the breakthrough curves. In this case, the packed column was excavated in 0.5–1 cm thick increments. The sand from each layer was dried and then homogenized with a mill. The crushed sand was then divided into five 500 mg replicates and combusted at 900°C with a biological oxidizer (OX 500, R.J. Harvey Instrumentation Corporation, Tappan, NY, USA). The emerging $^{14}CO_2$ was dissolved in vials filled with scintillation cocktail (Oxisolv®, MERCK KGAA, Darmstadt, Germany) and the radioactivity was measured by the liquid scintillation counter. Table 2 summarizes measured column properties determined from the conservative tracer experiments and mass balance information for MWCNTs.

Table 2. Experimental conditions, hydraulic parameters, and mass balance information (as fractions of the total applied mass; eff - effluent, soil - soil profile) for water-saturated column experiments. The electrolyte was 1 mM KCl.

C_o [mg L^{-1}]	Type of soil/d_c [µm]	Flow rate q [cm min^{-1}]	Porosity	Disp.[a] [cm]	CNT eff[b]	CNT soil[c]	Total mass balance
0.01	240	0.64	0.46	0.029	0.05	0.91	0.96
0.01	350	0.63	0.38	0.043	0.27	0.72	0.99
0.01	607	0.62	0.41	0.090	0.51	0.46	0.98
0.005	350	0.64	0.44	0.051	0.13	0.95	1.07
1	240	0.64	0.45	0.038	0.04	0.82	0.85
1	350	0.66	0.43	0.052	0.33	0.56	0.88
1	607	0.66	0.46	0.069	0.73	0.21	0.94
1	KAL	0.64	0.40	0.080	0.29	0.58	0.87

[a] Disp. is the longitudinal dispersivity estimated on basis of the conservative tracer BTC
[b] CNT eff is the total amount of MWCNTs in the liquid phase
[c] CNT soil is the total amount of MWCNTs in the solid phase

In addition to these column transport experiments, the influence of flow interruption on MWCNT transport in quartz sand (350 µm) was investigated using a C_o of 1 mg L^{-1}. First, the saturated column experiment was performed, as described above. After termination of the transport experiment, the flow was stopped. But instead of determining the RP, the saturated sand column with the retained MWCNTs was left at room temperature for 18 h. Then, it was flushed again with 1 mM KCl for around 5 pore volumes and the leachate was collected. Finally, the packing was removed to obtain the RP.

3.7 Water-unsaturated column setup

For unsaturated experiments, the polyvinyl chloride soil columns (Chapter 3.4) were mounted on acrylic glass plates covered with a high conductivity 20 µm nylon mesh. The air-entry value of the nylon mesh was approximately 50 mbar. The undisturbed soil columns were slowly saturated from bottom to top with 1 mM KCl. For repacked columns, soil and water were trickled alternately into an empty column. The water-saturated columns (repacked and undisturbed) were equipped with two tensiometers (inserted at 2.5 and 7.5 cm below the soil surface) to monitor the pressure head inside the columns. Then, the columns were installed into the setup including an irrigation head on top of the column and suction at the bottom. The suction was applied by a vacuum pump and four vacuum barrels. In brief, the columns were irrigated from the top with 1 mM KCl and suction between 0 and -35 mbar was applied to the bottom. Software controlled equipment (Unold et al., 2009b) was used to achieve steady-state flow conditions in the columns.

A unit gradient in the matrix potential (monitored using the two tensiometers) was achieved by automatically changing the irrigation rate or the bottom suction. The irrigation rate was recorded by weighing the storage bottle of the irrigation solution. The electrical conductivity of the leachate was continuously measured over the duration of the experiment. A schematic overview of the unsaturated column setup is given in Figure 9.

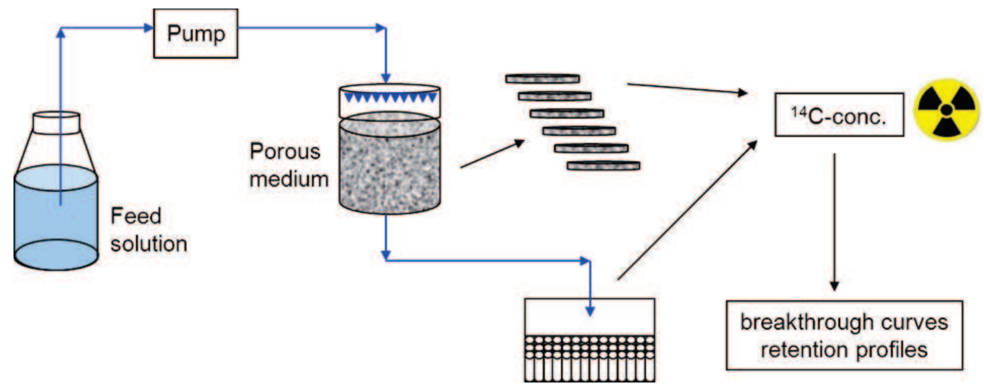

Figure 9. Schematic overview of the water-unsaturated column setup. Background solution and tracer were applied via the irrigation head while the MWCNT suspension was applied using a pipette.

Prior to the unsaturated transport experiment, it was tested if the application with the irrigation head was suitable for the MWCNTs. Therefore, the storage bottle with the MWCNT suspension was connected to the irrigation head and the particles were pumped into the irrigation head and dropped onto the soil surface with the irrigation solution. The pulse duration was 3 pore volumes, as for the saturated experiments, which was about 30 h for the applied flow rate. After this time period, black aggregates in the irrigation head were macroscopically observable. Obviously, the MWCNTs aggregated during the application resulting in an irregular outflow and thus non-uniform application to the column. In consequence, the actually applied MWCNT concentration (C_o) was overestimated.

Therefore, the pulse duration was reduced to 2 h and the radioactivity in the irrigation water was monitored at different time steps during the application procedure. The normalized MWCNT concentration started at 1 and decreased continuously until it was 0.8 after 2 h. This proved that a continuous outflow of MWCNTs was not achievable either. The initial concentration was not stable and the calculated C_o again overestimated the applied amount of MWCNTs. Therefore, the MWCNT suspensions were applied using a pipette.

For unsaturated transport experiments, the columns were flushed with 1 mM KCl until the conductivity of the leachate and the matrix potentials (water contents) were constant. Afterwards, a 1 h pulse of 10 mM KCl was applied to the column as conservative tracer using the irrigation head and its breakthrough curve was detected by measuring the conductivity of the leachate. The columns were flushed again with 1 mM KCl until the conductivity remained constant at background levels. Following the tracer experiment, 5 mL of MWCNT suspension (10 mg L^{-1}) were pipetted evenly on top of the soil. The columns were flushed again with 1 mM KCl and the leachate was collected using a fraction collector. The leachate was analyzed in the liquid scintillation counter and the experiment was stopped when the radioactivity in the effluent fell below the detection limit. After termination of the transport experiment, the soil was removed in 1 cm thick increments and the RP was determined with the same procedure as described above for the saturated column setup. Table 3 summarizes column properties determined from the conservative tracer experiments and mass balance information for MWCNTs.

Table 3. Experimental conditions, hydraulic parameters, and mass balance information (as fractions of the total applied mass) for water-unsaturated column experiments. The electrolyte was 1 mM KCl.

Type of core	Soil type	Water saturation [%]	q [cm min^{-1}]	Porosity	Disp.[a] [cm]	CNT eff[b]	CNT soil[c]	Total mass balance
Und.	KAL	96	0.0064	0.37	0.60	< 0.01	0.91	0.91
Und.	KAL	85	0.0084	0.32	0.69	< 0.01	0.98	0.98
Rep.	KAL	96	0.0067	0.38	0.37	< 0.01	0.86	0.86
Und.	MRZ	95	0.0063	0.49	2.41	< 0.01	1.01	1.01

[a] Disp. is the longitudinal dispersivity estimated on basis of the conservative tracer BTC
[b] CNT eff is the total amount of MWCNTs in the liquid phase
[c] CNT soil is the total amount of MWCNTs in the solid phase

3.8 Lysimeter

A stainless steel lysimeter (Figure 10) with a surface area of 0.5 m² and a depth of 115 cm was used for larger scale transport experiments (Burauel and Führ 2000). The lysimeter contained an undisturbed soil monolith from the test site in Kaldenkirchen-Hülst (KAL). It was equipped with two time-domain reflectrometry (TDR) sensors in 5 and 30 cm depth, respectively, to observe the water content during the experiment. The lysimeter was covered with a stainless steel plate and was artificially irrigated with tap water at a precipitation rate of 1200 mm y^{-1}.

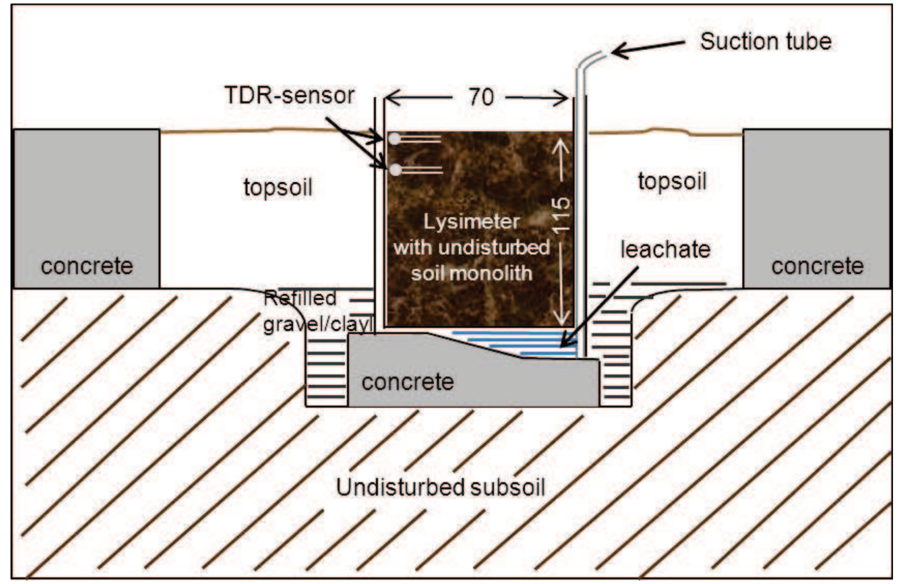

Figure 10. Cross-section through the lysimeter (all measures in cm). Adapted from Burauel and Führ (2000).

A pulse of 5 L of potassium bromide solution (approx. 16.5 g of KBr in total) was applied at first uniformly onto the soil's surface as a conservative tracer. One week later, the same procedure was repeated with 5 L of ^{14}C-MWCNT suspension (approx. 25 mg of MWCNTs in total). The leachate was collected in regular intervals from a stainless steel pan placed at the bottom of the lysimeter. The bromide concentration in the leachate was determined using the aforementioned high performance liquid chromatograph equipped with a UV-detector. For determination of the radioactivity, the previously described LSC was used. After termination of the experiment, soil samples were taken at different points using a Pürckhauer soil corer (Schierholz et al. 2000) to obtain quantitative information about the MWCNT distribution in the soil profile.

3.9 Batch adsorption experiments

The adsorption isotherm of CLD onto a loamy sand soil from the test site in Kaldenkirchen-Hülst was determined in batch trials according to the OECD-guideline 106. Therefore, 1 g of dry soil was weighed into glass centrifuge tubes. After pre-equilibration with 5 mL of 1 mM KCl for 24 h, 10 mL of radiolabeled CLD solution of different concentrations were added. The concentration steps of the isotherm were 0, 1, 2.5, 5, 7.5, and 10 mg kg^{-1}. To test the adsorption to the glass wall of the centrifuge beaker, the procedure was repeated with the CLD solution in centrifuge tubes without soil. Soil and CLD were equilibrated for 24 h in an over-head shaker to establish the sorption isotherm. Afterwards, the centrifuge tubes were removed from the shaker and centrifuged for 20 min at 10,000×g. Afterwards, two aliquots of 2.5 mL of each sample were taken, mixed with 5 mL of scintillation cocktail, shaken, and the radioactivity was measured using the LSC. All experiments were performed in triplicate. Finally, the adsorption isotherm was calculated using a graphical software program (Origin Pro 8, OriginLab Corporation, Northampton, MA, USA).

3.10 Dialysis adsorption experiments

Since centrifugation was not sufficient to separate the functionalized MWCNTs from solution, the dialysis technique (Telscher et al., 2005) was applied to determine the adsorption of CLD onto the MWCNTs. Therefore, half-cells made of PTFE with a holding capacity of about 5 mL were used. Two half-cells were connected (Figure 11), separated by a cellulose membrane with a cut off of 1 kDa (VWR International GmbH, Langenfeld, Germany), and inserted into a special frame.

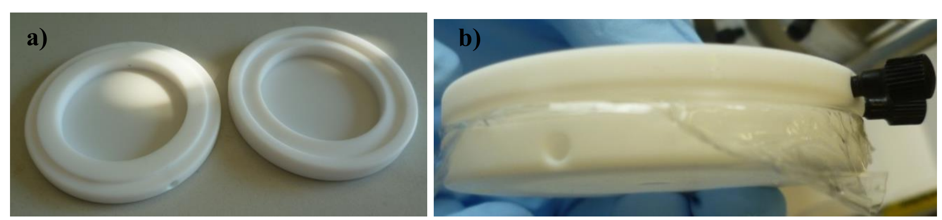

Figure 11. Picture of the two half cells before (a) and after connection (b). The half cells were separated by a membrane.

Then, the MWCNT suspension (1 mg L^{-1}) was injected into the bottom part of the half-cell using a syringe. The syringe was weighed with suspension before and after injection to determine the injected volume. This procedure was repeated with CLD solution of different concentrations (0, 2, 5, 10, 20 g kg^{-1}) for the top parts of the half-cells. To test the adsorption to the PTFE wall of the half-cell, the procedure was repeated with the CLD solution in half-cells without MWCNTs. Duplicates of each concentration step were run. After injection of CLD solution, the frames were inserted into a rotator and rotated at 10 rpm for 48 h to achieve equilibrium (Figure 12). Afterwards, the solution was removed from the top half-cell using a syringe and weighed into vials to measure the ^{14}C-CLD concentration in the LSC.

Figure 12. Equilibration of the dialysis half-cells in a rotator.

3.11 Mathematical modeling

To account for the various transport and retention mechanisms described in Chapter 2, the transport experiments were analyzed using the HYDRUS-1D code, a finite element model for simulating one-dimensional movement of water, heat, and multiple solutes in (variably) saturated media (Šimůnek et al., 2008). The code includes a nonlinear least squares optimization routine (Marquardt, 1963) that allows model parameters to be inversely fitted to experimental BTCs and RPs. Weights to data points were adjusted so that the contributions to the minimized objective function by the sum of squared deviations between measured and fitted values were approximately the same for the BTC and the RP. The conservative tracer BTC for each column was simulated using an equilibrium model based on the ADE and the column porosity and dispersivity was obtained by inverse optimization.

The theory of the ADE was already described above (Chapter 2.3). To model the results of this study, the parameter ψ of Equation 3 is given as a combination of Equations 4 and 5:

$$\psi = \left(1 - \frac{S}{S_{max}}\right)\left(\frac{d_c + x}{d_c}\right)^{-\beta} \tag{10}$$

where S_{max} [N_cM^{-1}] is the maximum solid phase particle concentration, d_c [L] is the median diameter of the sand grains, and β [-] is an empirical variable that controls the shape of the retention profile.

The above model formulation is very flexible and can account for time-dependent breakthrough curves and retention profiles that are exponential, uniform, and/or hyper-exponential with depth. The first term on the right side of Equation 10 accounts for time-dependent blocking/filling of retention sites using a Langmuirian approach (Gargiulo et al., 2007a). This blocking term implies that retention decreases with time and that the retention profile becomes uniform with depth as S approaches S_{max}. The second term on the right side of Equation 10 describes depth-dependent retention (e.g., a decreasing retention rate with depth). When $\beta = 0$, this term equals 1 and an exponential distribution of retained MWCNTs is predicted with depth, similar to conventional filtration theory. Conversely, when $\beta > 0$ is employed, the retention profile of MWCNTs exhibits a hyper-exponential shape (e.g., a higher deposition rate close to the column inlet). Bradford et al. (2003) found an optimal value of $\beta = 0.432$ for different spherical sized latex microspheres and sand grains. However, this value of β did not adequately describe the observed depth-dependency in retention profile shape for the non-spherical MWCNTs. This parameter was therefore re-estimated by simultaneously fitting β and k_1 to BTC and RP from the three sized sands. Based on this information a value of β for MWCNTs was estimated from the average value from these experiments as 0.765 (standard deviation = 0.1). A similar value for $\beta = 0.8$ was employed by Wang et al. (2012) in MWCNT transport studies.

Four model formulations based on Equations 1 to 5 and 10 were considered in this work. The conventional attachment and detachment model (M1) is obtained by setting ψ = 1. A model that includes attachment, detachment, and Langmuirian blocking (M2) is achieved when $\beta = 0$. A depth-dependent retention model (M3) is acquired by setting β = 0.765 and setting S_{max} to a large value so that the first term on the right side of Equation 10 goes to 1. Finally, a time- and depth-dependent retention model (M4) is given when $\beta = 0.765$ and S_{max} is set equal to a value resulting in the first term on the right side of Equation 10 being smaller than 1.

4. Results and discussion

4.1 Characterization of carbon nanotubes

Prior to transport experiments, the as-received and the functionalized MWCNTs were characterized by various methods. On the one hand, it was important to identify their general properties because particle shape, size, and stability affect their transport behavior in porous media. On the other hand, the effect of the acid treatment on the material was investigated in order to verify whether the functionalization procedure was successful in inducing oxygen-containing functional groups on the MWCNTs. The acid treatment described in Chapter 3.1 is a relatively rough functionalization method, and may affect the structure and properties of MWCNTs. Therefore, it was necessary to compare their size and shape before and after the functionalization procedure.

Chemical composition

The presence of functional groups was verified by X-ray photoelectron spectroscopy (XPS). Figure 13 shows the XPS spectra of as-received and functionalized MWCNTs. The intensity in the binding energy of the O 1s spectra (Figure 13a) was significantly higher after the acid treatment. This indicates that the functionalization method was successful and produced an increased amount of oxygen containing functional groups. The two materials also showed differences in their C 1s spectra (Figure 13b). The peak at 285 eV represents the sp^2 carbon atoms of the graphene sheets and was dominant for both samples (Xia et al., 2007). Between 287 eV and 293 eV, the spectra of the functionalized MWCNTs showed a shoulder that is attributable to carbon atoms exhibiting bonds to oxygen atoms (Xia et al., 2007). Oxygen-containing functional groups are known to enhance the stability of CNTs in the aqueous phase because they increase their hydrophilic properties (Smith et al., 2009).

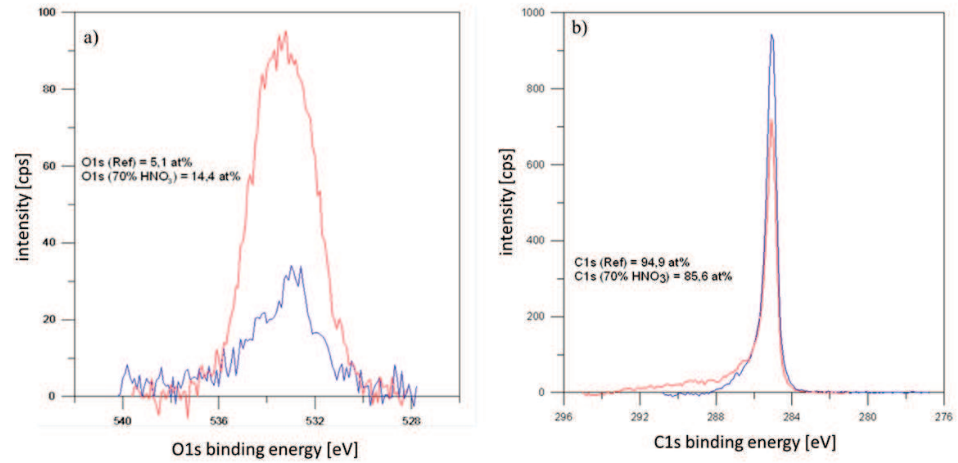

Figure 13. High-resolution O 1s (a) and C 1s (b) spectra of untreated (blue line) and functionalized (red line) multi-walled carbon nanotubes obtained using X-ray photoelectron spectroscopy. Reprinted from Kasel et al. (2013), with permission from Elsevier.

Prior to the acid treatment, metal catalyst particles were visible in the TEM images (Figure 14). A comparison of the TEM images before and after the acid treatment showed a reduction in metal catalyst particles (data not shown). An analysis of these particles with EDX revealed that the most common catalyst metals (Co, Mn, Mg, and Al) were present in the unpurified MWCNTs (Figure 15a) but that these metal peaks were lacking in the spectra of the purified MWCNTs (Figure 15b). The Cu peaks of the spectra are caused by the copper grid used as sample holder.

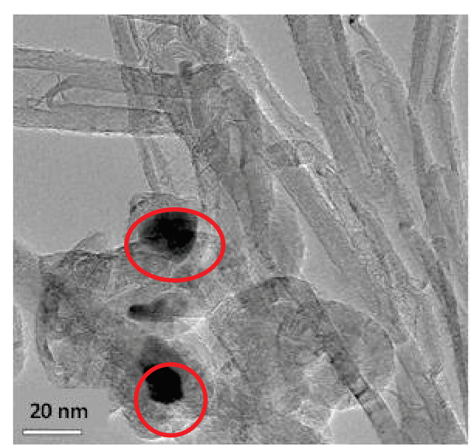

Figure 14. TEM image of unpurified CNTs. The dark particles (red circles) refer to the metal catalysts.

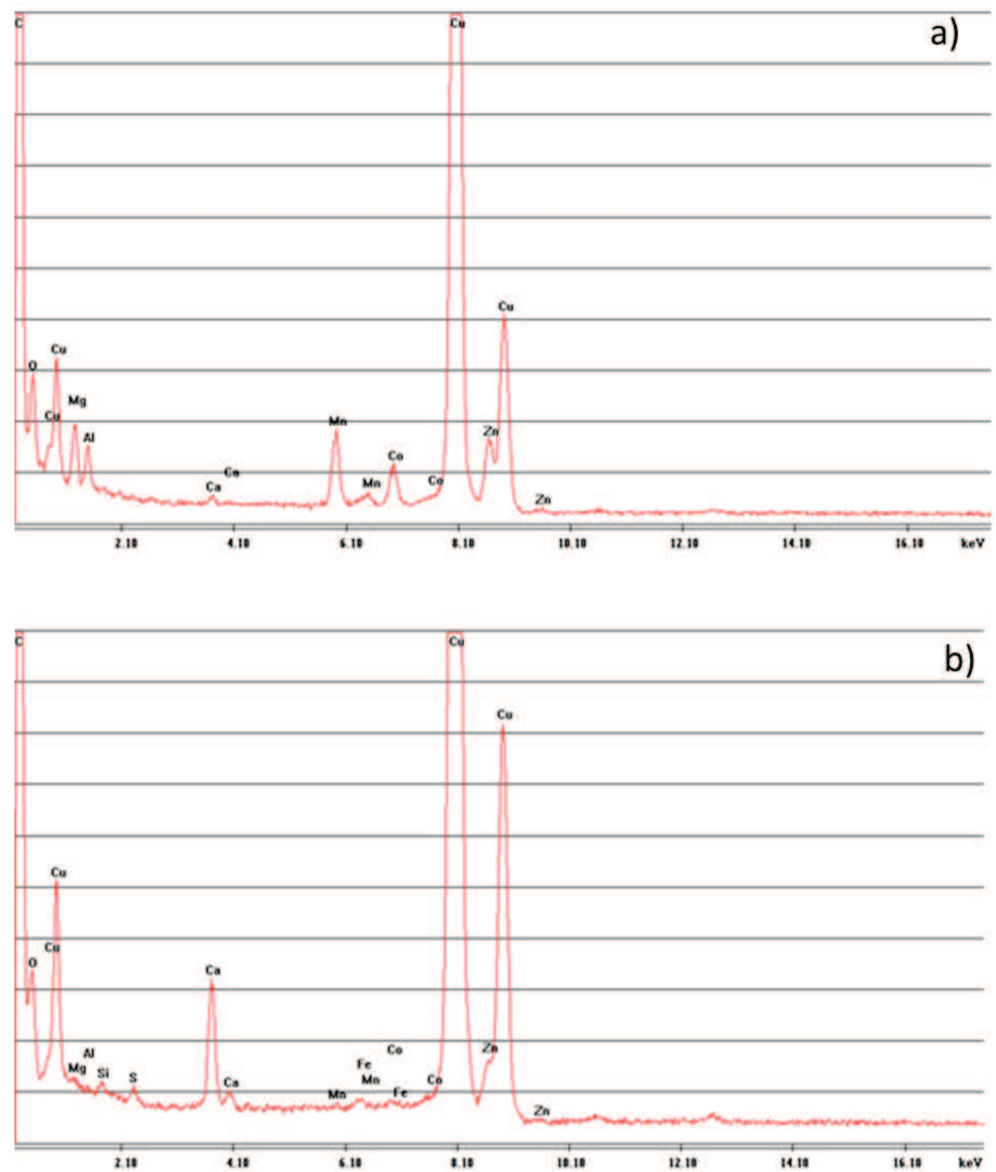

Figure 15. Energy-dispersive X-ray (EDX) spectra of metals in unpurified (a) and purified (b) MWCNTs.

The amount of these metals was quantified in the unmodified and functionalized MWCNTs using ICP-MS, as described in Chapter 3.5. The results of these measurements indicate that all four metals were present in the untreated material and that these catalyst impurities were significantly lower after the functionalization process. The acid treatment reduced the amount of Mg, Mn, Co, and Al from up to 3.26 wt% to less than 0.07 wt%. Thus, metal impurities were almost completely removed and were not expected to influence the interaction of MWCNTs with the porous media.

Shape and size

Further TEM images (Figure 16a) show that the MWCNTs were tortuous particles with a high aspect ratio. At higher magnification, the multiple walls of carbon were visible (Figure 16b). The size distribution of the MWCNTs was heterogeneous. The hydrodynamic radius of functionalized MWCNTs dispersed in 1 mM KCl was determined using DLS in the range of 170 nm to 210 nm.

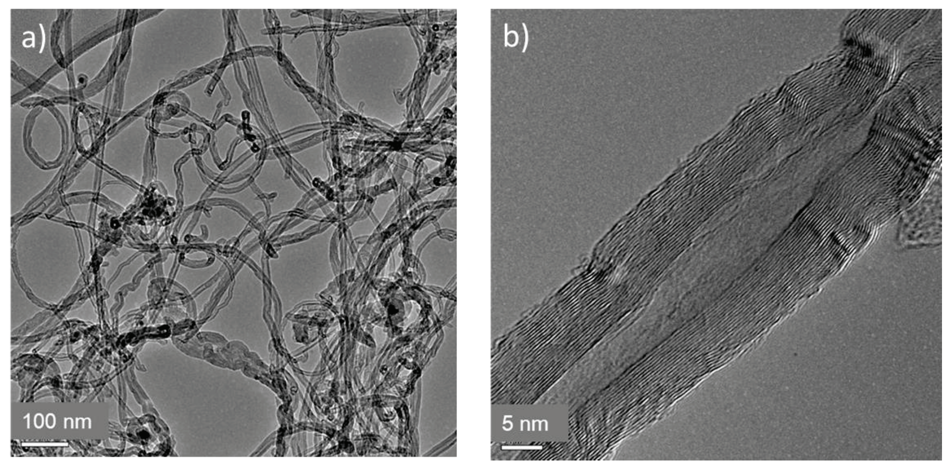

Figure 16. Transmission electron micrographs of multiwalled carbon nanotubes at different magnifications. Reprinted from Kasel et al. (2013), with permission from Elsevier.

The TEM images did not reveal significant changes in size or diameter after the functionalization process, although it is known that boiling in strong nitric acid may result in an opening and shortening of CNTs (Jia et al., 1999).

Colloid stability

Reliably determining MWCNT size, stability, and interaction energies using conventional approaches (DLS and DLVO calculations) is not trivial because of their complex size distribution and configuration (Figure 16). The hydrodynamic radius of colloids is frequently measured with DLS. However, for non-spherical particles, the hydrodynamic radius is not equal to the geometric particle diameter (Hassellöv et al., 2008;

Pecora, 2000). Therefore, the reliable size determination of carbon nanotubes using DLS is difficult. Nevertheless, it can be used for comparison. The DLVO theory (Chapter 2.1) provides information on the stability and aggregation of particles but it was developed for spherical particles (Tian et al., 2011) and may therefore be unreliable for non-spherical particles like CNTs. This was proven by Tian et al. (2011), who showed that DLVO energy profiles of SWCNTs differed greatly when the tube length instead of the tube diameter was applied for the calculations.

Simple aggregation experiments were performed to observe the stability of MWCNT suspension for the duration of the experiments. For a MWCNT concentration of 10 mg L^{-1}, no MWCNT aggregates were visible after 4 h in 1 mM KCl solution and the hydrodynamic radius at three measurement times (t = 0 h, t = 1 h, and t = 24 h) was in the same range (approx. 150 nm). For all transport experiments, MWCNT concentrations were equal to 10 mg L^{-1} or even lower (0.005–1 mg L^{-1}). Thus, it was assumed that all MWCNT suspensions were stable for the duration of particle application to the columns/lysimeter for transport studies (approx. 15 min to 1 h). The electrophoretic mobility of MWCNTs (1 mg L^{-1}) in 1 mM KCl solution (pH 8.5) was -2.85×10^{-8} m^2 V^{-1} s^{-1}. The negative charge on both MWCNTs and sand (Chapter 3.3) and the low IS conditions, suggest repulsive electrostatic conditions during the transport experiments that were unfavorable for attachment of MWCNTs. The critical coagulation concentration (CCC) was determined for unlabeled, functionalized MWCNTs in simple aggregation/sedimentation experiments (Figure 17).

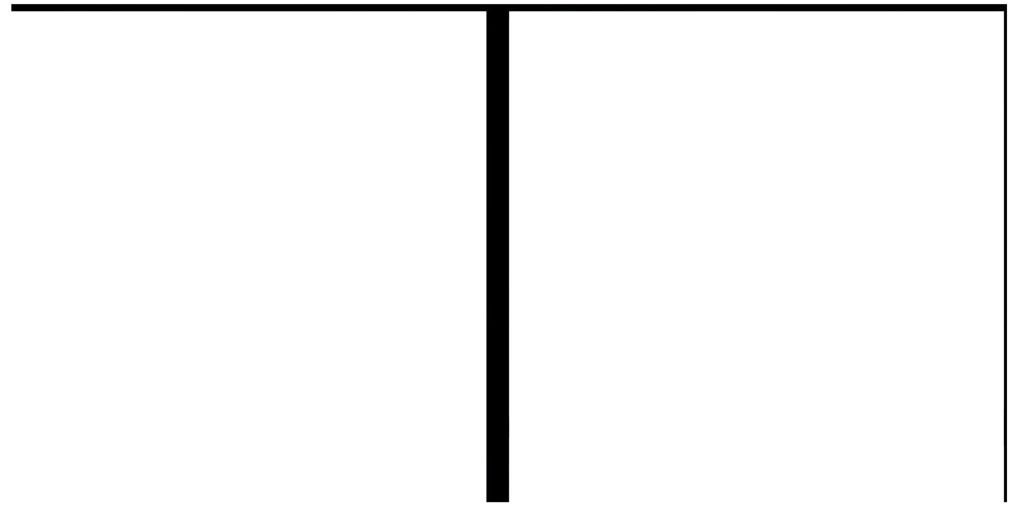

Figure 17. Determination of the critical coagulation concentration of KCl (a) and $CaCl_2$ (b) for a MWCNT concentration of 10 mg L^{-1}.

The critical coagulation concentration was 40 mM for KCl and 0.4 mM for $CaCl_2$ when the CNT concentration was 10 mg L^{-1}. This shows that the stability of MWCNTs in aqueous suspension is very sensitive to the ionic strength. It is known that divalent cations enhance the compression of the electric double layer surrounding the particles, thus leading to larger aggregation rates (Pan and Xing, 2012) compared to monovalent cations even when their concentrations are the same. This is explained by the Schulze-Hardy rule:

$$CCC \sim (1/z)^n \tag{11}$$

where z is the valency of the electrolyte counterions and n is 6 in three dimensions and 9 in two dimensions (Sano, 2001). The Schulze-Hardy rule can be explained by a combination of van der Waals attraction and electrostatic repulsion (Overbeek, 1980). This explains why the critical coagulation concentration is two orders of magnitude lower for $CaCl_2$ than for KCl. For all experiments, the electrolyte concentration (1 mM KCl) was significantly below the critical coagulation concentration. These findings support the assumption that all suspensions were stable, at least for the duration of the transport experiments. Nevertheless, Ca^{2+} is present in natural soils and may therefore also affect the stability of MWCNTs in natural porous media.

4.2 Transport and retention of carbon nanotubes in saturated porous media[2]

Column transport experiments in quartz sand were performed at water-saturated conditions to evaluate the effect of input concentration and sand grain size on MWCNT transport. Therefore, three sand grain sizes (607, 350, and 240 µm) and three MWCNT input concentrations (1, 0.01, and 0.005 mg L^{-1}) were considered. Since the available experimental setups were originally designed for solutes but nanoparticles behave like colloids, the setups were tested for MWCNTs and modified. This was done prior to the transport experiments and is described in Chapter 3.6. In addition to the breakthrough curves, retention profiles were measured and numerically modeled in order to obtain information on MWCNT mass balance, retention mechanisms, and to more accurately predict environmental fate. Finally, an experiment with intermittent flow was conducted.

4.2.1 Effect of grain size

Water-saturated column experiments were conducted to assess the effect of the collector grain size on MWCNT transport and retention. Figure 18 presents observed and simulated BTCs for MWCNTs in three different sized sands (240, 350, and 607 µm) when q = 0.62–0.66 cm min^{-1}, IS = 1 mM KCl, and C_o = 0.01 mg L^{-1}. The BTCs are plotted as the normalized effluent concentration (C/C_o) as a function of pore volumes that have been flushed through the column. The corresponding observed and simulated RPs for the MWCNTs are shown in Figure 19. The RPs are plotted as normalized solid phase concentration (S/C_o) as a function of distance. The total mass balance information presented in Table 2 ranged from 0.85 to 1.07.

The MWCNT breakthrough curves (Figure 18) reached the column outlet only slightly after the conservative tracer (data not shown) indicating that size exclusion was negligible for MWCNTs (Bradford et al., 2003). A clear decrease in the maximum MWCNT effluent concentration occurred with decreasing grain size. This can partially be explained by an increasing rate of mass transfer to the solid surface with a decrease in sand grain size as predicted by filtration theory (Tufenkji and Elimelech, 2004; Yao et al., 1971). The MWCNT BTCs in the 240 and 350 µm sands also exhibited some time-dependent blocking behavior (increasing breakthrough concentrations with time),

[2] Contains parts from "Water Research 47, Kasel, D., Bradford, S. A., Šimůnek, J., Heggen, M., Vereecken, H., Klumpp, E., Transport and retention of multi-walled carbon nanotubes in saturated porous media: Effects of input concentration and grain size. 933-944, 2013", with permission from Elsevier.

suggesting that retention locations were being filled over time. The observed concentration tailing was negligible after recovery of the BTC. The value of the detachment coefficient k_2 was therefore set equal to zero for all of these simulations.

The fitted model parameters to the BTCs (M1 and M2) as well as to BTCs and RPs (M3 and M4) are provided in Table 4, as well as the Pearson's correlation coefficient for the BTC (R_{eff}^2). A direct comparison between of the attachment coefficient k_1 for the four model formulations is not meaningful since models M1 and M2 do not account for a depth-dependency, whereas models M3 and M4 do. All four model formulations (M1, M2, M3, and M4) described the MWCNT BTCs quite well ($R_{eff}^2 > 0.85$). Improved agreement with the BTCs was obtained for models that included the Langmuirian blocking term (M2 and M4). The Akaike information criterion (AIC) (Akaike, 1974) was used to assess the relative ability of the four model formulations to describe the BTC and RP data. The AIC value is a measure of the goodness of a fit that penalizes for adding fitting parameters; i.e., the model with the lowest value of AIC is preferred. It can be calculated as:

$$AIC = 2(L + m) \tag{12}$$

where L is the negative log likelihood for the fitted model and m is the total number of independently optimized parameters (Russo and Bouton, 1992). When the inverse model parameters are calculated by least square optimization, the AIC can be calculated using the residual sum of squares from regression:

$$AIC = n * \ln(\frac{RSS}{n}) + 2m \tag{13}$$

where n is the number of experimental data points and RSS the residual sum of squares (Russo and Bouton, 1992).

The calculated AIC decreased from -258 (M1) to -496 (M4), indicating that M4 provides the best agreement with the observed data. For a particular model, k_1 and S_{max} increased with decreasing grain size. Previous studies on the transport and deposition of fullerene (C_{60}) nanoparticles reported similar trends (Li et al., 2008). These trends reflect an increasing rate of retention and more retention locations in the finer textured sand.

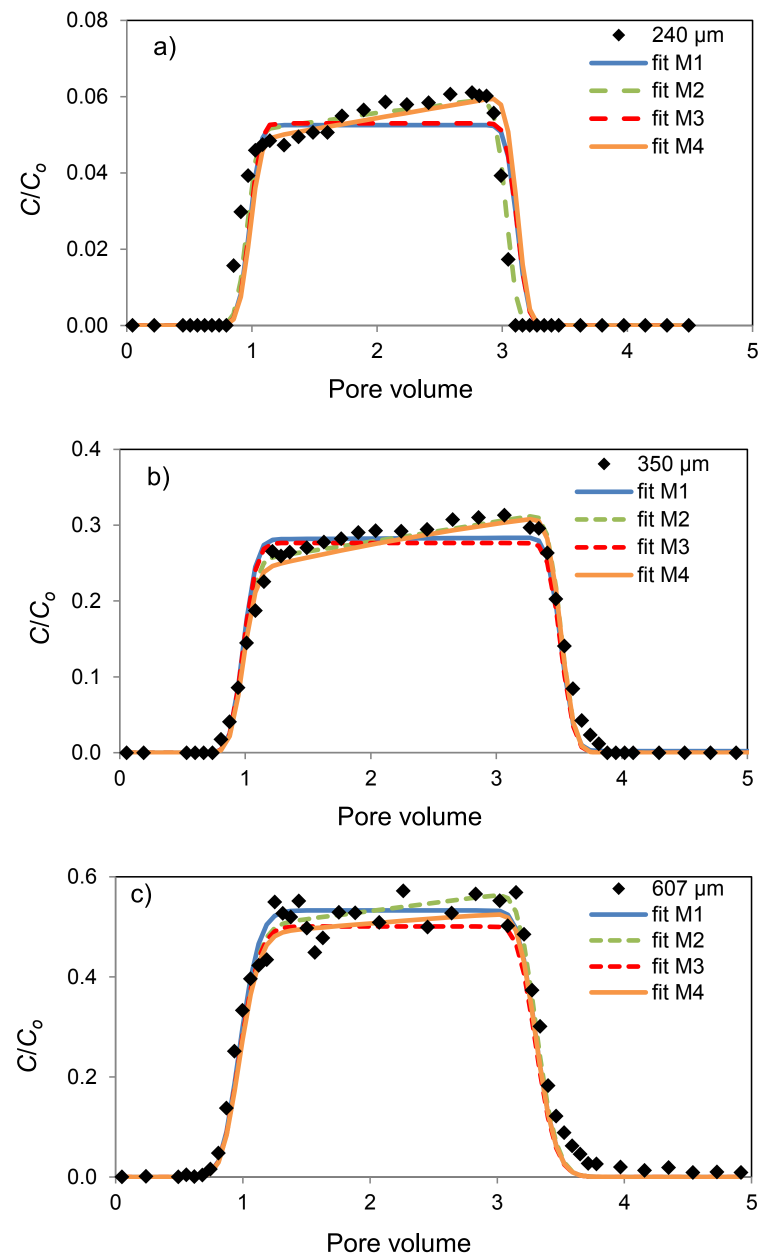

Figure 18. Observed and simulated breakthrough curves for MWCNTs in three different sized quartz sands: 240 µm (a), 350 µm (b), and 607 µm (c). Experimental data were fitted with four different models including: attachment and detachment (M1); attachment, detachment, and blocking (M2); depth-dependent retention (M3); and blocking combined with depth-dependent retention (M4). The flow rate was 0.62–0.66 cm min^{-1}, the electrolyte was 1 mM KCl, and the MWCNT input concentration was 0.01 mg L^{-1}. Note different vertical scales in the figures.

Table 4. Fitted model parameters using different model formulations. Correlation of observed and fitted data is reflected by $R_{eff+soil}^2$ for BTC and RP, by R_{eff}^2 for BTC, and by R_{soil}^2 for RP.

C_o [mg L^{-1}]	d_c [µm]	Model	$R_{eff+soil}^2$	R_{eff}^2	R_{soil}^2	β	k_1 [min^{-1}]	Standard error k_1	k_2 [min^{-1}]	Standard error k_2	S_{max} [Bq g^{-1}]	Standard error S_{max}
0.01	240	M1	0.57	0.88	0.44		0.34	0.47E+1				
0.01	350	M1	0.45	0.98	0.53		0.17	1.75E-1				
0.01	607	M1	0.32	0.98	0.49		0.08	2.90E-1				
0.01	240	M2	0.54	0.96	0.54		0.35	0.43E+1			289	0.15
0.01	350	M2	0.43	0.99	0.50		0.19	0.24E+1			68	5.40
0.01	607	M2	0.30	0.98	0.47		0.09	0.34E-2			49	14.40
0.01	240	M3	0.98	0.86	0.99	0.765	11.47	0.25E-2				
0.01	350	M3	0.96	0.98	0.99	0.765	4.70	0.47E+1				
0.01	607	M3	0.99	0.98	0.99	0.765	1.64	0.43E-1				
0.01	240	M4	0.98	0.91	0.99	0.765	11.97	2.37E-1			2760	717
0.01	350	M4	0.98	0.99	0.99	0.765	5.14	0.69E-1			338	45
0.01	607	M4	0.98	0.98	1.00	0.765	1.72	0.57E-1			303	129
0.01	240	M4	0.98	0.74	0.99	0.765	11.75	2.52E-3			11967	NF
0.01	350	M4	0.97	0.95	0.98	0.765	4.73	1.22E-1			4659	NF
0.01	607	M4	0.98	0.97	0.99	0.765	1.60	0.57E-1			1516	NF
1	240	M4	0.95	0.98	0.93	0.765	22.94	4.26E-1	0.5E-3	NF	11967	1419
1	350	M4	0.97	0.98	0.97	0.765	7.27	2.64E-1	0.3E-2	0.17E-2	4659	283
1	607	M4	0.98	0.97	0.81	0.765	1.69	1.09E-1	0.3E-2	0.22E-2	1516	129
0.005	350	M4	0.97	0.78	0.98	0.765	6.75	3.61E-1			4659	NF

NF – denotes not fitted

Figure 19 shows the corresponding retention profiles and reveals that MWCNT retention was highest close to the column inlet and then rapidly decreased with distance. Consistent with the BTCs shown in Figure 18, greater MWCNT retention occurred with decreasing sand size. Large deviations were observed between experimental and simulated RPs for models M1 and M2. The Pearson's correlation coefficient for the RP (R_{soil}^2) was less than 0.58. Models M1 and M2 tended to underestimate the high concentrations near the column inlet and overestimated the concentrations at greater distances, especially for coarser textured sand. Thus, RPs were not considered for fitting model parameters using models M1 and M2. These observations indicate that the experimental RPs were hyper-exponential with distance, and that the retention coefficient exhibited a depth-dependency. Models M3 and M4 include a depth-dependency in the retention coefficient, and therefore provided a much better description of the MWCNT RPs than either M1 or M2. The value of R_{soil}^2 for the M3 and M4 models was > 0.98. Model M4 provided the best overall description of the data when both BTCs and RPs were considered.

Hyper-exponential RPs have frequently been reported in the literature for colloids, microorganisms, and nanoparticles under unfavorable attachment conditions (Bradford and Bettahar, 2006; Bradford and Toride, 2007; Gargiulo et al., 2007a; Gargiulo et al., 2008; Wang et al., 2012a; Wang et al., 2011). A variety of reasons for hyper-exponential RPs have been identified, including: straining at grain-grain contacts and surface roughness locations (Bradford et al., 2003; Bradford et al., 2002; Shellenberger and Logan, 2001; Yoon et al., 2006), particle aggregation (Chatterjee et al., 2010; Chatterjee and Gupta, 2009; Chen and Elimelech, 2006, 2007), hydrodynamic factors (Bradford et al., 2009; Li et al., 2005; Wang et al., 2011), and chemical heterogeneity on the sand and the colloid (Bolster et al., 1999; Li et al., 2004; Tong and Johnson, 2006; Tufenkji and Elimelech, 2005). The relative contribution of each of these factors to the observed RP data is difficult to ascertain without additional information. However, the data does clearly indicate a strong dependency of the RP's shape on the grain size under low IS conditions. The contribution of physical processes to the observed hyper-exponential RPs has to be proven. However, other results in the literature indicate that straining played a dominant role in the CNT retention under low IS conditions (Jaisi et al., 2008; Wang et al., 2012b).

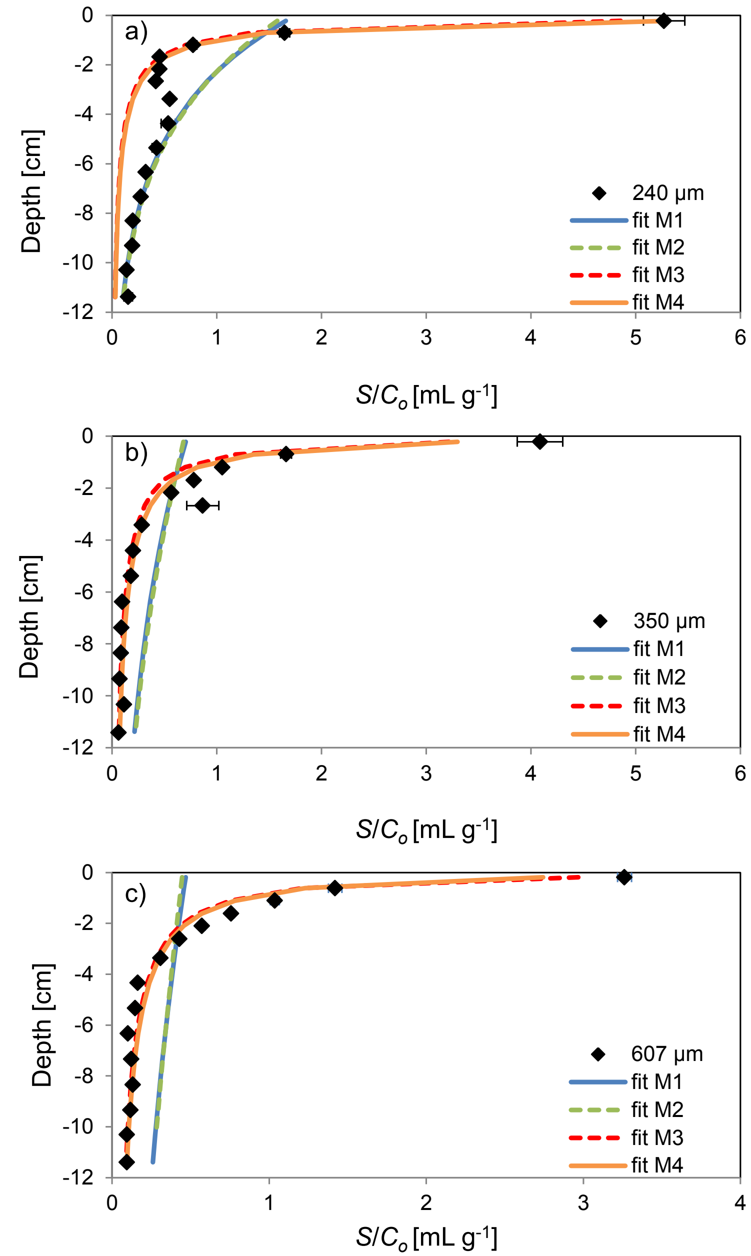

Figure 19. Observed and simulated retention profiles for MWCNTs in three different sized quartz sands: 240 µm (a), 350 µm (b), and 607 µm (c). Experimental data were simulated with four different models including: attachment and detachment (M1); attachment, detachment, and blocking (M2); depth-dependent retention (M3); and blocking combined with depth-dependent retention (M4). The flow rate was 0.62–0.66 cm min^{-1}, the electrolyte was 1 mM KCl, and the MWCNT input concentration was 0.01 mg L^{-1}.

Previous transport studies with CNTs measured and simulated only BTCs (Jaisi and Elimelech, 2009; Jaisi et al., 2008; Liu et al., 2009; Mattison et al., 2011). Determination and modeling of retention profile are scarce (Wang et al., 2012b). Accurate simulation of both BTCs and RPs is needed in order to assess the fate and risks associated with MWCNT migration. To illustrate this point, Figure 20 presents the simulated RPs of MWCNTs in the three different sized sands over a distance of 500 cm when using the various model formulations that were calibrated to the column BTC (M1 and M2) or BTC and RP (M3 and M4) data, respectively. In Figure 20 and the discussion below, the lower limit of the predicted S/C_o was set to 1E-5 mL g^{-1}. Increasing deviations in the model predictions occurred with transport distance and grain size. The M1 and M2 predictions were quite similar for a given grain size, with no breakthrough at a depth of 500 cm. The maximum transport distance predicted by the M1 and M2 models was around 200 cm in the coarsest textured 607 µm sand. In contrast, models M3 and M4 predict similar low levels of MWCNT breakthrough at 500 cm for the two largest grain sizes (350 and 607 µm). Consequently, using M1 and M2 to predict MWCNT fate would lead to the conclusion that MWCNTs will be retained in the various sands before reaching a depth of around 200 cm. In contrast, M3 and M4 would predict a transport of MWCNTs to depths greater than 500 cm. Since models M3 and M4 provided the best description of the BTCs and RPs at the column scale (Figure 18 and Figure 19), the predictions of these models are more reliable than the predictions obtained from the other two models (M1 and M2).

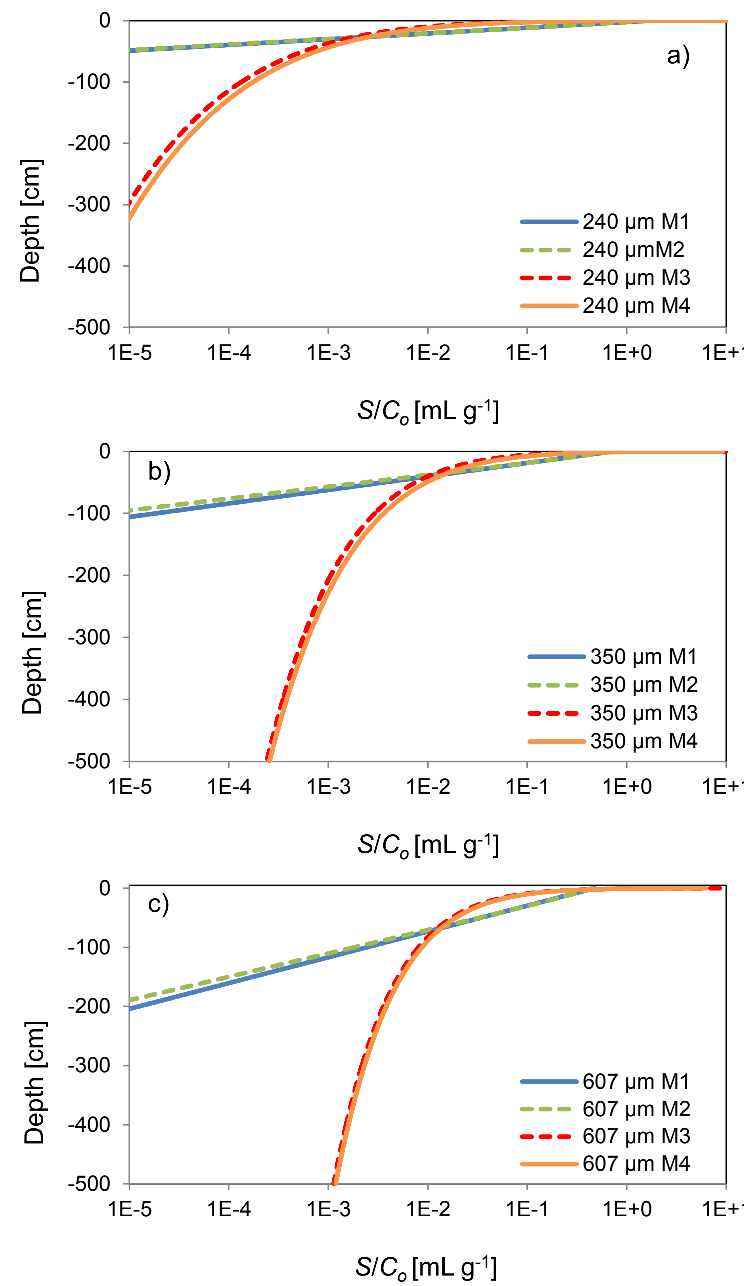

Figure 20. Predicted retention profiles for MWCNTs in 500 cm long columns packed with 240 µm (a), 350 µm (b), and 607 µm (c) sand. Here the normalized solid phase concentration (S/C_o) is plotted on a log-scale as a function of distance. Simulations employed model parameters determined in Figures 18 and 19. Four different model formulations were considered, namely: attachment and detachment (M1); attachment, detachment, and blocking (M2); depth-dependent retention (M3); and blocking combined with depth-dependent retention (M4).

4.2.2 Effect of input concentration

Additional column experiments were performed to investigate the influence of MWCNT input concentrations. Figure 21 presents observed and simulated BTCs (Figure 21a) and RPs (Figure 21b) for MWCNTs in 350 µm sand when q = 0.62–0.66 cm min^{-1}, IS = 1 mM KCl, and C_o = 1, 0.01, and 0.005 mg L^{-1}. Based on the findings of Chapter 4.2.1, only simulation results from model M4 were considered in Figure 21. Simulation fits to BTCs and RPs were very good, with a $R_{eff}^2 > 0.97$ and $R_{soil}^2 > 0.96$. Table 2 and Table 4 provide a summary of the associated experimental, mass balance, and model parameters.

Inspection of Figure 21a indicates that the fraction of the injected mass of MWCNTs that was recovered in the effluent increased with C_o. In addition, the shape of the BTC was much steeper for the highest C_o = 1 mg L^{-1} condition. These trends may be explained by blocking behavior as retention locations fill up over time and produce increasing effluent concentrations (Bradford and Bettahar, 2006). Consistent with observations in Figure 21a, a higher C_o is expected to fill a given number of retention locations ($S_{\max}$) more rapidly. The value of $S_{\max}$ was fitted for the highest C_o and then kept constant for the lower input concentrations. The fitted retention rate parameter k_1 was similar for all C_o. After recovery of the BTC, concentration tailing tended to be low, but was most pronounced for the highest C_o = 1 mg L^{-1} condition. This indicates that some of the MWCNT retention was reversible at higher C_o when $S_{\max}$ was filled to a greater extent (Kretzschmar et al., 1995).

Similar to the BTCs (Figure 21a), the shape of the RPs was also sensitive to C_o (Figure 21b). In particular, the fraction of MWCNTs retained close to the column inlet increased with decreasing C_o. Conversely, the RPs became less hyper-exponential (more uniform) with increasing C_o. Blocking provides an explanation for changes in the RP shape with C_o (Bradford and Bettahar, 2006; Bradford et al., 2009; Kim et al., 2011; Zhang et al., 2010). As MWCNT retention approaches $S_{\max}$ the overall rate of retention decreases and the RPs become uniform with depth (Bradford et al., 2009).

Results from Figure 21 demonstrate that C_o can have a large impact on the transport and retention behavior of MWCNTs. Enhanced retention and limited mobility of MWCNTs is expected for lower, more environmentally relevant concentrations of MWCNTs. These C_o effects need to be considered in models that are used to predict MWCNT fate and risk, otherwise they may overestimate their transport potential and groundwater concentrations.

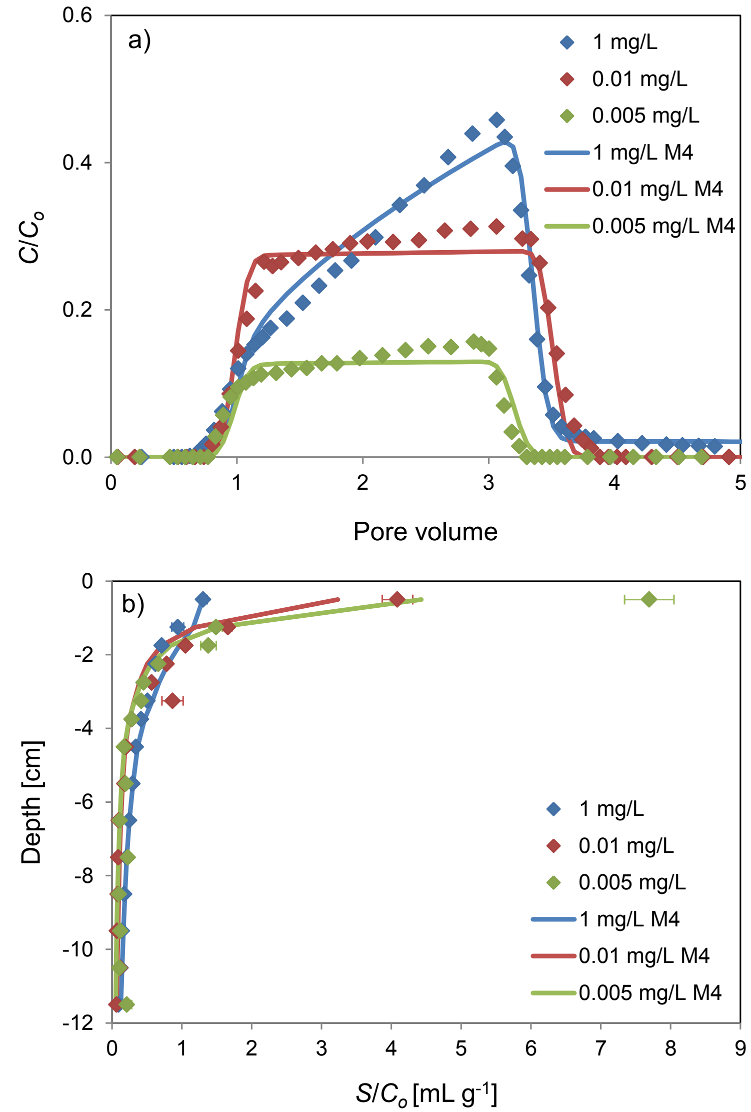

Figure 21. Observed and simulated breakthrough curves (a) and retention profiles (b) for MWCNTs at input concentrations (C_o) equal to 1, 0.01, and 0.005 mg L^{-1}. The flow rate was 0.62-0.66 cm min^{-1}, the electrolyte was 1 mM KCl, and the grain size of the quartz sand was 350 µm. The data was simulated using a model combining depth- and time-dependent retention (M4).

4.2.3 Effect of grain size and input concentration

Figure 22 presents observed and simulated BTCs (Figure 22a) and RPs (Figure 22b) for MWCNTs in three different sized sands (240, 350, and 607 µm) when q = 0.62–0.66 cm min^{-1}, IS = 1 mM, and C_o = 1 mg L^{-1}. Simulation results from model M4 were considered in Figure 22. Simulation fits to BTCs and RPs were good, with a $R_{eff}^2 > 0.97$ and $R_{soil}^2 > 0.81$. Table 2 and Table 4 provide a summary of the associated experimental, mass balance, and model parameters. Similar to Figure 18 and Figure 19, Figure 22 examines the influence of grain size on MWCNT transport and retention. However, the experiments shown in Figure 22 were conducted at a C_o that was two orders of magnitude higher than in Figure 18 and Figure 19.

Comparison of Figure 18, Figure 19, and Figure 22 reveals a similar trend of increasing MWCNT retention (decreasing breakthrough) with decreasing grain size at both C_o levels. In contrast, the time-dependent blocking behavior shown in the BTCs (e.g., increase in the normalized effluent concentrations shown in Figure 18 and Figure 22a) was much steeper for experiments conducted at the higher C_o. The RPs were also more hyper-exponential at the lower C_o (see Figure 19 and Figure 22b). As explained in Chapter 4.2.2, these trends occur because retention locations were filled more rapidly at a higher C_o. However, close inspection of Figure 18, Figure 19, and Figure 22 indicates that this concentration-dependent transport behavior was also a function of the sand grain size.

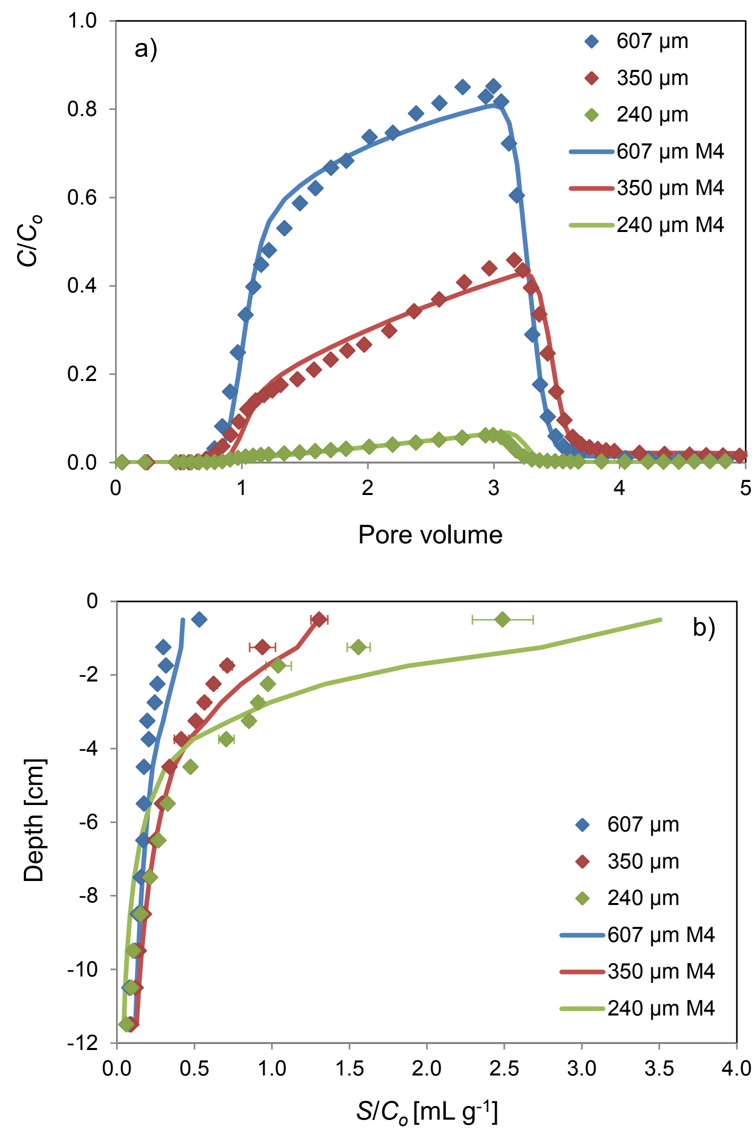

Figure 22. Observed and simulated breakthrough curves (a) and retention profiles (b) for MWCNTs in three different sized quartz sands: 240 µm (a), 350 µm (b), and 607 µm (c). The flow rate was 0.62-0.66 cm min^{-1}, the electrolyte was 1 mM KCl, and the MWCNT input concentration was 1 mg L^{-1}. The data was simulated using a model combining depth- and time-dependent retention (M4).

Examination of parameters k_1 (Figure 23a) and S_{max} (Figure 23b) as a function of grain size for the two C_o levels revealed that the values of k_1 and S_{max} both increased with decreasing grain size. As mentioned above, this reflects greater MWCNT retention rates and number of retention locations in the finer textured sand. However, higher C_o values accentuated this trend with k_1 and this rate of enhancement increased with decreasing grain size. Hence, the observed concentration dependency of MWCNT transport became more important with increasing C_o and decreasing grain size. In contrast to these observations with MWCNTs, Bradford and Bettahar (2006) observed for spherical latex microspheres that concentration-dependent colloid transport behavior became more important with increasing grain size. These trends can be explained by the effect of porous media's pore structure on MWCNT retention (Tan et al., 1994). The non-spherical MWCNTs have a high aspect ratio and it is hypothesized that solid phase MWCNTs may create a porous network with the ability to retain particles (Sumanasekera et al., 2010; Xin et al., 2012). It is logical to anticipate that the retained MWCNT network will become more significant at higher C_o and in smaller grain sized sand. This finding suggests that the particle shape will have a strong influence on concentration-dependent colloid transport.

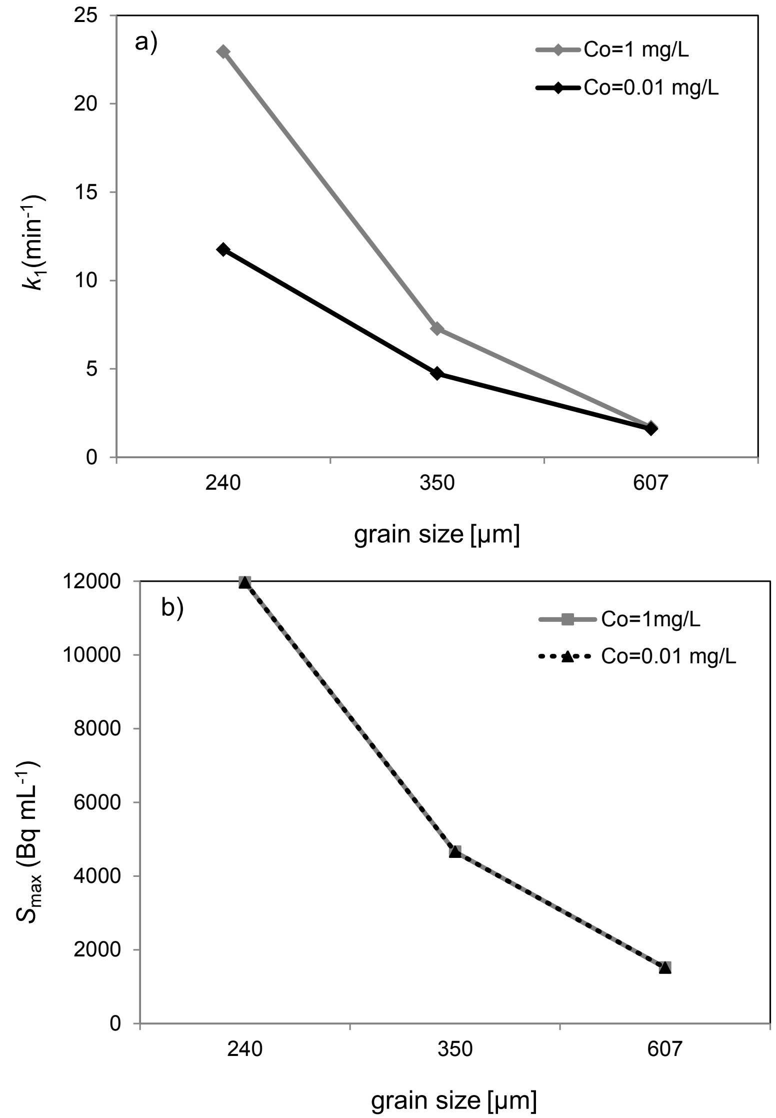

Figure 23. Plots of the depth-dependent (model M4) retention coefficient (k_1) (a) and the maximum solid phase particle concentration (S_{max}) (b) as a function of sand grain size for input MWCNT concentrations (C_o) of 1 and 0.01 mg L^{-1}.

4.2.4 Transport of carbon nanotubes with flow interruption

To investigate the influence of flow interruption on MWCNT transport, a transport experiment with intermittent flow conditions was performed as described in Chapter 3.6. The most important parameters for this experiment are summarized in Table 5.

Table 5. Experimental conditions, hydraulic parameters, fitted model parameters, and mass balance information (as fractions of the total applied mass; eff - effluent, sand - profile) for the intermittent flow experiment. Quartz sand with an average grain size of 350 µm served as porous medium, the electrolyte was 1 mM KCl, the flow rate was 0.64 cm min^{-1}, and C_o was 1 mg L^{-1}. A β of 0.765 was used for parameter estimation.

C_o [mg L^{-1}]	Type of soil/d_c [µm]	Flow rate q [cm min^{-1}]	Porosity	Disp.[a] [cm]	CNT eff_1[b]	CNT eff_2[c]	CNT sand[d]	Total mass balance
1	350	0.64	0.41	0.047	0.57	0.03	0.33	0.93

[a] Disp. is the longitudinal dispersivity estimated on basis of the conservative tracer BTC
[b] CNT eff_1 is the total amount of MWCNTs in the liquid phase in the first peak
[c] CNT eff_2 is the total amount of MWCNTs in the liquid phase after flow interruption
[d] CNT sand is the total amount of MWCNTs in the solid phase

Since quartz sand and MWCNTs were both negatively charged (Chapters 3.3 and 4.1), the presence of unfavorable attachment conditions was assumed. At these conditions, pore straining was expected to be the major mechanism for colloid retention in porous media (Grassian, 2008). Figure 24 shows the observed BTC (a) and RP (b) after the flow interruption and the second period of flushing with KCl. Two peaks of MWCNT breakthrough were observed for this experiment: the first peak reflects the BTC of the MWCNTs in the saturated sand, and the second peak the release of MWCNTs after flow interruption for 18 h. The second peak indicates that the flow interruption resulted in a remobilization of retained MWCNTs, although the amount of particles quantified in this peak was relatively low (approx. 3%). This suggests that the interactions between MWCNTs and sand grains are partially reversible, indicating that straining is the dominant mechanism for MWCNT retention but that attachment also occurs.

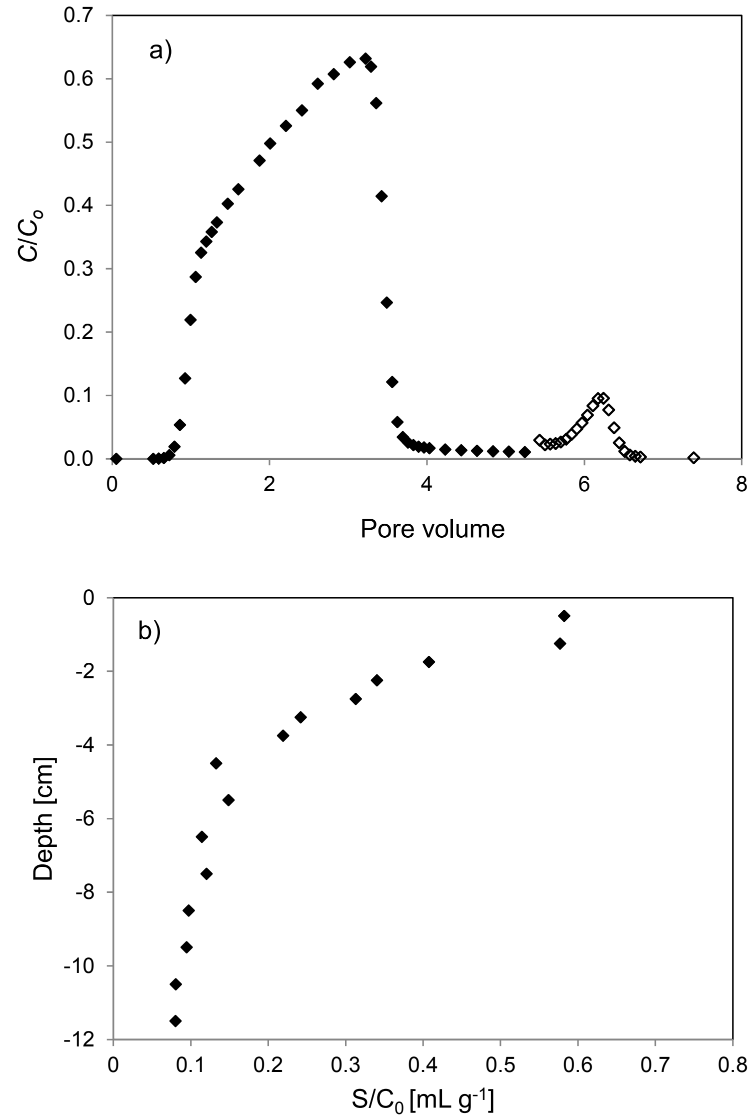

Figure 24. Breakthrough curve (a) and retention profile (b) for MWCNTs in a saturated sand column experiment with intermittent flow conditions. The MWCNT input concentration (C_o) was 1 mg L^{-1}, the flow rate was 0.64 cm min^{-1}, the electrolyte was 1 mM KCl, and the grain size of the quartz sand was 350 μm.

Kim et al. (2010) reported a successive release of retained oocysts (a stage of development of unicellular organisms) after several steps of flow interruption and flushing with deionized water where the release peaks became smaller with each step. They stated that this effect might be due to the release of oocysts retained by weak attractive forces and in low velocity regions by flushing after flow interruption. Their results support the statement that classic theories (CFT and DLVO) have limitations in quantifying the transport and retention mechanisms of colloids (Kim et al., 2010). It is known, that colloid transport in porous media is affected by the water flow regime and that transient flow can enhance colloid detachment from porous media (Zhang et al., 2012). The results of this flow interruption experiment indicate that a remobilization of functionalized MWCNTs in environmental compartments might be possible as flow conditions are not constant. For example, high flow rates can be present in natural soil due to heavy rainfall and a high infiltration rate and thus, remobilize retained particles. Furthermore, consecutive water pulses could be used for remediation of contaminated aquifers (Brusseau et al., 1989). Nevertheless, it has to be considered that quartz sand was investigated here and that saturated conditions and high flow rates were present in this experiment.

4.3 Transport of carbon nanotubes in natural soils[3]

In addition to the experiments in quartz sand, experiments were performed in repacked and undisturbed soil columns under water-saturated and -unsaturated conditions, respectively. A more heterogeneous pore size distribution and different pore water chemistry in soil compared to quartz sand were expected. Two soil types with different physico-chemical properties and texture were used. A detailed description of the soils is provided in Chapter 3.4. The aim of these experiments was to investigate the influence of soil structure and texture as well as water content on MWCNT transport.

4.3.1 Transport in disturbed soil under water-saturated conditions

A transport experiment was performed in a column packed with the loamy sand soil (KAL, < 2mm) under water-saturated conditions at high flow rates (0.64 cm min^{-1}) using a MWCNT concentration of 1 mg L^{-1}. The negative charge on both MWCNTs and soil (Chapters 3.4 and 4.1), and the low ionic strength conditions (1 mM KCl) suggest that highly unfavorable attachment conditions existed for MWCNTs during the transport experiments. The observed RP and BTC (Figure 25) were simultaneously numerically modeled using M4 accounting for time- and depth-dependent behavior. The associated experimental, mass balance, and model parameters are summarized in Table 2 and Table 6.

Table 6. Fitted model parameters for the breakthrough curve and retention profile of MWCNTs in water-saturated, disturbed soil. Correlation of observed and fitted data is reflected by R^2.

C_o [mg L^{-1}]	R^2	β	S_{max} [Bq g^{-1}]	Standard error S_{max}	k_1 [min^{-1}]	Standard error k_1	k_2 [min^{-1}]	Standard error k_2
1.00	0.98	0.765	6728	374	10.69	0.37	0.007	NF

NF – denotes not fitted

Similar as for the sand columns (Figure 22), the BTC of MWCNTs in disturbed soil at water-saturated conditions (Figure 25a) showed a slow increase of C/C_o with time indicating that blocking occurs. The shape of the RPs was also hyper-exponential (Figure 25b) which refers to straining.

[3] Contains parts from "Environmental Pollution 180, Kasel, D., Bradford, S. A., Šimůnek, J., Pütz, T., Vereecken, H., Klumpp, E., Limited transport of functionalized multi-walled carbon nanotubes in two natural soils. 152-158, 2013", with permission from Elsevier.

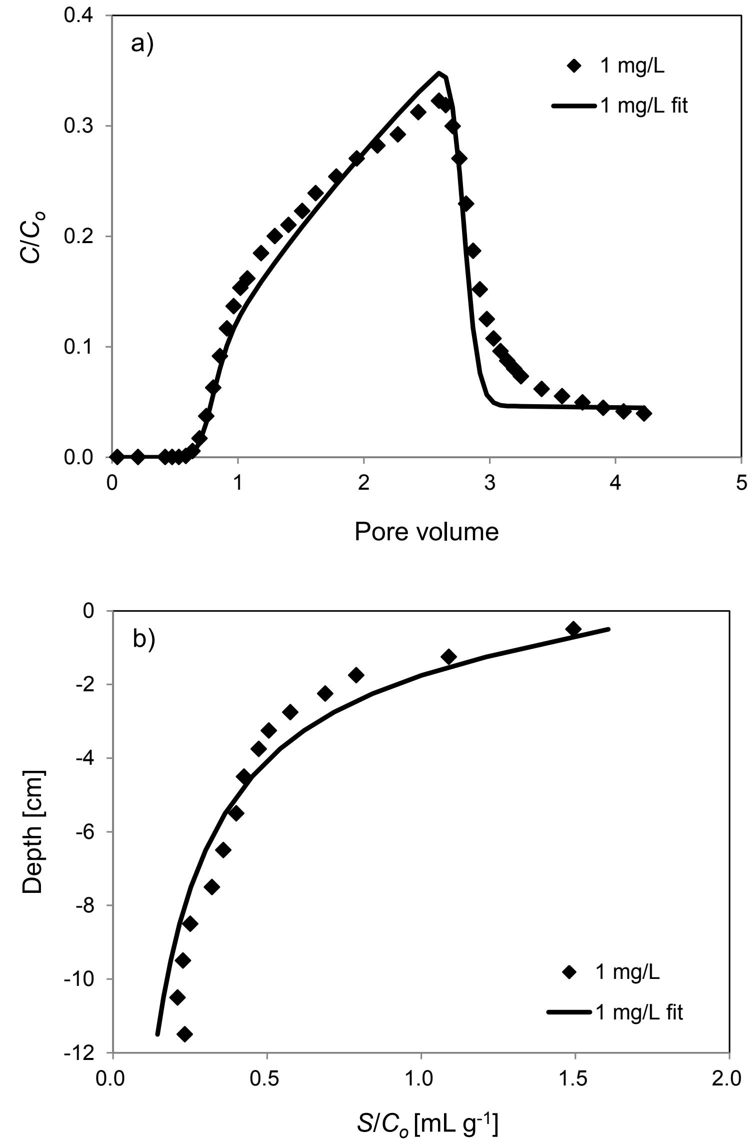

Figure 25. Observed and simulated breakthrough curves (a) and retention profiles (b) for MWCNTs at an input concentrations (C_o) equal to 1 mg L^{-1}. The experiment was conducted in a column packed with soil (< 2mm) from the test site KAL. The flow rate was 0.64 cm min^{-1}, the electrolyte was 1 mM KCl. The data was simulated using a model combining depth- and time-dependent retention (M4).

Around 30% of the applied MWCNTs were found in the column effluent and about 60% were recovered in the soil profile (Table 2). This indicates a certain mobility of MWCNTs in the disturbed sandy loam soil at water-saturated conditions. Possible explanations for this result may be the relatively homogenous pore size distribution due to the uniform packing of sieved soil and the high flow rate.

The concentration tailing observed in the BTC (Figure 25a) indicates that some of the MWCNT retention was reversible when flushing with background solution (Kretzschmar et al., 1995). In general, tailing is an indicator for colloid detachment (Mattison et al., 2011). The model simulations resulted in a detachment coefficient k_2 of 0.007 min^{-1} (Table 6) supporting the hypothesis that some detachment of MWCNTs took place in the disturbed soil column.

Jaisi and Elimelech (2009) report little transport (< 10%) of functionalized SWCNTs in saturated columns packed with the sand fraction of a soil (420–1,000 µm). Furthermore, they expect only limited transport of SWCNTs in soils and no risk of groundwater contamination. In contrast, Fang et al. (2013) found high mobility (up to 85%) of surfactant stabilized MWCNTs in different disturbed soils (< 1,000 µm) at water-saturated flow and predict a transport to layers > 30 cm and thus the possibility of groundwater contamination. A high mobility (up to 90%) in homogenous soil columns under water-saturated conditions was also described for TiO_2 nanoparticles (Fang et al., 2009).

Reliable predictions on the environmental fate of MWCNTs are difficult based on the results discussed in this chapter. Therefore, experiments considering more environmentally relevant scenarios (e.g., low flow rates, undisturbed soil, no surfactants, water-unsaturated conditions) were performed for this thesis.

4.3.2 Transport in undisturbed soil at two water-saturation levels

Transport and retention of MWCNTs in an undisturbed soil core of the loamy sand soil (KAL) were investigated at water contents close to saturation (approx. 96% and 85%, respectively).

There was no detectable breakthrough of MWCNTs in the soil core at a water content of 96%. Quantification of the retention profile (Table 7) revealed that 91% of MWCNTs were retained in the soil. The main fraction of MWCNTs was retained close to the column inlet and the retention profile exhibited a hyper-exponential shape. The same shape was observed in the described experiments for functionalized MWCNTs in saturated sand columns in Chapter 4.2 and was attributed to a depth-dependent retention mechanism. The determined retention profile for the soil column was simulated using M3 and is shown in Figure 26. The retention coefficient accounting for depth-dependency was able to describe the shape of the experimental RP well.

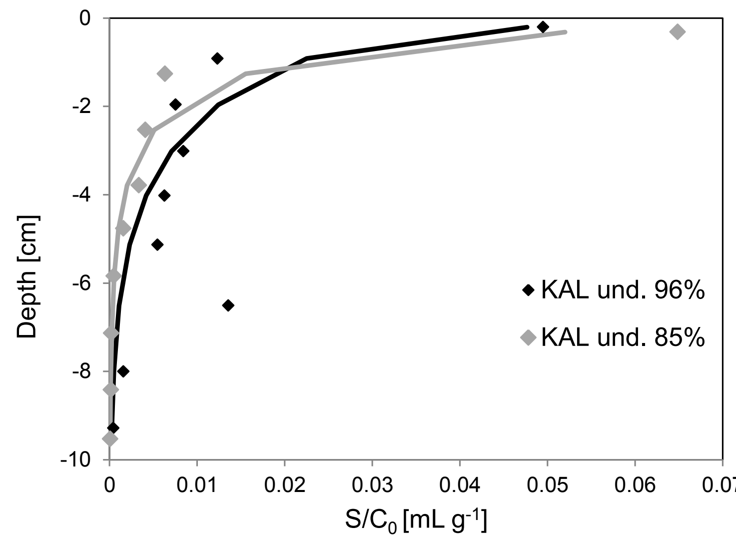

Figure 26. Observed and simulated retention profiles for MWCNTs in undisturbed (und.) loamy sand soil cores from the test site in Kaldenkirchen-Hülst (KAL) at two water-saturation levels (85 and 96%). For detailed experimental conditions see Table 2. The dots are the experimental data and the lines represent the model fits.

At lower water saturation (approx. 85%), no breakthrough of MWCNTs was observed and 98% of the applied radioactivity was detected in the soil profile. The shape of the retention profile was also hyper-exponential (Figure 26) and was fitted well using a model including a depth-dependent retention term (M3).

Though both experiments were performed at different water-saturation levels and thus, different amounts of air in the column, the retention profiles were similar. Complete retention occurred already at 96% water-saturation but reduction of the water content to 85% changed the MWCNT distribution in the soil. When comparing the profiles (Figure 26), the MWCNT concentrations in layers deeper than 2 cm were higher at the higher water content than for the lower water content. This implies that MWCNT transport was slightly enhanced at the higher water content. An increase in retention was expected with decreasing water-saturation because of a larger air-water interfacial area and a greater amount of flow through small pore spaces (Gargiulo et al., 2008). In contrast to the expected trend, the fitted retention coefficient (k_1) was higher at the higher water content (Table 7). One potential explanation is the insensitivity in the retention coefficient k_1 when complete retention occurs. In this case, higher values of k_1 will produce similar amounts of retention. This hypothesis is supported by the high standard error for k_1 for the experiment at 85% water content (Table 7).

Table 7. Fitted model parameters for the retention profiles of the different experiments. Correlation of observed and fitted data is reflected by R².

Type of core	Soil type	Water saturation [%]	R^2	β	k_1 [min^{-1}]	Standard error k_1	k_2 [min^{-1}]	Standard error k_2
Und	KAL	96	0.89	0.765	10.93	16.87	0.62E-02	0.89E-02
Und	KAL	85	0.96	0.765	2.56	1.55	0.16E-02	0.13E-02
Rep	KAL	96	0.86	0.765	0.42	0.59	NF	NF
Und	MRZ	95	0.97	0.765	0.21	0.25	NF	NF

NF – denotes not fitted
Und – Undisturbed
Rep – Repacked

Nevertheless, for both experiments, no significant transport to distances greater than 10 cm occurred and the highest fraction of MWCNTs was retained in the top layer of the soil. In consistency with these results, Jaisi and Elimelech (2009) reported limited transport of CNTs in a particular fraction of soil (420-1000 µm) in water-saturated column experiments. Based on their findings and the presented results, it is assumed that there is no transport of functionalized MWCNTs through the studied loamy sand soil at water contents lower than 85%.

It is known that CNT suspensions can be stabilized by natural organic matter (Hyung et al., 2006) and that humic acid can enhance CNT transport (Wang et al., 2008). Nevertheless there was no breakthrough of MWCNTs in the loamy sand soil containing about 1% organic carbon. Similarly, Wang et al. (2010) observed complete retention of fullerene (C_{60}) nanoparticles in saturated columns packed with two different soils containing 0.75% and 3.3% organic carbon, respectively. One possible explanation for the high retention of MWCNTs in soils compared to quartz sand might be adsorption via negatively charged carboxylic groups of the MWCNTs onto positively charged metal oxides. However, the iron content of the soil from KAL was relatively low (Table 1). Thus, it was assumed that physical factors (e.g., straining) play a dominant role for the MWCNT retention in soil (Jaisi and Elimelech, 2009). Since MWCNTs are non-spherical particles, they are easily trapped in small pore spaces and may create additional retention locations (Pan and Xing, 2012). Another reason for enhanced MWCNT retention may be the low, but environmentally relevant, flow rate (0.006 and 0.008 cm min^{-1}) in the described experiments. It is already known, that the flow rate strongly influences MWCNT transport and that retention increases with decreasing flow rate (Liu et al., 2009). In addition, the chemical heterogeneity of soils may also enhance MWCNT retention compared to quartz sand (Pan and Xing, 2012). Aggregation also influences CNT mobility in porous media (Pan and Xing, 2012) but could not be measured in this study.

In summary, results show that even at water contents close to saturation (96%) no detectable breakthrough of functionalized MWCNTs occurred in undisturbed cores of the loamy sand soil from KAL. The observed high retention of MWCNTs in soil at experimental conditions might be due to an interplay of low flow rate (Liu et al., 2009), soil composition (Fang et al., 2009), heterogeneous pore size distribution (Pan and Xing, 2012), and the presence of an air phase (Gargiulo et al., 2008). Based on the results of the environmentally relevant setup (undisturbed soil core, precipitation from the top, point application of MWCNTs, leaching from top to bottom, and low particle concentrations) no significant transport of MWCNTs in the loamy sand soil through the vadose zone is expected.

4.3.3 Comparison of undisturbed and repacked soil at water-unsaturated conditions

An additional experiment was performed in a repacked column with soil from KAL at a water content of approx. 96% and compared with the experiment performed in the undisturbed column at the same conditions (Figure 27). The dispersivity of the undisturbed soil column was almost twice as high as that for the repacked column (Table 3), indicating more heterogeneity in the undisturbed soil (Unold et al., 2009b). Additionally, the conservative tracer BTCs (data not shown) were described well for both repacked and undisturbed soil columns using the classical ADE model. This finding indicates that physical non-equilibrium processes (e.g., preferential flow) did not play a dominant role in these experiments (Unold et al., 2009b). In general, preferential flow will be more prominent in fully water-saturated media because macropores drain fast when the water level falls below full saturation, unless high rainfall intensities occur (Beven and Germann, 1982).

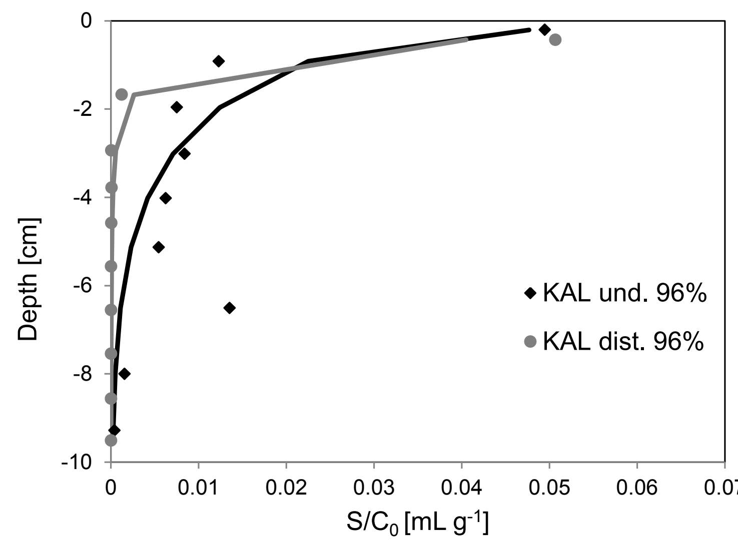

Figure 27. Observed and simulated retention profiles for MWCNTs in a disturbed (dist.) soil column from the test site in Kaldenkirchen-Hülst (KAL) compared with the previously shown RP for the undisturbed soil column from the same test site. The water-saturation was around 96%. For detailed experimental conditions see Table 2. The dots are the experimental data and the lines represent the model fits.

The transport results were similar for both undisturbed and repacked column experiments. The only difference was that the MWCNT concentration in layers deeper than 2 cm was higher in the undisturbed soil compared to the disturbed soil (Figure 27). This observation suggests a higher transport potential in the undisturbed soil. Nevertheless, no breakthrough was found in both columns. In the repacked column, more than 86% of MWCNTs were recovered in the RP which also exhibited a hyper-exponential shape (Figure 27). This result indicates that the structure of the undisturbed loamy sand soil was very homogenous without fractures or macropores, similar to the structure of the repacked soil column.

The saturated transport experiment with disturbed soil from KAL (Chapter 4.3.1) revealed certain mobility (approx. 30%) of MWCNTs. In contrast, the experiment with the same soil at unsaturated conditions presented in this chapter resulted in complete retention of MWCNTs in the soil. One possible explanation could be the presence of air in the unsaturated experiments. But, more important seems to be the role of the flow rate (Liu et al., 2009). The flow rate of the water-saturated experiment (0.64 cm min^{-1}) was about two orders of magnitude higher than for the unsaturated column (0.0067 cm min^{-1}). The sensitivity of CNT transport to the flow rate indicates that straining is an operative mechanism (Li et al., 2004). The increase of CNT breakthrough with increasing flow rate can also be explained by a decreased number of collisions between particles and collectors at high flow rates (Li et al., 2004; Liu et al., 2009). Thus, the experiments are only comparable when the same flow conditions are applied which can be difficult due to technical limitation of the setups.

4.3.4 Transport in undisturbed soil from two test sites at unsaturated conditions

In addition to the previously described experiments with a loamy sand soil, an experiment with a silty loam soil (MRZ) at conditions close to water-saturation (96%) was performed. In general, soil from MRZ was expected to exhibit stronger sorption than the loamy sand soil from KAL due to a higher clay content which causes a larger specific surface area (Unold et al., 2009b). Surface deposition and physical straining are expected to be the dominant retention mechanisms for CNT retention in soil (Fang et al., 2013; Jaisi and Elimelech, 2009).

Nevertheless, various factors influence the mobility of CNTs in soils. Soil texture (e.g., clay content) affects the pore size distribution in the soil and thus, straining. In agreement with this, Fang et al. (2013) found that the transport of surfactant stabilized MWCNTs through various soils was negatively correlated with the soil clay content. For TiO_2 nanoparticles, Fang et al. (2009) described a significantly increased retention with increasing salinity and clay contents.

The comparison of KAL and MRZ soils at similar experimental conditions did not reveal any detectable differences in transport behavior of MWCNTs in both soils. No MWCNT breakthrough was detected and more than 90% was recovered in the soil profile of MRZ soil (Figure 28). The retention profiles in the two soils were very similar despite significant differences in their dispersivity and porosity (Table 3). In fact, the MWCNT concentration in layers deeper than 2 cm was slightly higher for the KAL soil that had less clay. Thus in the absence of preferential flow, no transport of MWCNTs through the vadose zone in the MRZ soil is expected because of its higher clay content and lower water contents.

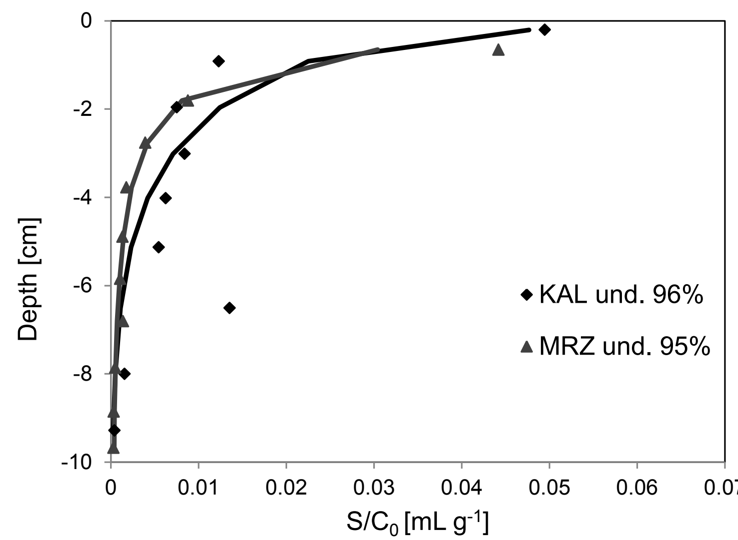

Figure 28. Observed and simulated retention profiles for MWCNTs in an undisturbed silty loam soil from the test site in Merzenhausen (MRZ) compared with the previously shown RP for the undisturbed loamy sand soil from the test site in Kaldenkirchen-Hülst (KAL). The water-saturation was around 96%. For detailed experimental conditions see Table 3. The dots are the experimental data and the lines represent the model fits.

In summary, results indicated that the transport behavior of MWCNTs was not significantly different for these two soils. It is hypothesized that physical filtration mechanisms are the dominant processes controlling MWCNT retention in these natural soils. These processes are expected to be influenced by water content (Gargiulo et al., 2007a), flow rate (Liu et al., 2009), and particle concentration (Bradford and Bettahar, 2006).

4.3.5 Transport in a soil lysimeter

In addition to the laboratory experiments, a lysimeter study was performed to investigate the transport of MWCNTs on a larger scale over a longer time period. The lysimeter experiment also represents intermittent flow conditions.

The results of the lysimeter experiment revealed that 100% of the bromide tracer was recovered in the effluent after 107 days. In dramatic contrast, no radioactivity was detected in the lysimeter effluent after 220 days (Figure 29a) even at a relatively high irrigation rate (1200 mm y^{-1}). Therefore, the lysimeter experiment was stopped and the MWCNT distribution in the soil profile was determined. The corresponding RP (Figure 29b) exhibited the same hyper-exponential shape as in repacked and undisturbed columns.

The main fraction of MWCNTs was retained in the upper 20 cm of the soil column. Consistent with the findings of Jaisi and Elimelech (2009) and the unsaturated column experiments (Chapters 4.3.2 and 4.3.3), this indicates that no significant MWCNT transport occurred in the undisturbed loamy sand soil under unsaturated conditions.

No effect of the irrigation events on MWCNT breakthrough was observed which suggests that the effect of intermittent flow might not be as relevant for unsaturated conditions in undisturbed soil compared to saturated flow in sand (Chapter 4.2.4). Furthermore, no preferential flow resulting in a fast transport and thus a detectable concentration of MWCNTs in the leachate was proven for the loamy sand soil from KAL. In addition, it is known that the flow rate strongly influences MWCNT transport in porous media (Liu et al., 2009). One reason for the breakthrough of MWCNTs in the disturbed saturated soil (Chapter 4.3.1) may be the high flow rate applied in this experiment. Since there was no high, continuous flow applied to the lysimeter it is not surprising that transport was limited.

Finally, the lysimeter experiment proved that complete retention of MWCNTs occurred in the undisturbed loamy sand soil from the test site KAL for a time period of 8 months. Nevertheless, the influence of certain weather conditions (e.g., oversaturation due to heavy rainfall, drainage and imbibition) and environmental factors (e.g., preferential flow paths, soil type, uptake by organisms) generally need to be considered when evaluating potential risks of MWCNTs to humans and the environment.

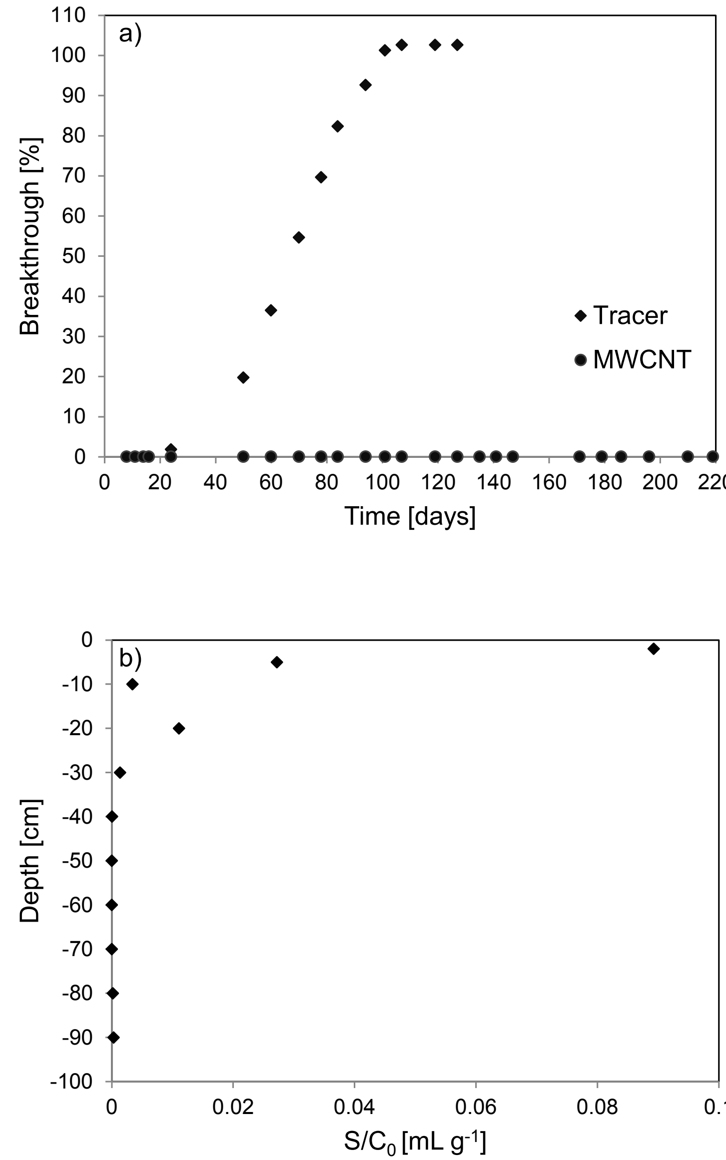

Figure 29. Cumulative breakthrough of tracer (Br^-) and radiolabeled MWCNTs (a) as well as an averaged retention profile (b) 220 days after application of MWCNTs to a lysimeter. The lysimeter was filled with an undisturbed loamy sand soil from the test site Kaldenkirchen-Hülst.

4.4 Outlook: Influence of carbon nanotubes on transport and deposition of chlordecone in soils

On the one hand, carbon nanotubes were considered for soil and groundwater remediation (Chapter 1.1) and may therefore have a potential to decontaminate soils polluted with chlordecone (CLD). On the other hand, a remobilization of the strongly retained CLD in the presence of CNTs might be also possible. Furthermore, CNTs could also enhance the retention of CLD and thus increase its persistence in soil. Therefore, investigations into the effect of MWCNTs on the mobility of CLD are of special interest and may be a promising topic for further research. In this study, sorption isotherms of CLD onto a loamy sand soil (KAL) and functionalized MWCNTs were determined.

The adsorption isotherm for CLD onto the loamy sand soil from KAL is shown in Figure 30. In control experiments without soil, 100% of the applied CLD was recovered in the solution after equilibration for 24 h. This indicates that there was no adsorption onto the glass wall or the cap of the centrifuge tubes. A linear regression of the adsorption isotherm yielded a sorption coefficient (K_d) of 56 L kg^{-1} with a R^2 of 0.99.

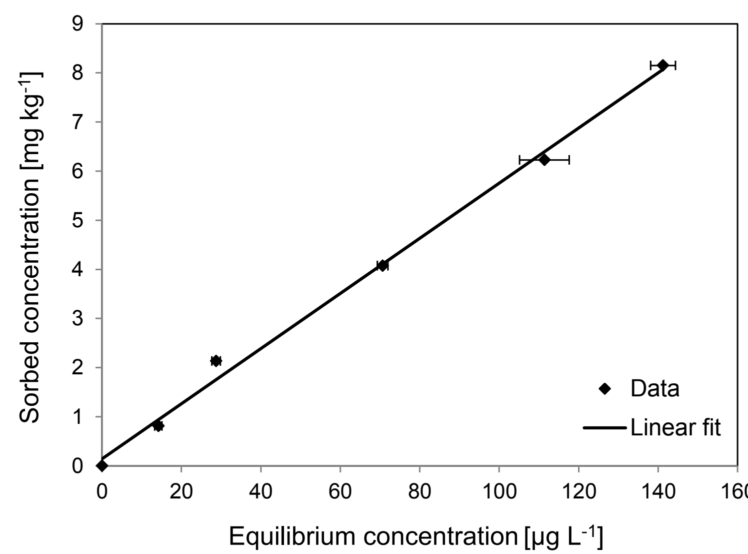

Figure 30. Adsorption isotherm of chlordecone onto the loamy sand soil (KAL).

The partition coefficient K_d is not only influenced by the properties of the solute (e.g., solubility, octanol-water partition coefficient, vapor pressure), but also by the physico-chemical composition of the soil (e.g., electrolytes in the soil solution, clay minerals, oxides and hydroxides, organic material) (Blume et al., 2010). The determined high value indicates a relatively high removal rate of CLD from water by the loamy sand soil which was expected because of the hydrophobic properties of CLD. Since most of the organic solutes preferably adsorb onto the soil organic matter, the linear relation between the equilibrium liquid and solid phase concentration of hydrophobic organic solutes is often referred to as a partition process in the soil organic matter (Blume et al., 2010; Li, 2011).

Based on the assumption that CLD was adsorbed on the organic matter of the soil, the K_d was normalized by the organic carbon content of the soil (Table 1) and resulted in a K_{oc} of 5090 L kg^{-1}. This is in the range of the known literature values for the K_{oc} of CLD which are reported to range between 2500 L kg^{-1} and 20,000 L kg^{-1} (Woignier et al., 2012). This K_{oc}-value indicates that the hydrophobic adsorption of CLD onto this soil was controlled by the interaction between CLD and the organic carbon of the soil (Li et al., 2012b). In general, a high K_{oc}-value represents limited mobility of organic chemicals which is consistent with the aforementioned persistent contamination of soils in the French West Indies. Fernández-Bayo et al. (Fernández-Bayo et al., 2013) reported a strong linear sorption of CLD onto soil and a high K_{oc}-value. They also found that the sorption of CLD was not only influenced by the amount of organic matter but also by its composition and structure. In conclusion, they hypothesized that even in soils with low organic carbon content, a high sorption of CLD can occur.

The adsorption isotherm for CLD onto functionalized MWCNTs is shown in Figure 31 and demonstrates a strong adsorption of CLD onto the functionalized MWCNTs. The data were corrected for adsorption of CLD onto the PTFE of the dialysis half-cells. The isotherm was successfully fitted using the Freundlich model (R^2 = 0.99). Thereby, the estimated values for the two parameters were K_F = 229 $\mu g^{(1-1/n)}$ $L^{1/n}$ g^{-1} and n = 1.49. In consequence, 1/n was 0.67, indicating that adsorption occurred at relatively heterogeneous surfaces (Blume et al., 2010). Pan and Xing (2008) state that the presence of high energy adsorption sites (e.g., functional groups) may be one possible explanation for the heterogeneous adsorption of organic chemicals onto CNTs. The K_F-value describes the affinity of the adsorbate onto the surface of the adsorbent (Blume et al., 2010). The strong adsorption of CLD onto the MWCNTs is in agreement with the results of Yan et al. (2008) who observed strong adsorption of atrazine onto MWCNTs and were also able to describe the isotherm using the Freundlich model.

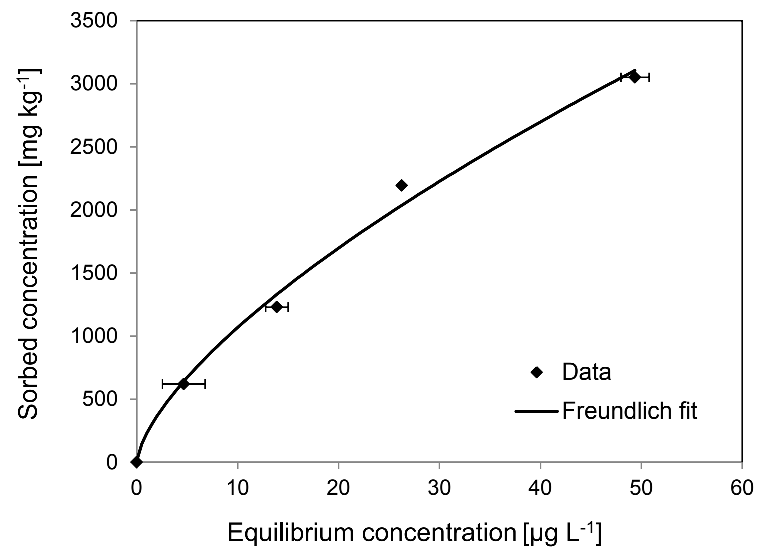

Figure 31. Adsorption isotherm of chlordecone onto functionalized multi-walled carbon nanotubes.

The estimated K_d-value for the adsorption isotherm of CLD onto the functionalized MWCNTs was 60,000 L kg^{-1} (R^2 = 0.95). The K_d was three orders of magnitude higher than for the loamy sand soil (56 L kg^{-1}). This proves that there was a strong adsorption of CLD onto the functionalized MWCNTs. Thus, it can be hypothesized that MWCNTs might influence the mobility of CLD in the soil.

It was proven that the modified MWCNTs contained functional groups (e.g., carboxylic groups; Chapter 4.1). These may also affect the adsorption of chemicals. The negative charge of the MWCNTs increases with an increasing pH-value because of enhanced deprotonation of the functional groups (Li, 2011). The importance of the amount of carboxylic groups on the adsorption of organic chemicals was investigated by Cho et al. (2008). They reported a decrease in naphthalene adsorption onto MWCNTs with an increasing level of adsorbent oxidation. This effect can be explained by increased polarity of the MWCNTs after functionalization (Cho et al., 2008). Although, the MWCNTs used in this study demonstrably contained carboxylic groups (Chapter 4.1), they exhibited a strong adsorption capacity for CLD.

To investigate the effect of the MWCNTs on the transport and retention of CLD in the soil, various experiments are of interest. First, a normal column transport experiment could be performed with CLD in the soil from KAL. Based on the determined adsorption isotherm, limited transport of CLD through the loamy sand soil is expected. Thus, a high retention of CLD is very likely in the top layer of the soil.

Since CLD also strongly adsorbs onto MWCNTs and a breakthrough of 30% of the particles was found in a disturbed water-saturated soil at high flow rates (Figure 25), a simultaneous injection of these two compounds would be of interest to investigate the MWCNT-facilitated transport of CLD. In similar experiments, Fang et al. (2013) showed that, in the presence of surfactants, MWCNTs could enhance the mobility of phenanthrene depending on the soil type. They also showed that in soils with a high adsorption affinity, the phenanthrene adsorbed to the MWCNTs was stripped off and retained in the soil (Fang et al., 2013). Since CLD also adsorbed onto the soil tested in this study, it is unclear if the MWCNTs enhance the mobility of CLD when they are applied to the soil after the CLD. In addition, no significant transport of MWCNTs in undisturbed soil under environmentally relevant conditions was found (Chapters 4.2.2 – 4.2.4). Thus, MWCNTs are not expected to enhance the mobility of pollutants but rather to limit it.

In general, it is relatively unlikely that suspensions of MWCNTs and pesticides will be released into the environment simultaneously. The MWCNTs retained in the soil may also alter the adsorption capacity of the soil and may therefore affect the transport and deposition of CLD. Thus, experiments with MWCNTs injected to the column first, followed by the CLD pulse, would also be interesting to understand the mechanisms of CLD sorption in the soil. The CLD might adsorb to both the retained MWCNTs and to the soil.

Finally, the hypotheses presented here have to be verified in co-transport experiments considering different scenarios (e.g., variation of soils, flow rate, order of CLD and MWCNT application) to obtain information on the potential of groundwater contamination by MWCNT-enhanced transport of CLD or the possibility of remediation of contaminated soil using MWCNT.

5. Summary and conclusions

Since an increasing production and use of NPs may result in their release into the environment, it is important to gain knowledge on their fate in the environment. The aim of this study was to investigate the transport and retention of functionalized MWCNTs in saturated and unsaturated porous media. Column experiments were performed in quartz sand and soil columns under different conditions. In addition, a soil lysimeter study was conducted. This study provided new insights into the environmental behavior and fate of MWCNTs and helped to evaluate the risks of MWCNT release into soils and sediments.

Prior to the transport experiments, the MWCNTs were modified with strong nitric acid in order to remove metal impurities and to enhance their stability in aqueous suspensions. The MWCNTs were characterized before and after modification to determine their properties and the effect of the modification process. Characterization by different techniques (e.g., TEM, ICP-MS, XPS) showed that the modification process significantly lowered catalyst impurities and induced oxygen-containing functional groups. Nevertheless, some characterization techniques (e.g., DLS) reached their limitations for CNTs because of their high aspect ratio. Further work on the analytical techniques for NPs in general and CNTs in particular, especially in environmental matrices, is needed to improve the characterization and detection of this new class of emerging pollutants.

Nanoparticles behave like colloids and tend to aggregate. However, the available and commonly used experimental setups and methods for transport studies were originally designed for solutes. Therefore, the setups were tested for MWCNTs and modified. The colloidal nature of NPs must be considered when analyzing these materials, making most of the common guidelines for testing chemicals inapplicable for nanoparticles unless they are adapted.

The transport experiments under water-saturated conditions showed that the grain size of the porous medium and the input concentration of MWCNTs play an important role on MWCNT transport. Furthermore, this study highlights the importance of considering environmentally relevant concentrations and retention profiles to allow reliable predictions of MWCNT transport and fate. This was enabled by the ^{14}C-labeling of MWCNTs. This work provides new information on the mobility of functionalized multi-walled carbon nanotubes. Results show that normalized MWCNT transport increases with higher input concentrations and in coarser textured sand. The retention profiles showed that the majority of MWCNT retention occurred near the column inlet, especially for lower input concentrations and smaller sand sizes. Simulations that considered a combination of time-and depth-dependent retention provided a good description of the experimental data. An analysis of model parameters demonstrated that concentration-dependent transport behavior became more important for smaller grain sizes and higher input concentrations. These trends were attributed to the complex shape and deposition morphology of MWCNTs in smaller pore spaces at higher input concentrations. The results of this study with quartz sand suggest that functionalized MWCNTs tend to be mobile in sandy subsurface environments, and may be transported to depths greater than 500 cm. Thus, aquifer contamination cannot be excluded.

An experiment with flow interruption showed a release of a small fraction of the applied MWCNTs after flow interruption. This indicates that some remobilization of functionalized MWCNTs in the environment might occur because natural flow conditions are not constant. Experiments with disturbed soil at water-saturated conditions showed a certain mobility of MWCNTs at high flow rates. Additionally, a concentration tailing of the BTC and the detachment coefficient indicated that retention in the disturbed soil was not completely irreversible.

Experiments in undisturbed soils under water-unsaturated conditions were performed to assess the mobility of MWCNTs in natural porous media. The results revealed an almost complete retention of functionalized MWCNTs in undisturbed cores of two well characterized soils (loamy sand and silty loam) at low flow rates. There was no detectable breakthrough of MWCNTs. More than 86% of MWCNTs were recovered in the soil profile at conditions close to saturation. At lower water-saturation, MWCNT retention was enhanced in the upper soil layers. A long-term lysimeter study confirmed that the MWCNTs were retained in the top soil layer. Soils are therefore expected to act as an effective sink for MWCNTs. Reasons for the high retention of MWCNTs in soil might be physical and chemical heterogeneity, particle aggregation, the heterogeneous soil pore size distribution, and the presence of air. Although it is known that organic matter can stabilize CNT suspensions and enhance their transport, no transport in the investigated soil was found – possibly due to the low organic carbon content (approx. 1%). The results suggest little potential for MWCNT transport through the vadose zone and for subsequent groundwater contamination in the considered soils. Nevertheless, MWCNT incorporation by earthworms, sediment-dwelling animals or filter feeders and transport to deeper soil layers and groundwater under conditions of heavy rainfall and/or preferential flow cannot be excluded. In addition, transient drainage and imbibition events might remobilize retained particles.

Since colloid-facilitated transport is an important mechanism for the transport and translocation of pollutants, the effect of MWCNTs on the transport of organic contaminants is a promising topic for further research. In this study, preliminary experiments revealed strong adsorption of chlordecone onto a loamy sand soil and the MWCNTs. Since the adsorption of CLD onto the MWCNTs was significantly higher compared to onto the soil, a potential influence of MWCNTs on the mobility of CLD in the soil has to be investigated.

This study provides fundamental information on the mobility of MWCNTs in natural porous media under environmentally relevant conditions. Nevertheless, further research is needed to better evaluate the environmental risk and to establish regulations for the production and use of these materials. The colloidal stability of CNTs is an important factor influencing their toxicity to organisms and their mobility in porous media. Since most of the commercial applications demand stable particles, the use of stabilized CNTs will increase and so too will the environmental risk. Therefore, investigations are needed on stabilized CNTs and their fate and transport after release from products. In addition, the effect of natural weather conditions (e.g., natural rainfall, drainage and imbibition) and plants on CNT transport would be a potential topic for further research. Investigations on the co-transport of CNTs and other compounds (e.g., heavy metals, organic chemicals) in soils of different chemical and physical composition are also of interest.

References

Akaike, H., 1974. A new look at the statistical model identification. Automatic Control, IEEE Transactions on 19, 716-723.

Allen, S.J., McKay, G., Porter, J.F., 2004. Adsorption isotherm models for basic dye adsorption by peat in single and binary component systems. Journal of Colloid and Interface Science 280, 322-333.

Batley, G.E., Kirby, J.K., McLaughlin, M.J., 2012. Fate and Risks of Nanomaterials in Aquatic and Terrestrial Environments. Accounts of Chemical Research.

Baughman, R.H., Zakhidov, A.A., de Heer, W.A., 2002. Carbon Nanotubes-the Route Toward Applications. Science 297, 787.

Beven, K., Germann, P., 1982. Macropores and water flow in soils. Water Ressources Research 18, 1311-1325.

Bierdel, M., Buchholz, S., Michele, V., Mleczko, L., Rudolf, R., Voetz, M., Wolf, A., 2007. Industrial production of multiwalled carbon nanotubes. physica status solidi (b) 244, 3939-3943.

Blume, H.-P., Brümmer, G.W., Horn, R., Kandeler, E., Kögel-Knabner, I., Kretzschmar, R., Stahr, K., Wilke, B.-M., 2010. Scheffer/Schachtschabel: Lehrbuch der Bodenkunde. Spektrum Akademischer Verlag.

Bolster, C.H., Mills, A.L., Hornberger, G.M., Herman, J.S., 1999. Spatial distribution of deposited bacteria following Miscible Displacement Experiments in intact cores. Water Ressources Research 35, 1797-1807.

Boxall, A.B., 2007. Engineered nanomaterials in soils and water: How do they behave and could they pose a risk to human health? Nanomedicine 2, 919-927.

Bradford, S.A., Bettahar, M., 2005. Straining, Attachment, and Detachment of Oocysts in Saturated Porous Media. J. Environ. Qual. 34, 469-478.

Bradford, S.A., Bettahar, M., 2006. Concentration dependent transport of colloids in saturated porous media. Journal of Contaminant Hydrology 82, 99-117.

Bradford, S.A., Bettahar, M., Simunek, J., van Genuchten, M.T., 2004. Straining and Attachment of Colloids in Physically Heterogeneous Porous Media. Vadose Zone Journal 3, 384-394.

Bradford, S.A., Kim, H.N., Haznedaroglu, B.Z., Torkzaban, S., Walker, S.L., 2009. Coupled Factors Influencing Concentration-Dependent Colloid Transport and Retention in Saturated Porous Media. Environmental Science & Technology 43, 6996-7002.

Bradford, S.A., Simunek, J., Bettahar, M., van Genuchten, M.T., Yates, S.R., 2003. Modeling Colloid Attachment, Straining, and Exclusion in Saturated Porous Media. Environmental Science & Technology 37, 2242-2250.

Bradford, S.A., Simunek, J., Bettahar, M., van Genuchten, M.T., Yates, S.R., 2006. Significance of straining in colloid deposition: Evidence and implications. Water Ressources Research 42.

Bradford, S.A., Toride, N., 2007. A Stochastic Model for Colloid Transport and Deposition. Journal of Environmental Quality 36, 1346-1356.

Bradford, S.A., Yates, S.R., Bettahar, M., Simunek, J., 2002. Physical factors affecting the transport and fate of colloids in saturated porous media. Water Ressources Research 38, 12.

Brusseau, M.L., Rao, P.S.C., Jessup, R.E., Davidson, J.M., 1989. Flow interruption: A method for investigating sorption nonequilibrium. Journal of Contaminant Hydrology 4, 223-240.

Burauel, P., Führ, F., 2000. Formation and long-term fate of non-extractable residues in outdoor lysimeter studies. Environmental pollution 108, 45-52.

Cabidoche, Y.M., Achard, R., Cattan, P., Clermont-Dauphin, C., Massat, F., Sansoulet, J., 2009. Long-term pollution by chlordecone of tropical volcanic soils in the French West Indies: A simple leaching model accounts for current residue. Environmental pollution 157, 1697-1705.

Cabidoche, Y.M., Lesueur-Jannoyer, M., 2012. Contamination of Harvested Organs in Root Crops Grown on Chlordecone-Polluted Soils. Pedosphere 22, 562-571.

Camobreco, V.J., Richards, B.K., Steenhuis, T.S., Peverly, J.H., McBride, M.B., 1996. Movement of Heavy Metals Through Undisturbed and Homogenized Soil Columns. Soil Science 161, 740-750.

Chatterjee, J., Abdulkareem, S., Gupta, S.K., 2010. Estimation of colloidal deposition from heterogeneous populations. Water Research 44, 3365-3374.

Chatterjee, J., Gupta, S.K., 2009. An Agglomeration-Based Model for Colloid Filtration. Environmental Science & Technology 43, 3694-3699.

Chen, K.L., Elimelech, M., 2006. Aggregation and deposition kinetics of fullerene (C60) nanoparticles. Langmuir 22, 10994.

Chen, K.L., Elimelech, M., 2007. Influence of humic acid on the aggregation kinetics of fullerene (C60) nanoparticles in monovalent and divalent electrolyte solutions. Journal of Colloid & Interface Science 309, 126-134.

Chen, W., Duan, L., Zhu, D., 2007. Adsorption of Polar and Nonpolar Organic Chemicals to Carbon Nanotubes. Environmental Science & Technology 41, 8295-8300.

Cheng, X., Kan, A.T., Tomson, M.B., 2005. Study of C_{60} transport in porous media and the effect of sorbed C_{60} on naphthalene transport. Journal of Materials Research 20, 3244-3254.

Cho, H.-H., Smith, B.A., Wnuk, J.D., Fairbrother, D.H., Ball, W.P., 2008. Influence of Surface Oxides on the Adsorption of Naphthalene onto Multiwalled Carbon Nanotubes. Environmental Science & Technology 42, 2899-2905.

Coat, S., Bocquené, G., Godard, E., 2006. Contamination of some aquatic species with the organochlorine pesticide chlordecone in Martinique. Aquatic Living Resources 19, 181-187.

De Volder, M.F., Tawfick, S.H., Baughman, R.H., Hart, A.J., 2013. Carbon Nanotubes: Present and Future Commercial Applications. Science 339, 535-539.

Eckelman, M.J., Mauter, M.S., Isaacs, J.A., Elimelech, M., 2012. New Perspectives on Nanomaterial Aquatic Ecotoxicity: Production Impacts Exceed Direct Exposure Impacts for Carbon Nanotoubes. Environmental Science & Technology 46, 2902-2910.

Fang, J., Shan, X.-q., Wen, B., Huang, R.-x., 2013. Mobility of TX100 suspended multiwalled carbon nanotubes (MWCNTs) and the facilitated transport of phenanthrene in real soil columns. Geoderma 207, 1-7.

Fang, J., Shan, X.-q., Wen, B., Lin, J.-m., Owens, G., 2009. Stability of titania nanoparticles in soil suspensions and transport in saturated homogeneous soil columns. Environmental pollution 157, 1101-1109.

Farré, M., Gajda-Schrantz, K., Kantiani, L., Barceló, D., 2009. Ecotoxicity and analysis of nanomaterials in the aquatic environment. Analytical and Bioanalytical Chemistry 393, 81-95.

Ferguson, P.L., Chandler, G.T., Templeton, R.C., DeMarco, A., Scrivens, W.A., Englehart, B.A., 2008. Influence of Sediment−Amendment with Single-walled Carbon Nanotubes and Diesel Soot on Bioaccumulation of Hydrophobic Organic Contaminants by Benthic Invertebrates. Environmental Science & Technology 42, 3879-3885.

Fernández-Bayo, J.D., Saison, C., Geniez, C., Voltz, M., Vereecken, H., Berns, A.E., 2013. Sorption characteristics of chlordecone and cadusafos in tropical agricultural soils. Current organic chemistry, In press.

Franchi, A., O'Melia, C.R., 2003. Effects of Natural Organic Matter and Solution Chemistry on the Deposition and Reentrainment of Colloids in Porous Media. Environmental Science & Technology 37, 1122-1129.

Galloway, T., Lewis, C., Dolciotti, I., Johnston, B.D., Moger, J., Regoli, F., 2010. Sublethal toxicity of nano-titanium dioxide and carbon nanotubes in a sediment dwelling marine polychaete. Environmental pollution 158, 1748-1755.

Gargiulo, G., Bradford, S., Šimůnek, J., Ustohal, P., Vereecken, H., Klumpp, E., 2007a. Bacteria transport and deposition under unsaturated conditions: The role of the matrix grain size and the bacteria surface protein. Journal of Contaminant Hydrology 92, 255-273.

Gargiulo, G., Bradford, S.A., Simunek, J., Ustohal, P., Vereecken, H., Klumpp, E., 2008. Bacteria Transport and Deposition under Unsaturated Flow Conditions: The Role of Water Content and Bacteria Surface Hydrophobicity. Vadose Zone Journal 7, 406-419.

Gargiulo, G., Bradford, S.A., Šimůnek, J., Ustohal, P., Vereecken, H., Klumpp, E., 2007b. Transport and Deposition of Metabolically Active and Stationary Phase Deinococcus radiodurans in Unsaturated Porous Media. Environmental Science & Technology 41, 1265-1271.

Gottschalk, F., Sonderer, T., Scholz, R.W., Nowack, B., 2009. Modeled Environmental Concentrations of Engineered Nanomaterials (TiO2, ZnO, Ag, CNT, Fullerenes) for Different Regions. Environmental Science & Technology 43, 9216-9222.

Grassian, V.H., 2008. Nanoscience and nanotechnology : environmental and health impacts / ed. by Vicki H. Grassian. Wiley, Hoboken, NJ.

Grathwohl, P., 1990. Influence of organic matter from soils and sediments from various origins on the sorption of some chlorinated aliphatic hydrocarbons: implications on Koc correlations. Environmental Science & Technology 24, 1687-1693.

Grolimund, D., Elimelech, M., Borkovec, M., Barmettler, K., Kretzschmar, R., Sticher, H., 1998. Transport of in Situ Mobilized Colloidal Particles in Packed Soil Columns. Environmental Science & Technology 32, 3562-3569.

Grubek-Jaworska, H., Nejman, P., Czumińska, K., Przybyłowski, T., Huczko, A., Lange, H., Bystrzejewski, M., Baranowski, P., Chazan, R., 2006. Preliminary results on the pathogenic effects of intratracheal exposure to one-dimensional nanocarbons. Carbon 44, 1057-1063.

Hammond, B., Katzenellenbogen, B.S., Krauthammer, N., McConnell, J., 1979. Estrogenic activity of the insecticide chlordecone (Kepone) and interaction with uterine estrogen receptors. Proceedings of the National Academy of Sciences 76, 6641-6645.

Harvey, R.W., Garabedian, S.P., 1991. Use of colloid filtration theory in modeling movement of bacteria through a contaminated sandy aquifer. Environmental Science & Technology 25, 178-185.

Hassellöv, M., Readman, J., Ranville, J., Tiede, K., 2008. Nanoparticle analysis and characterization methodologies in environmental risk assessment of engineered nanoparticles. Ecotoxicology 17, 344-361.

Hsu, J.-P., Liu, B.-T., 1998. Effect of Particle Size on Critical Coagulation Concentration. Journal of Colloid and Interface Science 198, 186-189.

Hull, M.S., Kennedy, A.J., Steevens, J.A., Bednar, A.J., Weiss, J.C.A., Vikesland, P.J., 2009. Release of Metal Impurities from Carbon Nanomaterials Influences Aquatic Toxicity. Environmental Science & Technology 43, 4169-4174.

Hussain, F., Hojjati, M., Okamoto, M., Gorga, R.E., 2006. Review article: Polymer-matrix Nanocomposites, Processing, Manufacturing, and Application: An Overview. Journal of Composite Materials 40, 1511-1575.

Hyung, H., Fortner, J.D., Hughes, J.B., Kim, J.-H., 2006. Natural Organic Matter Stabilizes Carbon Nanotubes in the Aqueous Phase. Environmental Science & Technology 41, 179-184.

Iijima, S., 1991. Helical microtubules of graphitic carbon. Nature 354, 56-58.

Jaisi, D.P., Elimelech, M., 2009. Single-Walled Carbon Nanotubes Exhibit Limited Transport in Soil Columns. Environmental Science & Technology 43, 9161-9166.

Jaisi, D.P., Saleh, N.B., Blake, R.E., Elimelech, M., 2008. Transport of Single-Walled Carbon Nanotubes in Porous Media: Filtration Mechanisms and Reversibility. Environmental Science & Technology 42, 8317-8323.

Jia, Z., Wang, Z., Liang, J., Wei, B., Wu, D., 1999. Production of short multi-walled carbon nanotubes. Carbon 37, 903-906.

Jiang, L., Gao, L., Sun, J., 2003. Production of aqueous colloidal dispersions of carbon nanotubes. Journal of Colloid and Interface Science 260, 89-94.

Jorio, A., Dresselhaus, G., Dresselhaus, S., 2008. Carbon Nanotubes: Advanced Topics in the Synthesis, Structure, Properties and Applications. Springer.

Kang, S., Herzberg, M., Rodrigues, D.F., Elimelech, M., 2008. Antibacterial Effects of Carbon Nanotubes: Size Does Matter! Langmuir 24, 6409-6413.

Kasel, D., Bradford, S.A., Šimůnek, J., Heggen, M., Vereecken, H., Klumpp, E., 2013. Transport and retention of multi-walled carbon nanotubes in saturated porous media: Effects of input concentration and grain size. Water Research 47, 933-944.

Kasteel, R., Mboh, C.M., Unold, M., Groeneweg, J., Vanderborght, J., Vereecken, H., 2010. Transformation and Sorption of the Veterinary Antibiotic Sulfadiazine in Two

Soils: A Short-Term Batch Study. Environmental Science & Technology 44, 4651-4657.

Khodakovskaya, M., Dervishi, E., Mahmood, M., Xu, Y., Li, Z., Watanabe, F., Biris, A.S., 2009. Carbon Nanotubes Are Able To Penetrate Plant Seed Coat and Dramatically Affect Seed Germination and Plant Growth. ACS Nano 3, 3221-3227.

Kim, H., Lee, M., Chae, W., Ezeh, T.D., Walker, S.L., 2011. Coupled Effect of Input Concentration and Solution Ionic Strength on Colloid Transport in Saturated Porous Media. International Proceedings of Chemical, Biological, and Environmental Engineering 17, 195-198.

Kim, H.N., Walker, S.L., Bradford, S.A., 2010. Coupled factors influencing the transport and retention of Cryptosporidium parvum oocysts in saturated porous media. Water Research 44, 1213-1223.

Klaine, S.J., Alvarez, P.J.J., Batley, G.E., Fernandes, T.F., Handy, R.D., Lyon, D.Y., Mahendra, S., McLaughlin, M.J., Lead, J.R., 2008. Nanomaterials in the environment: Behavior, fate, bioavailability, and effects. Environmental Toxicology and Chemistry 27, 1825-1851.

Köhler, A.R., Som, C., Helland, A., Gottschalk, F., 2008. Studying the potential release of carbon nanotubes throughout the application life cycle. Journal of Cleaner Production 16, 927-937.

Koyama, S., Endo, M., Kim, Y.-A., Hayashi, T., Yanagisawa, T., Osaka, K., Koyama, H., Haniu, H., Kuroiwa, N., 2006. Role of systemic T-cells and histopathological aspects after subcutaneous implantation of various carbon nanotubes in mice. Carbon 44, 1079-1092.

Kretzschmar, R., Barmettler, K., Grolimund, D., Yan, Y.-d., Borkovec, M., Sticher, H., 1997. Experimental determination of colloid deposition rates and collision efficiencies in natural porous media. Water Ressources Research 33, 1129-1137.

Kretzschmar, R., Robarge, W.P., Amoozegar, A., 1995. Influence of Natural Organic Matter on Colloid Transport Through Saprolite. Water Resour. Res. 31, 435-445.

Lam, C.-W., James, J.T., McCluskey, R., Hunter, R.L., 2004. Pulmonary Toxicity of Single-Wall Carbon Nanotubes in Mice 7 and 90 Days After Intratracheal Instillation. Toxicological Sciences 77, 126-134.

Lecoanet, H.F., Bottero, J.-Y., Wiesner, M.R., 2004. Laboratory Assessment of the Mobility of Nanomaterials in Porous Media. Environmental Science & Technology 38, 5164-5169.

Lecoanet, H.F., Wiesner, M.R., 2004. Velocity Effects on Fullerene and Oxide Nanoparticle Deposition in Porous Media. Environmental Science & Technology 38, 4377-4382.

Levillain, J., Cattan, P., Colin, F., Voltz, M., Cabidoche, Y.M., 2012. Analysis of environmental and farming factors of soil contamination by a persistent organic pollutant, chlordecone, in a banana production area of French West Indies. Agriculture Ecosystems & Environment 159, 123-132.

Li, C., 2011. Sorption of a branched nonylphenol isomer and perfluorooctanoic acid on geosorbents and carbon nanotubes. Schriften des Forschungszentrums Jülich, Energiy & Environment 110, Forschungszentrum jülich GmbH, Zentralbibliothek, Jülich.

Li, C., Schäffer, A., Séquaris, J.-M., László, K., Tóth, A., Tombácz, E., Vereecken, H., Ji, R., Klumpp, E., 2012a. Surface-associated metal catalyst enhances the sorption of perfluorooctanoic acid to multi-walled carbon nanotubes. Journal of Colloid and Interface Science 377, 342-346.

Li, C.L., Ji, R., Schaffer, A., Sequaris, J.M., Amelung, W., Vereecken, H., Klumpp, E., 2012b. Sorption of a branched nonylphenol and perfluorooctanoic acid on Yangtze River sediments and their model components. Journal of Environmental Monitoring 14, 2653-2658.

Li, X., Scheibe, T.D., Johnson, W.P., 2004. Apparent Decreases in Colloid Deposition Rate Coefficients with Distance of Transport under Unfavorable Deposition Conditions: A General Phenomenon. Environmental Science & Technology 38, 5616-5625.

Li, X., Zhang, P., Lin, C.L., Johnson, W.P., 2005. Role of Hydrodynamic Drag on Microsphere Deposition and Re-entrainment in Porous Media under Unfavorable Conditions. Environmental Science & Technology 39, 4012-4020.

Li, Y., Wang, Y., Pennell, K.D., Abriola, L.M., 2008. Investigation of the Transport and Deposition of Fullerene (C60) Nanoparticles in Quartz Sands under Varying Flow Conditions. Environmental Science & Technology 42, 7174-7180.

Lin, D., Tian, X., Wu, F., Xing, B., 2010. Fate and Transport of Engineered Nanomaterials in the Environment. J. Environ. Qual. 39, 1896-1908.

Lin, S., Reppert, J., Hu, Q., Hudson, J.S., Reid, M.L., Ratnikova, T.A., Rao, A.M., Luo, H., Ke, P.C., 2009. Uptake, Translocation, and Transmission of Carbon Nanomaterials in Rice Plants. Small 5, 1128-1132.

Liu, X., Hurt, R.H., Kane, A.B., 2010. Biodurability of single-walled carbon nanotubes depends on surface functionalization. Carbon 48, 1961-1969.

Liu, X., O'Carroll, D.M., Petersen, E.J., Huang, Q., Anderson, C.L., 2009. Mobility of Multiwalled Carbon Nanotubes in Porous Media. Environmental Science & Technology 43, 8153-8158.

Lu, C., Chung, Y.-L., Chang, K.-F., 2005. Adsorption of trihalomethanes from water with carbon nanotubes. Water Research 39, 1183-1189.

Marquardt, D., 1963. An Algorithm for Least-Squares Estimation of Nonlinear Parameters. Journal of the Society for Industrial and Applied Mathematics 11, 431-441.

Mattison, N.T., O'Carroll, D.M., Kerry Rowe, R., Petersen, E.J., 2011. Impact of Porous Media Grain Size on the Transport of Multi-walled Carbon Nanotubes. Environmental Science & Technology 45, 9765-9775.

Mauter, M.S., Elimelech, M., 2008. Environmental Applications of Carbon-Based Nanomaterials. Environmental Science & Technology 42, 5843-5859.

Maynard, A.D., 2007. Nanotechnology: The Next Big Thing, or Much Ado about Nothing? Annals of Occupational Hygiene 51, 1-12.

McGinley, P.M., Katz, L.E., Weber, W.J., 1993. A distributed reactivity model for sorption by soils and sediments. 2. Multicomponent systems and competitive effects. Environmental Science & Technology 27, 1524-1531.

Mueller, N.C., Nowack, B., 2008. Exposure Modeling of Engineered Nanoparticles in the Environment. Environmental Science & Technology 42, 4447-4453.

Murr, L.E., Esquivel, E.V., Bang, J.J., de la Rosa, G., Gardea-Torresdey, J.L., 2004. Chemistry and nanoparticulate compositions of a 10,000 year-old ice core melt water. Water Research 38, 4282-4296.

Nagasawa, S., Yudasaka, M., Hirahara, K., Ichihashi, T., Iijima, S., 2000. Effect of oxidation on single-wall carbon nanotubes. Chemical Physics Letters 328, 374-380.

Nel, A., Xia, T., Madler, L., Li, N., 2006. Toxic Potential of Materials at the Nanolevel. Science 311, 622-627.

Nelson, K.E., Ginn, T.R., 2005. Colloid Filtration Theory and the Happel Sphere-in-Cell Model Revisited with Direct Numerical Simulation of Colloids. Langmuir 21, 2173-2184.

Nowack, B., Bucheli, T.D., 2007. Occurrence, behavior and effects of nanoparticles in the environment. Environmental pollution 150, 5-22.

O'Carroll, D.M., Liu, X., Mattison, N.T., Petersen, E.J., 2013. Impact of diameter on carbon nanotube transport in sand. Journal of Colloid and Interface Science 390, 96-104.

Overbeek, J.T.G., 1980. The rule of Schulze and Hardy.

Pan, B., Xing, B., 2008. Adsorption Mechanisms of Organic Chemicals on Carbon Nanotubes. Environmental Science & Technology 42, 9005-9013.

Pan, B., Xing, B., 2012. Applications and implications of manufactured nanoparticles in soils: a review. European Journal of Soil Science 63, 437-456.

Pecora, R., 2000. Dynamic Light Scattering Measurement of Nanometer Particles in Liquids. Journal of Nanoparticle Research 2, 123-131.

Peng, X., Li, Y., Luan, Z., Di, Z., Wang, H., Tian, B., Jia, Z., 2003. Adsorption of 1,2-dichlorobenzene from water to carbon nanotubes. Chemical Physics Letters 376, 154-158.

Petersen, E.J., Akkanen, J., Kukkonen, J.V.K., Weber, W.J., 2009a. Biological Uptake and Depuration of Carbon Nanotubes by Daphnia magna. Environmental Science & Technology 43, 2969-2975.

Petersen, E.J., Huang, Q., Weber, J.W.J., 2008a. Bioaccumulation of Radio-Labeled Carbon Nanotubes by Eisenia foetida. Environmental Science & Technology 42, 3090-3095.

Petersen, E.J., Huang, Q., Weber, W.J., 2008b. Ecological Uptake and Depuration of Carbon Nanotubes by Lumbriculus variegatus. Environmental Health Perspectives 116, 496-500.

Petersen, E.J., Huang, Q., Weber, W.J., 2010. Relevance of octanol–water distribution measurements to the potential ecological uptake of multi-walled carbon nanotubes. Environmental Toxicology and Chemistry 29, 1106-1112.

Petersen, E.J., Pinto, R.A., Landrum, P.F., Weber, J.W.J., 2009b. Influence of Carbon Nanotubes on Pyrene Bioaccumulation from Contaminated Soils by Earthworms. Environmental Science & Technology 43, 4181-4187.

Petersen, E.J., Zhang, L., Mattison, N.T., O'Carroll, D.M., Whelton, A.J., Uddin, N., Nguyen, T., Huang, Q., Henry, T.B., Holbrook, R.D., Chen, K.L., 2011. Potential Release Pathways, Environmental Fate, And Ecological Risks of Carbon Nanotubes. Environmental Science & Technology 45, 9837-9856.

Petosa, A.R., Jaisi, D.P., Quevedo, I.R., Elimelech, M., Tufenkji, N., 2010. Aggregation and Deposition of Engineered Nanomaterials in Aquatic Environments: Role of Physicochemical Interactions. Environmental Science & Technology 44, 6532-6549.

Pillay, K., 2012. Carbon Nanomaterials – A New orm of Ion E changers, in: Kilislio lu, A. (Ed.), Ion Exchange Technologies. InTech, pp. 91-100.

Pumera, M., 2007. Carbon Nanotubes Contain Residual Metal Catalyst Nanoparticles even after Washing with Nitric Acid at Elevated Temperature Because These Metal Nanoparticles Are Sheathed by Several Graphene Sheets. Langmuir 23, 6453-6458.

Russier, J., Menard-Moyon, C., Venturelli, E., Gravel, E., Marcolongo, G., Meneghetti, M., Doris, E., Bianco, A., 2011. Oxidative biodegradation of single- and multi-walled carbon nanotubes. Nanoscale 3, 893-896.

Russo, D., Bouton, M., 1992. Statistical analysis of spatial variability in unsaturated flow parameters. Water Ressources Research 28, 1911-1925.

Saleh, N.B., Pfefferle, L.D., Elimelech, M., 2008. Aggregation Kinetics of Multiwalled Carbon Nanotubes in Aquatic Systems: Measurements and Environmental Implications. Environmental Science & Technology 42, 7963-7969.

Salerno, M.B., Flamm, M., Logan, B.E., Velegol, D., 2006. Transport of Rodlike Colloids through Packed Beds. Environmental Science & Technology 40, 6336-6340.

Sangermano, M., Pegel, S., Pötschke, P., Voit, B., 2008. Antistatic Epoxy Coatings With Carbon Nanotubes Obtained by Cationic Photopolymerization. Macromolecular Rapid Communications 29, 396-400.

Sano, M., 2001. Colloidal nature of single-walled carbon nanotubes in electrolyte solution: The Schulze-Hardy rule. Langmuir CCCS, 7172-7173.

Schäffer, A., von Lochow, H.E.C., Baumgartner, W., Daniels, B., Deutschmann, B., Rhiem, S., Simon, A., Stibany, F., Maes, H.M., 2011. Umweltverhalten und -effekte von kohlenstoff-basierten Nanopartikeln, Skript zur Präsentation auf der Tagung Nanotechnologie und Wasserwirtschaft, p. 12.

Schlagenhauf, L., Chu, B.T.T., Buha, J., Nüesch, F., Wang, J., 2012. Release of Carbon Nanotubes from an Epoxy-Based Nanocomposite during an Abrasion Process. Environmental Science & Technology 46, 7366-7372.

Schwab, F., Bucheli, T.D., Lukhele, L.P., Magrez, A., Nowack, B., Sigg, L., Knauer, K., 2011. Are Carbon Nanotube Effects on Green Algae Caused by Shading and Agglomeration? Environmental Science & Technology 45, 6136-6144.

Shellenberger, K., Logan, B.E., 2001. Effect of Molecular Scale Roughness of Glass Beads on Colloidal and Bacterial Deposition. Environmental Science & Technology 36, 184-189.

Simon-Deckers, A.l., Loo, S., Mayne-L'hermite, M., Herlin-Boime, N., Menguy, N., Reynaud, C.c., Gouget, B., Carri re, M., 200 . Size-, Composition- and Shape-Dependent Toxicological Impact of Metal Oxide Nanoparticles and Carbon Nanotubes toward Bacteria. Environmental Science & Technology 43, 8423-8429.

Šimůnek, J., van Genuchten, M.T., Šejna, M., 2008. Development and Applications of the HYDRUS and STANMOD Software Packages and Related Codes. Vadose Zone Journal 7, 587-600.

Sinnott, S.B., 2002. Chemical Functionalization of Carbon Nanotubes. Journal of Nanoscience and Nanotechnology 2, 113-123.

Smith, B., Wepasnick, K., Schrote, K.E., Cho, H.-H., Ball, W.P., Fairbrother, D.H., 2009. Influence of Surface Oxides on the Colloidal Stability of Multi-Walled Carbon Nanotubes: A Structure-Property Relationship. Langmuir 25, 9767-9776.

Smith, C.J., Shaw, B.J., Handy, R.D., 2007. Toxicity of single walled carbon nanotubes to rainbow trout, (Oncorhynchus mykiss): Respiratory toxicity, organ pathologies, and other physiological effects. Aquatic Toxicology 82, 94-109.

Som, C., Wick, P., Krug, H., Nowack, B., 2011. Environmental and health effects of nanomaterials in nanotextiles and facade coatings. Environment international 37, 1131-1142.

Sumanasekera, G.U., Chen, G., Takai, K., Joly, J., Kobayashi, N., Enoki, T., Eklund, P.C., 2010. Charge transfer and weak chemisorption of oxygen molecules in nanoporous carbon consisting of a disordered network of nanographene sheets. Journal of Physics: Condensed Matter 22, 334208.

Sun, Y.-P., Fu, K., Lin, Y., Huang, W., 2002. Functionalized Carbon Nanotubes: Properties and Applications. Accounts of Chemical Research 35, 1096-1104.

Tan, Y., Gannon, J.T., Baveye, P., Alexander, M., 1994. Transport of bacteria in an aquifer sand: Experiments and model simulations. Water Resour. Res. 30, 3243-3252.

Telscher, M.J.H., Schuller, U., Schmidt, B., Schaffer, A., 2005. Occurrence of a nitro metabolite of a defined nonylphenol isomer in soil/sewage sludge mixtures. Environmental Science & Technology 39, 7896-7900.

Templeton, R.C., Ferguson, P.L., Washburn, K.M., Scrivens, W.A., Chandler, G.T., 2006. Life-Cycle Effects of Single-Walled Carbon Nanotubes (SWNTs) on an Estuarine Meiobenthic Copepod†. Environmental Science & Technology 40, 7387-7393.

Tian, Y., Gao, B., Silvera-Batista, C., Ziegler, K., 2010. Transport of engineered nanoparticles in saturated porous media. Journal of Nanoparticle Research 12, 2371-2380.

Tian, Y., Gao, B., Wang, Y., Morales, V.L., Carpena, R.M., Huang, Q., Yang, L., 2012. Deposition and transport of functionalized carbon nanotubes in water-saturated sand columns. Journal of Hazardous Materials 213–214, 265-272.

Tian, Y., Gao, B., Ziegler, K.J., 2011. High mobility of SDBS-dispersed single-walled carbon nanotubes in saturated and unsaturated porous media. Journal of Hazardous Materials 186, 1766-1772.

Tong, M., Johnson, W.P., 2006. Colloid Population Heterogeneity Drives Hyperexponential Deviation from Classic Filtration Theory. Environmental Science & Technology 41, 493-499.

Torkzaban, S., Bradford, S.A., van Genuchten, M.T., Walker, S.L., 2008. Colloid transport in unsaturated porous media: The role of water content and ionic strength on particle straining. Journal of Contaminant Hydrology 96, 113-127.

Tufenkji, N., Elimelech, M., 2004. Deviation from the Classical Colloid Filtration Theory in the Presence of Repulsive DLVO Interactions. Langmuir 20, 10818-10828.

Tufenkji, N., Elimelech, M., 2005. Spatial Distributions of Cryptosporidium Oocysts in Porous Media: Evidence for Dual Mode Deposition. Environmental Science & Technology 39, 3620-3629.

Unold, M., Kasteel, R., Groeneweg, J., Vereecken, H., 2009a. Transport and transformation of sulfadiazine in soil columns packed with a silty loam and a loamy sand. Journal of Contaminant Hydrology 103, 38-47.

Unold, M., Simunek, J., Kasteel, R., Groeneweg, J., Vereecken, H., 2009b. Transport of Manure-Based Applied Sulfadiazine and Its Main Transformation Products in Soil Columns. Vadose Zone Journal 8, 677-689.

Upadhyayula, V.K.K., Deng, S., Mitchell, M.C., Smith, G.B., 2009. Application of carbon nanotube technology for removal of contaminants in drinking water: A review. Science of The Total Environment 408, 1-13.

Van Eerdenbrugh, B., Van den Mooter, G., Augustijns, P., 2008. Top-down production of drug nanocrystals: Nanosuspension stabilization, miniaturization and transformation into solid products. International Journal of Pharmaceutics 364, 64-75.

Vecchia, E.D., Luna, M., Sethi, R., 2009. Transport in Porous Media of Highly Concentrated Iron Micro- and Nanoparticles in the Presence of Xanthan Gum. Environmental Science & Technology 43, 8942-8947.

Wan, J., Tokunaga, T.K., 1997. Film Straining of Colloids in Unsaturated Porous Media: Conceptual Model and Experimental Testing. Environmental Science & Technology 31, 2413-2420.

Wang, D., Bradford, S.A., Harvey, R.W., Hao, X., Zhou, D., 2012a. Transport of ARS-labeled hydroxyapatite nanoparticles in saturated granular media is influenced by surface charge variability even in the presence of humic acid. Journal of Hazardous Materials 229–230, 170-176.

Wang, D., Paradelo, M., Bradford, S.A., Peijnenburg, W.J.G.M., Chu, L., Zhou, D., 2011. Facilitated transport of Cu with hydroxyapatite nanoparticles in saturated sand: Effects of solution ionic strength and composition. Water Research 45, 5905-5915.

Wang, P., Shi, Q., Liang, H., Steuerman, D.W., Stucky, G.D., Keller, A.A., 2008. Enhanced Environmental Mobility of Carbon Nanotubes in the Presence of Humic Acid and Their Removal from Aqueous Solution. Small 4, 2166-2170.

Wang, Y., Kim, J.-H., Baek, J.-B., Miller, G.W., Pennell, K.D., 2012b. Transport behavior of functionalized multi-wall carbon nanotubes in water-saturated quartz sand as a function of tube length. Water Research 46, 4521-4531.

Wang, Y., Li, Y., Kim, H., Walker, S.L., Abriola, L.M., Pennell, K.D., 2010. Transport and Retention of Fullerene Nanoparticles in Natural Soils. Journal of Environmental Quality 39, 1925-1933.

Warheit, D.B., Laurence, B.R., Reed, K.L., Roach, D.H., Reynolds, G.A.M., Webb, T.R., 2004. Comparative Pulmonary Toxicity Assessment of Single-wall Carbon Nanotubes in Rats. Toxicological Sciences 77, 117-125.

Waychunas, G.A., 2001. Structure, Aggregation and Characterization of Nanoparticles. Reviews in Mineralogy and Geochemistry 44, 105-166.

Weber, W.J., McGinley, P.M., Katz, L.E., 1992. A distributed reactivity model for sorption by soils and sediments. 1. Conceptual basis and equilibrium assessments. Environmental Science & Technology 26, 1955-1962.

Wiesner, M.R., Bottero, J.Y., 2007. Environmental Nanotechnology: Applications and Impacts of Nanomaterials. McGraw-Hill.

Wiesner, M.R., Lowry, G.V., Alvarez, P., Dionysiou, D., Biswas, P., 2006. Assessing the Risks of Manufactured Nanomaterials. Environmental Science & Technology 40, 4336-4345.

Woignier, T., Fernandes, P., Jannoyer-Lesueur, M., Soler, A., 2012. Sequestration of chlordecone in the porous structure of an andosol and effects of added organic matter: an alternative to decontamination. European Journal of Soil Science 63, 717-723.

Xia, W., Wang, Y., Bergsträßer, R., Kundu, S., Muhler, M., 2007. Surface characterization of oxygen-functionalized multi-walled carbon nanotubes by high-resolution X-ray photoelectron spectroscopy and temperature-programmed desorption. Applied Surface Science 254, 247-250.

Xin, S., Guo, Y.-G., Wan, L.-J., 2012. Nanocarbon Networks for Advanced Rechargeable Lithium Batteries. Accounts of Chemical Research 45, 1759-1769.

Yan, X.M., Shi, B.Y., Lu, J.J., Feng, C.H., Wang, D.S., Tang, H.X., 2008. Adsorption and desorption of atrazine on carbon nanotubes. Journal of Colloid and Interface Science 321, 30-38.

Yao, K.-M., Habibian, M.T., O'Melia, C.R., 1971. Water and waste water filtration. Concepts and applications. Environmental Science & Technology 5, 1105-1112.

Yates, D.E., Levine, S., Healy, T.W., 1974. Site-binding model of the electrical double layer at the oxide/water interface. J. Chem. Soc., Faraday Trans. 1 70, 1807-1818.

Yoon, J.S., Germaine, J.T., Culligan, P.J., 2006. Visualization of particle behavior within a porous medium: Mechanisms for particle filtration and retardation during downward transport. Water Resour. Res. 42, W06417.

Zhang, L., Petersen, E.J., Huang, Q., 2011. Phase Distribution of 14C-Labeled Multiwalled Carbon Nanotubes in Aqueous Systems Containing Model Solids: Peat. Environmental Science & Technology 45, 1356-1362.

Zhang, Q., Hassanizadeh, S.M., Raoof, A., van Genuchten, M.T., Roels, S.M., 2012. Modeling Virus Transport and Remobilization during Transient Partially Saturated Flow. Vadose Zone Journal 11.

Zhang, W., Morales, V.n.L., Cakmak, M.E., Salvucci, A.E., Geohring, L.D., Hay, A.G., Parlange, J.-Y., Steenhuis, T.S., 2010. Colloid Transport and Retention in Unsaturated Porous Media: Effect of Colloid Input Concentration. Environmental Science & Technology 44, 4965-4972.

List of Figures

List of Tables

List of Abbreviations

ADE	Advection-dispersion equation
AIC	Akaike information criterion
Al	Aluminum
BTC	Breakthrough curve
Bq	Becquerel
$CaCl_2$	Calcium chloride
CCC	Critical coagulation concentration
CFT	Classical colloid filtration theory
CLD	Chlordecone
CNTs	Carbon nanotubes
^{14}C	Radioactive carbon isotope
$^{14}CO_2$	Radioactively labeled carbon dioxide
C_{60}	Fullerene nanoparticles
Co	Cobalt
DLS	Dynamic light scattering
DLVO	Derjaguin–Landau–Verwey–Overbeek
EDX	Energy-dispersive X-ray spectroscope
ICP-MS	Inductively coupled plasma-mass spectrometry
IS	Ionic strength
KAL	Test site Kaldenkirchen-Hülst
KBr	Potassium bromide
KCl	Potassium chloride
LSC	Liquid scintillation counter
M1	Conventional attachment and detachment model
M2	Model that includes attachment, detachment, and blocking
M3	Depth-dependent retention model
M4	Time- and depth-dependent retention model
MBq	Mega-Becquerel
Mg	Magnesium
Mn	Manganese
MRZ	Test site Merzenhausen
MWCNTs	Multi-walled carbon nanotubes
NP	Nanoparticle
PTFE	Polytetrafluoroethylene
RP	Retention profile
SDBS	Sodium dodecylbenzenesulfonate
SWCNTs	Single-walled carbon nanotubes
TDR	Time-domain reflectrometry
TEM	Transmission electron microscope
TiO_2	Titanium dioxide
XPS	X-ray photoelectron spectroscopy

List of Symbols

C	Particle concentration in the aqueous phase [Bq mL^{-1}]
C_o	Initial particle concentration [Bq mL^{-1}]
C_e	Liquid phase equilibrium concentration [g L^{-1}]
D	Dispersion coefficient
d_c	Median diameter of the sand grains [cm]
f_{oc}	Organic carbon content [kg kg^{-1}]
k_1	First-order retention coefficient
k_2	First-order detachment coefficient
K_d	Linear sorption coefficient [L kg^{-1}]
K_{oc}	Linear sorption coefficient normalized by organic carbon content [L kg^{-1}]
K_F	Freundlich sorption coefficient [$\mu g^{(1-1/n)}$ $L^{1/n}$ g^{-1}]
K_L	Langmuir sorption coefficient [L μg^{-1}]
L	Units of length [cm]
L	Negative log likelihood for the fitted model
M	Units of mass [g]
m	Total number of independently optimized parameters
n	Number of experimental data points
n	Describes nonlinearity of the isotherm after Freundlich
N_c	Number of particles
q	Flow rate [cm min^{-1}]
Q	Limited adsorption capacity of the monolayer [µg kg^{-1}]
q_e	Solid phase equilibrium concentration [g kg^{-1}]
RSS	Residual sum of squares
S	Solid phase particle concentration [Bq g^{-1}]
S_max	Maximum solid phase particle concentration [Bq g^{-1}]
t	Time [min]
T	Units of time [min]
wt%	Percent of weight
x	Spatial coordinate
y	Year
z	Valency of the electrolyte counterions
β	Empirical variable that controls the shape of the retention profile
ρ	Bulk density of the porous media [g cm^{-3}]
θ	Volumetric water content
ψ	Dimensionless function to account for time-/depth-dependent retention
η	Single collector efficiency
α	Sticking efficiency
$<$	Smaller than
$>$	Larger than

Curriculum vitae

Daniela Kasel (environmental scientist)

Hof Mulbach 7
54526 Landscheid, Germany
Phone: 0049-176-24207741
E-Mail: danielakasel@gmail.com
Born on 14.07.1985 in Trier, Germany

Work Experience

02/2010 – 11/2013	Ph.D.-student at the Institute of Bio- and Geosciences, IBG-3, Agrosphere Institute at Forschungszentrum Jülich GmbH, Germany in cooperation with RWTH Aachen University, Germany; Topic: Mobility of Nanoparticles in Saturated and Unsaturated Porous Media
05/2012 – 08/2012	Visiting Scholar at the Department of Environmental Sciences at University of California Riverside, USA, cooperation with Jiří Šimůnek and Scott Bradford on modeling of nanoparticle transport and retention
02/2009 – 03/2009	Short-term employment as a scientific assistant at the Department for Analytical und Ecological Chemistry at the University of Trier, Germany; mentoring of undergraduates during lab courses in inorganic chemistry
04/2008 – 05/2008	Internship with the district government of Düsseldorf, Germany; working on the Water Framework Directive
11/2007 – 12/2007	Internship at the Federal Institute for Geosciences and Natural Resources, Hannover, Germany; water sampling, data processing and analysis
04/2004 – 01/2010	Part-time job as a restaurant service employee at Mc Donald’s Bitburg, Germany

Education

03/2009 – 11/2009	Diploma thesis: Sorption of Azo Dyes in Soils Final grade: 1.3 (approximate equivalent: A)
04/2004 – 11/2009	Studies in environmental sciences at the University of Trier, Germany Main areas of study: chemistry, soil science, geology, and hydrology Final grade: 1.5 (approximate equivalent: A)
08/1995 – 03/2004	Cusanus secondary school, Wittlich, Germany Abitur (German highschool exam with university entrance qualification) Final grade: 2.1 (approximate equivalent: B)

Further Work and Qualifications

Since 11/2010	Practical work with radionuclides (^{14}C) in liquid and solid samples and the corresponding analytical techniques
Since 09/2010	Experience with transmission electron microscopy at the Ernst-Ruska-Centre, Forschungszentrum Jülich GmbH, Germany
04/2011 – 08/2011	Supervision of a diploma student of the FH Aachen; thesis about transport of carbon nanotubes in porous media
12/2010 – 05/2012	Ph.D.-representative at IBG-3, Forschungszentrum Jülich GmbH, Germany

Trainings

7/2010	Summer school on 'Upscaling and Modeling of Reactive Transport in Partially-Saturated Porous Media' in Utrecht, the Netherlands
6/2010	Three day workshop on 'Scientific Writing and Ethics' held by Markus Flury
05/2010 – 10/2011	Participation at the 'Programme for generic qualification of PhD students' at the orschungszentrum Jülich GmbH, Germany, including project management, team communication, scientific writing and career strategies

Languages

German (native)
English (fluent)
French (basic)
Spanish (basic)

Software

Microsoft Office (daily use)
HYDRUS-1D (fair)
Origin (basic)

Memberships

Since 3/2011	German Soil Science Society

Further Interests

Playing tennis (since 2010 as active member of the Tennisvereinigung Blau-Weiß Jülich e.V.)

Furthermore running, swimming, and reading

Publications

The content of this doctoral thesis was partly published and presented before in the following publications and scientific conference contributions. The permission of Elsevier was obtained for the reuse of the journal articles.

Journal articles:

1. Kasel, D., Bradford, S. A., Šimůnek, J., Heggen, M., Vereecken, H., Klumpp, E., (2013). Transport and retention of multi-walled carbon nanotubes in saturated porous media: Effects of input concentration and grain size. Water Research 47, 933-944. http://dx.doi.org/10.1016/j.watres.2012.11.019.

2. Kasel, D., Bradford, S. A., Šimůnek, J., Pütz, T., Vereecken, H., Klumpp, E., (2013). Limited transport of functionalized multi-walled carbon nanotubes in two natural soils. Environmental Pollution 180, 152-158. http://dx.doi.org/10.1016/j.envpol.2013.05.031.

Conference contributions (oral):

1. Kasel, D., Bradford, S. A., Šimůnek, J., Heggen, M., Vereecken, H., Klumpp, E., (2012). Transport and Deposition of Multiwalled Carbon Nanotubes in Saturated Porous Media. American Geophysical Union's 45th annual all Meeting, San Francisco, USA, 03-07/12/2012.

2. Klumpp, E., Kasel, D., Liang, Y., Bradford, S. A., Šimůnek, J., Heggen, M., Vereecken, H., (2012). Transport and Deposition of Nanoparticles in (Model) Soils. Interfaces against Pollution, Nancy, France, 11-14/06/2012

3. Kasel, D., Philipp, H., Kasteel, R., Vereecken, H., Klumpp, E., (2011). Transport and Deposition of Multiwalled Carbon Nanotubes in Saturated Porous Media. EuCheMS International Conference on Chemistry and the Environment 2011, Zurich, Switzerland, 11-14/09/2011.

Conference contributions (poster):

1. Kasel, D., Vereecken, H., Klumpp, E., (2012). Transport and Deposition of Multiwalled Carbon Nanotubes in (Model) Soils. 2. Clustertreffen der BMBF-Fördermaßnahmen NanoCare und NanoNature, Frankfurt (Main), Germany, 13-14/03/2012.

2. Kasel, D., Schierenberg, W., Philipp, H., Heggen, M., Kasteel, R., Vereecken, H., Klumpp, E., (2011). Transport of Multiwalled Carbon Nanotubes in Saturated Porous Media. Jahrestagung der Deutschen Bodenkundlichen Gesellschaft, Berlin, Germany, 03-09/09/2011.

3. Liang, Y., Kasel, D., Heggen, M., Vereecken, H., Klumpp, E., (2011). Transport of carbon nanotubes and silver nanoparticles in saturated porous media. 1. Clustertreffen der BMBF-Fördermaßnahmen NanoCare und NanoNature, Frankfurt (Main), Germany, 10-11/05/2011.

Acknowledgments

First of all, I would like to thank the Federal Ministry of Education and Research for funding the Nanoflow project and, thus, my thesis.

My gratitude goes to my doctoral advisor Prof. Dr. Erwin Klumpp for his support. Detailed discussions, constructive words and his open door helped me to overcome diverse difficulties during the past three years at IBG-3. Thanks for everything.

I would also like to thank Prof. Dr. Andreas Schäffer for valuable discussions and the opportunity to complete my Ph.D. at the Chair of Environmental Biology and Chemodynamics (UBC), RWTH Aachen University.

Special thanks to Prof. Dr. Harry Vereecken for the opportunity to write my thesis at the Agrosphere. He always supports the Ph.D. students, and all of the presentations and reports were good preparation for conferences, papers, and my thesis.

I am very grateful for the opportunity to visit Dr. Scott A. Bradford and Prof. Dr. Jiří Šimůnek in Riverside, California. Thank you very much for all your patience and support.

Dr. Marc Heggen supported me with the transmission electron microscope at the Ernst Ruska Centre for Microscopy and Spectroscopy with Electrons, Forschungszentrum Jülich GmbH. Thank you very much.

I would also like to thank Peter Klahre, Stephan Köppchen, Martina Krause, Ulrike Langen, Herbert Philipp, Claudia Walraf, Dr. Lutz Weihermüller, and Ansgar Weuthen for all their support. Thanks for always helping me.

Thanks to Wolfgang Schierenberg and Miaoyue Zhang for their practical assistance in the lab.

The lysimeter experiment would not have been possible without the help of Dr. Anne Berns, Dr. Diana Hofmann, Stephan Köppchen, Martina Krause, Ulrike Langen, Yan Liang, Dr. Bastian Niedrée, Herbert Philipp, Dr. Thomas Pütz, Herbert Rützel, and Dr. Lutz Weihermüller. Thank you very much.

I would like to thank Dr. Hanna Maes from the Chair of Environmental Biology and Chemodynamics (UBC) at RWTH Aachen University for her valuable hints at the beginning of my work and the opportunity to synthesize ^{14}C-labeled MWCNTs.

Thanks to Dr. Anne Berns, Markus Duschl, and Dr. Wolfgang Tappe for all your time discussing smaller and bigger problems, reading diverse manuscripts, and continuously motivating me.

Thanks to Basti, Christian, Meli, Sascha, Sirgit, Thomas, and Wolfgang for all of the enjoyable and informative lunch breaks. I will miss you.

I would also like to thank all of my colleagues at IBG-3 who have become friends over the past three years. Our shared leisure activities were a welcome distraction.

Finally, thanks to my family who always support me in everything I do and for bearing with me despite various desperate phone calls.

Danksagung

Zunächst gilt mein Dank dem Bundesministerium für Bildung und Forschung welches das Projekt NanoFlow gefördert und so meine Promotion ermöglicht hat.

Mein besonderer Dank gilt meinem Doktorvater, Prof. Dr. Erwin Klumpp für die vielfältige Unterstützung während der Promotion. Ausführliche Diskussionen, aufbauende Worte und seine immer offen stehende Tür haben mir über verschiedene Schwierigkeiten während der dreieinhalb Jahre am IBG-3 hinweg geholfen. Danke für alles.

Ich möchte mich herzlich bei Prof. Dr. Andreas Schäffer für wertvolle Diskussionen und die Möglichkeit der Promotion am Lehrstuhl für Umweltbiologie und Chemodynamik der RWTH Aachen University bedanken.

Ein großer Dank geht an Prof. Dr. Harry Vereecken für die Möglichkeit der Durchführung der Doktorarbeit in der Agrosphäre. Die Unterstützung der Doktoranden war stets exzellent und die zahlreichen Vorträge und Ph.D.-Reports waren eine gute Vorbereitung für Konferenzen, Paper und die Dissertation.

Ich bin sehr dankbar für die Möglichkeit Dr. Scott A. Bradford und Prof. Dr. Jiří Šimůnek in Riverside, Californien, besuchen zu können. Vielen Dank für Eure Geduld und Unterstützung.

Besonders bedanken möchte ich mich auch bei Dr. Marc Heggen für seine Unterstützung bei der Transmissionselektronenmikroskopie am Ernst Ruska-Zentrum für Mikroskopie und Spektroskopie mit Elektronen der Forschungszentrum Jülich GmbH und die Möglichkeit diese Technik zu erlernen.

Außerdem danke ich Peter Klahre, Stephan Köppchen, Martina Krause, Ulrike Langen, Herbert Philipp, Claudia Walraf, Dr. Lutz Weihermüller und Ansgar Weuthen für ihre vielfältige Unterstützung. Danke, dass ihr mir immer weitergeholfen (oder es zumindest versucht) habt.

Für die Hilfe bei der Durchführung von Laborversuchen danke ich außerdem Wolfgang Schierenberg und Miaoyue Zhang.

Das Lysimeterexperiment wäre ohne die Hilfe von Dr. Anne Berns, Dr. Diana Hofmann, Stephan Köppchen, Martina Krause, Ulrike Langen, Yan Liang, Dr. Bastian Niedrée, Herbert Philipp, Dr. Thomas Pütz, Herbert Rützel und Dr. Lutz Weihermüller nicht möglich gewesen. Vielen Dank.

Mein Dank gilt außerdem Dr. Hanna Maes, Mitarbeiterin am Lehrstuhl für Umweltbiologie und Chemodynamik der RWTH Aachen University, für die wertvollen Ratschläge vor allem zu Beginn meiner Doktorarbeit und die Ermöglichung der Synthese ^{14}C-markierter MWCNTs.

Außerdem möchte ich mich von Herzen bei Dr. Anne Berns, Markus Duschl und Dr. Wolfgang Tappe bedanken, die sich oft Zeit genommen haben kleinere und größere Probleme mit mir zu diskutieren, Korrektur zu lesen und die mich immer wieder (re)animiert haben.

Danke an Basti, Christian, Meli, Sascha, Sirgit, Thomas und Wolfgang für die schöne und lehrreiche Zeit während der Mittagspause. Ich werde Euch vermissen.

Ich möchte mich auch bei allen Kollegen bedanken, die mir in den 3 Jahren besonders ans Herz gewachsen sind und die mir des Öfteren über kleine und große Krisen hinweg geholfen haben. Die gemeinsamen Freizeitaktivitäten waren eine willkommene Abwechslung.

Außerdem möchte ich mich bei meiner Familie bedanken, die einige verzweifelte Anrufe über sich ergehen lassen mussten und die mich immer in allem unterstützen.

Band / Volume 188
Entwicklung protonenleitender Werkstoffe und Membranen auf Basis von Lanthan-Wolframat für die Wasserstoffabtrennung aus Gasgemischen
J. Seeger (2013), V, 130 pp
ISBN: 978-3-89336-903-4

Band / Volume 189
Entwicklung und Herstellung von metallgestützten Festelektrolyt-Brennstoffzellen (MSC-SOFC) mit einem Sol-Gel-Elektrolyten
S. D. Vieweger (2013), xviii, 176 pp
ISBN: 978-3-89336-904-1

Band / Volume 190
Mobile Brenngaserzeugungssysteme mit Mitteldestillaten für Hochtemperatur-PEFC
C. Wiethege (2013), iii, 179 pp
ISBN: 978-3-89336-905-8

Band / Volume 191
Verbundvorhaben Öko-effiziente Flugzeugsysteme für die nächste Generation (EFFESYS) - Teilprojekt Brennstoffzelle, Infrastruktur, Komponenten und System (BRINKS) – Schlussbericht
J. Pasel, R.C. Samsun, H. Janßen, W. Lehnert, R. Peters, D. Stolten (2013), xii, 152 pp
ISBN: 978-3-89336-908-9

Band / Volume 192
Analyse des Betriebsverhaltens von Hochtemperatur-Polymerelektrolyt-Brennstoffzellen
L. Lüke (2013), 150 pp
ISBN: 978-3-89336-909-6

Band / Volume 193
Full-waveform inversion of crosshole GPR data for hydrogeological applications
A. Klotzsche (2013), X, 164 pp
ISBN: 978-3-89336-915-7

Band / Volume 194
Long Term Stability and Permeability of Mixed Ion Conducting Membranes under Oxyfuel Conditions
X. Li (2013), III, 143 pp
ISBN: 978-3-89336-916-4

Band / Volume 195
Innovative Beschichtungs- und Charakterisierungsmethoden für die nasschemische Herstellung von asymmetrischen Gastrennmembranen auf Basis von SiO_2
J. Hoffmann (2013), V, 152 pp
ISBN: 978-3-89336-917-1

Band / Volume 196
Aerosol processes in the Planetary Boundary Layer: High resolution Aerosol Mass Spectrometry on a Zeppelin NT Airship
F. Rubach (2013), iii, 141 pp
ISBN: 978-3-89336-918-8

Band / Volume 197
Institute of Energy and Climate Research IEK-6: Nuclear Waste Management - Report 2011 / 2012 Material Science for Nuclear Waste Management
M. Klinkenberg, S. Neumeier, D. Bosbach (Eds.) (2013), 195 pp
ISBN: 978-3-89336-980-1

Band / Volume 198
Material migration in tokamak plasmas with a three-dimensional boundary
R. Laengner (2013), vi, 140, XVII pp
ISBN: 978-3-89336-924-9

Band / Volume 199
Improved characterization of river-aquifer interactions through data assimilation with the Ensemble Kalman Filter
W. Kurtz (2013), xxv, 125 pp
ISBN: 978-3-89336-925-6

Band / Volume 200
Innovative SANEX process for trivalent actinides separation from PUREX raffinate
A. Sypula (2013), 220 pp
ISBN: 978-3-89336-927-0

Band / Volume 201
Transport and deposition of functionalized multi-walled carbon nanotubes in porous media
D. Kasel (2013), VI, 103 pp
ISBN: 978-3-89336-929-4

Weitere ***Schriften des Verlags im Forschungszentrum Jülich*** unter
http://wwwzb1.fz-juelich.de/verlagextern1/index.asp

Energie & Umwelt / Energy & Environment
Band / Volume 201
ISBN 978-3-89336-929-4

JÜLICH
FORSCHUNGSZENTRUM